An investigation into a technique of reconstruction tomography.

MCCOMBIE, W.F.

1982

An Investigation into a Technique

of Reconstruction Tomography

by

William Francis McCombie

This thesis is submitted in partial fulfilment of the requirements of the Council for National Academic Awards, for the degree of Master of Philosophy (M.Phil.)

School of Electronic and Electrical Engineering,
Robert Gordon's Institute of Technology,
Aberdeen.

In collaboration with

Department of Bio-Medical Physics and Bio-Engineering,
University of Aberdeen,
Foresterhill,
Aberdeen.

October 1982

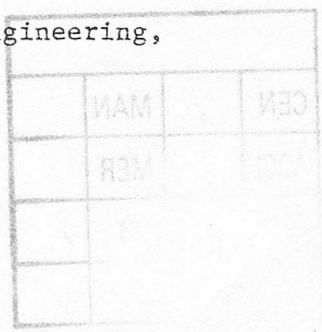

DECLARATION

I hereby declare that this thesis is a record of work undertaken by myself, that it has not been the subject of any previous application for a degree, and that all sources information have been duly acknowledged.

In the course of this research, the following were included in an approved programme of advanced studies.

(1) 8085 micro processor course at R.G.I.T., November 1979

(2) Attended all relevant seminars held at the Medical Physics Department, Aberdeen University on techniques in nuclear medicine.

(3) Visits to Dr P E Undrill (Department of Medical Physics, Aberdeen University) and Dr J E Bateman (Rutherford and Appleton Laboratories) for discussions and information exchanges.

William Francis McCombie

October 1982

An Investigation into a Technique of Reconstruction Tomography

by

William Francis McCombie

ABSTRACT

The aim of this research was to investigate a new technique of reconstruction tomography to be applied to a new type of radioactivity detecting 'camera'. Radioactive isotopes can be injected into a human and their paths through the body can be monitored by these 'cameras'. Conventional 'cameras' involve a moving detector, whereas the static type of 'camera' being developed by Dr J E Bateman at Rutherford Laboratory, has fixed detectors. The purpose was to convert the information collected by this static type of 'camera' into a picture of the cross-section of the human body.

The first part of the work involved writing a program to simulate the effects of known geometry, three-dimensional containers, 'phantoms', filled with the radioactive isotopes. The two containers simulated were the cuboid and the sphere, and these could be either hollow or solid. The program could create 'simulated phantoms' anywhere in three-dimensional space. It also had the capability of producing data which took into account the defects and limitations of the 'camera'.

The second part involved writing a program to reconstruct a layer of the body from the data produced by the 'camera'. This involved having to process the data to remove unwanted information from the picture. New processes, for improving information content of a picture, have been developed and evaluated. These processes produced encouraging results, but displayed some problems. These were investigated to try and minimise their effect. These processes were also compared with conventional techniques of picture processing.

Acknowledgements

I would like to express my thanks to my director of studies Dr J D Eades for his encouragement and guidance throughout the project. In addition, to note the information and criticism supplied by my external supervisor Dr P E Undrill (Medical Physics Dept., Aberdeen University) and by Dr J E Bateman (Rutherford and Appleton Laboratories, Dicot, Oxon).

I am grateful for the assistance of the staff of the Computer Services Unit, in particular Mr G J C Smith, in connection with any problems associated with the computer used. Also to Mr E Forrest for his help with the mathematical problems encountered during this project. I also note the welcome criticism from Mr D P Mann throughout this project.

I would like to thank Mr B Davidson for his help in the drawing of most of the diagrams in this thesis. Finally I acknowledge the support of a Scottish Education Department research studentship.

SUMMARY

This work was involved with computer assisted reconstruction tomography. The synthesis and analysis of the data for devices such as these, was carried out totally as a computer software project. The computer used was that of the Robert Gordon's Institute of Technology, which was a DECsystem-2050. The computer language used throughtout was FORTRAN.

Chapter One gives a brief history of tomographic techniques, as well as the basic criteria which are involved. Chapter Two outlines the device that was simulated by the computer programs. Chapter Three then goes on to describe the operation of the computer program that simulates the device. Chapter Four details the new processes, which were created to improve the quality of the final output. Chapter Five shows the different types of output device and their output. Chapter Six compares all the processes that were described in Chapter Four. Chapter Seven compares the best process in Chapter Six with one of the techniques currenty used, and finally Chapter Eight concludes and describes the possible further work.

CONTENTS

CHAPTER ONE

HISTORY OF TOMOGRAPHIC TECHNIQUES

Tomography is concerned with the study of the human body by the use of 'body scanners', which produce an image of a section through the body. These body scanners have come into existence through advances in medical technology, brought about by social demands for a longer and healthier life. This involved the clinician in not only being able to cure diseases or ailments, but also being able to detect them at an early stage. Most of these diseases were concerned with the internal organs of the body, such as the brain, liver or the heart. The techniques originally employed to diagnose the condition, either used the clinician's experience, or involved a surgical procedure. A technique was needed, to enable the examination of these internal organs, which minimised the risk to the patient.

The following chapter will give a brief history of the development of tomographic body scanners. Different types of these scanners will be described and their relative merits discussed.

1.1 Whole Body Scanners

The first attempt at showing the organs within a body was by using a source of x-ray radiation and a photographic plate. The x-ray source transmitted radiation through the body, and was collected by the photographic plate on the opposite side. The principle with which this arrangement operated, was that dense objects affect the trajectories of

x-rays. As the x-rays were absorbed, the photographic plate, directly behind those objects, received less radiation. Thus a picture was formed on the film, which contains information relating to that body. The main drawback to the result obtained, was that any section that required to be observed, was superimposed with the rest of the body on the one picture. Selection of one plane through the body was not possible.

However a system of a moving source of x-rays with a moving photographic plate, as shown in Figure 1.1, could be used to produce the effect of highlighting a particular section. As can be seen, the points on the focal plane X have kept their relative positions, whereas any points off the plane have moved, and thus caused them to be recorded as a blur. The technique was analogous to using a narrow depth of field in photography, which meant that the other sections of the body were still present, but in a highly blurred state.

In the late 1960's, the work carried out by G N Hounsfield [1.1] led to considerable developments in the ability to study internal organs of bodies. New machines were engineered which could generate and store three dimensional information about these organs of the body. Using this information, a particular section through the body could be reconstructed and displayed. The effect of radiation from other sections in the body was greatly reduced compared with the technique using x-rays with a photographic plate. One disadvantage of the new system, was that pre-processing of the information had to be performed, before a meaningful image could be formed. However, the application of a computer to this task overcame this problem. The presence of the computer also enabled the capability of modifying the information obtained from the body scanner, and thus enhance the final picture to give a clearer, more meaningful reconstruction of a discrete section.

There were two distinct types of body scanner available which used different methods of irradiating the body. These were transmission and emission devices. How they operated and their individual advantages will be described in the following sections.

1.2 Transmission Tomography

The types of body scanners that used transmission tomography, all involved the basic construction shown in Figure 1.2, which consisted of a source of radiation at A and a suitable radiation detector at B. The object of these devices was to produce a picture of the density of the material within the section to be viewed.

The principle of operation was that radiation from the source at A was transmitted through the body, and the intensity of the radiation was detected at B. The amount of radiation detected and the position of the detector were recorded, while a complete scan of the body was made. A scan consisted of two distinct motions, these were a movement in a straight line sweep across the body, and a rotation which moved the system round to a new angle for another sweep. The movement in a straight line was carried out, by moving the source of radiation and the detector in unison, in a linear sweep across the body from position X to X′. Once this was done, the whole apparatus was rotated through a pre-determined angle and the linear sweep was carried out again. The apparatus followed a scanning pattern as shown in Figure 1.3. This procedure was continued until at least one complete revolution had been completed round that part of the body.

1.2.1 Single Detector [1.2,1.3]

The single detector type of body scanner had a single collimated beam of x-ray radiation at A and a single scintillation detector at B with the linear sweeps around the body at typically six degree intervals, as shown in Figure 1.4. A scintillation detector converts x-rays to photons of light [1.4]. These photons can then be amplified using a photo-multiplier, to generate a reasonably large signal to be used by normal electronics.

The amount of radiation detected by B, would obviously depend on the quantity and density of the material, on the line between the two positions A and B. Therefore, each linear sweep across the body would create a profile of intensities. To remove the error introduced when converting from the profile of the scans onto the array, the profile was passed through a mathematical filter which had the characteristic shown in Figure 1.5. The modified profiles were used to produce an array of intensities to be used for the final picture.

Each profile was divided up into a finite number of elements and 'rays' orthogonal to these profiles were projected across the display array. Each square of the array, that a particular 'ray' passed through, was incremented by the value of the profile at that 'ray' position, as shown in Figure 1.6. This procedure was continued until the whole scan had been processed. The array could be further filtered to enhance the picture before it was displayed.

Some of the radiation detected, did not come directly from the source but arrived after bouncing off high density objects, such as bones or the detector equipment. To reduce the effect of these indirect x-rays, the acceptance angle of the collimator was limited. Thus increasing the probability that only x-rays emanating from the direction of the source, would be accepted.

As there was only one detector, this technique would only produce the section of the body in the plane of the scan. The information obtained from the body by this method, was therefore only two dimensional. If the information required was not in that section, another scan would have to be performed.

1.2.2 Array of Detectors

The next logical step to improve the detection system, was to replace the single detector by an array of detectors [1.5], as shown in Figure 1.7. The main advantage that the array of detectors had over a single detector, was that it took less time to gather the same amount of information. This was achieved by the array being able to catch more of the radiation passing through the body, thus the dose of radiation the patient received could be reduced. Due to the reduced amount of time for gathering the same amount of information, the picture would have less blur due to movement by the patient. However, this system was normally used to gather a larger amount of information, as a large number of rays used in the creation of the array increased the signal to noise ratio of the system, which in turn resulted in clearer pictures. A disadvantage of the system was the increased complexity due to the addition of more detectors.

The array of detectors have two possible modes of scanning. These were dependent on the number of the detectors per metre within the array. If this value was low, then the action of the scan was the same as in the single detector case, but with the number of linear sweeps reduced. If on the other hand the density was high, the scan consisted of only the rotation.

When there was a low density of detectors in the array, the source of radiation was usually collimated. This reduced the effect of indirect rays, by lowering the number of possible ray trajectories. However, when the density of detectors was high, limited collimation is used on the source of radiation, as shown in Figure 1.8. This type of source was known as a 'fan beam'. With a high density of detectors, it was more economic to use xenon gas detectors rather than scintillation detectors.

The array of detectors not only extended in the direction that was scanned previously, but also along the body. Thus enabling the body scanner to be placed approximately, rather than precisely as in the technique in 1.2.1. As there was now a third dimension, the analysis software could produce a three dimensional picture of the body.

1.3 Emission Tomography

The basic principle of emission tomography was that the radiation was emanating from within the body as opposed to being fired through the body by an external source of radiation, as in the case of transmission tomography. This was carried out by injecting the patient with a suitable source of radiation. This produced information relating to the distribution of the radiation within the body, rather than the density of the material.

There were two distinct types of radiation emission available, which in turn used different methods of detection. These are described in the following sections.

1.3.1 Single Gamma Ray Emission

The first of the two types of emission sources, produced a single gamma ray for each emission [1.6]. This was achieved by using an element or compound which was radioactively unstable and was decaying. The material that was injected was the source of the radiation. The gamma rays emitted were detected using a single scintillation detector, as described in 1.2.1. A good inorganic scintillor, for use with gamma rays, was crystalline sodium iodide activated with thallium, NaI(Tl). The detector was collimated so that only those gamma rays which were orthogonal to the linear sweep of the detector were detected. The line of the gamma ray in space, was therefore defined by the position of the collimated scintillation detector, when the gamma ray was detected. However, this differed from 1.2.1 in that only positional information could be detected with any real accuracy, due to uncertainty in the intensity of the radiation. For example, a value detected could be a weak source close to the detector or a large source far away.

With only one detector, most of the radiation emanating from the body was lost. Therefore, the patients have to be given higher doses of radiation to enable a reasonable amount of data to be collected. To improve on this system, an array of collimated scintillation detectors [1.7] could be used, as described in 1.2.2. However, as the source was not one point but a whole volume, there was an increase in the amount of indirect rays.

1.3.2 Pair of Gamma Rays Emission

The other type of radiation emission produced two simultaneous gamma rays. This effect was achieved by using a substance which emitted positrons. When a positron came in contact with an electron, they annihilate and produce two gamma rays. The trajectories of these gamma

rays were along the same straight line in space, but in opposite directions. Using this phenomenon, a system for reconstructing an image of a section through the body was designed using a pair of two dimensional, large area detectors. These detectors could be of three basic types; those using arrays of sodium iodide crystals [1.8,1.9], those using multiwire proportional chambers with lead converters [1.10,1.11] and those using multi-proportional chambers with liquid xenon [1.12,1.13,1.14]. There were also circular detectors available [1.15,1.16], using sodium iodide crystals.

The two dimensional large area detectors could give the (X,Y) co-ordinates where a gamma ray passed through their faces. Using two such detectors, positioned facing each other as shown in Figure 1.9, the pairs of gamma rays emitted from the body could be detected. The control electronics for the detectors operate such that, when one gamma ray was detected, the system waited within a set period of time for the other one to strike the other detector (coincidence detection). When the other gamma ray was detected, the position information of each detector was stored on magnetic tape or disc, for processing by a computer at a later date. But if only one gamma ray was detected within the set time period, it was discarded, as a unique straight line cannot be produced through only one point.

As the value of the source of each pair of gamma rays was unknown, the only information that could be gathered from the body, was the trajectories of the gamma rays. Therefore, any square in the array used for the final picture, that the ray passed through, was incremented by the same value, usually one.

As this arrangement of detectors did not move, it was not really a scanner but more akin to a camera. The device is often refered to as a 'positron camera', due to the radiation being generated by the annihilation of positrons. An example of this type of device was the

camera being developed by Dr J E Bateman of Rutherford and Appleton Laboratories. This Camera will be described in more detail in Chapter Two.

1.4 Desirable Qualities of a Whole Body Scanner

A system for studying the organs within the human body should not introduce any undesirable risk to the patient. The system should also take as short a period of time as is reasonable to gather the information to produce the picture and the resultant picture should be as accurate as possible. These points will now be highlighted in the following sections.

1.4.1 Speed and Dose

The speed of the scan was dependent on the dose of radiation. The larger the dose, the faster the scan could be. However, there was a limit to the amount of radiation which could be administered to a patient, without exposing them to the dangers involved from excessive amounts of radiation. To prevent these effects, the dose was carefully controlled. The time taken for the scan must, therefore, be increased to enable the equivalent amount of radiation to be collected. But this increase in time, meant that the time that the patient had to remain in the same position, was longer. Due to the greater time for a scan, there is a higher probability that the patient would move. The longer time could also affect the amount of radiation emitted, as the value of the half-life of the radio-isotope became significant. An isotope with a longer half-life could be used, but this increased the overall exposure time to the patient. As the type of isotope used may be collected by one particular organ, the increase in half-life may therefore cause local damage to this organ.

To justify buying a system, it had to be able to attain a certain through-put of patients. The longer the scan took, the fewer patients per hour that could be checked. Therefore, it may not be economically justifiable to buy a whole body scanning system.

Typical ranges of times taken for a scan by each of the different devices described, are given in the following table.

Transmission

Type	Scan Time
Single	4min - 4.5min
Multi	10sec - 2.5min

Emission

Type	Scan Time
Single	2min - 30min
Multi	2min - 15min
Positron	20sec - 10min

The main advantages of a fast scan time, was the decrease in the effect of blurring in the picture, due to movement of the patient. But for faster scans, a larger dose of radiation had to be administered. For a good quality picture, a large number of gamma rays need to be detected. This could be achieved by either a large dose or a slow scan. But during a slow scan the patient could move and introduce error anyway. There is a compromise between the quality of picture, speed of production and radiation dose. However, during the past ten years, using technological advances in collecting and processing, the scan times of all types of machines have reduced.

1.4.2 Accuracy

The accuracy of the picture produced by the body scanner was dependent on its spatial resolution. The spatial resolution is a measure of the ability to distinguish between two objects close together. It can be obtained by using a line source, and measuring the 'full width half maximum' value of the orthogonal slice of the picture, to the direction of the line source. The smaller this value, the better the resolution, and hence the sharper the reconstruction will be. The resolution of a body scanner picture had to be greater than the smallest object or distance that had to be seen. It had been found that the spatial resolution is independent of the distance between the pairs of detectors in a positron camera, unlike the effect on collimated scintillation detectors [1.17].

The value of the spatial resolution of a body scanner, could be reduced by the algorithm for removing any noise and unwanted signal, before producing the final picture. Due to the capability of some algorithms to highlight specific effects such as edge enhancement, this could produce a picture that did not fully represent what actually exists within that section of the body.

1.5 Summary

A body scanner system should produce accurate pictures of a section through a human body using a small dose of radiation. It should also gather the relevant information in the shortest time possible, so that there is as little discomfort to the patient. The body scanner interface to the operator should be as simple and as easy to understand as possible, and should inform the operator when a mistake has been made. This lowers the average overall time for processing by reducing the effect of errors. To optimise through-put of patients, the time for

gathering and processing the information obtained from the patient, should be about the same.

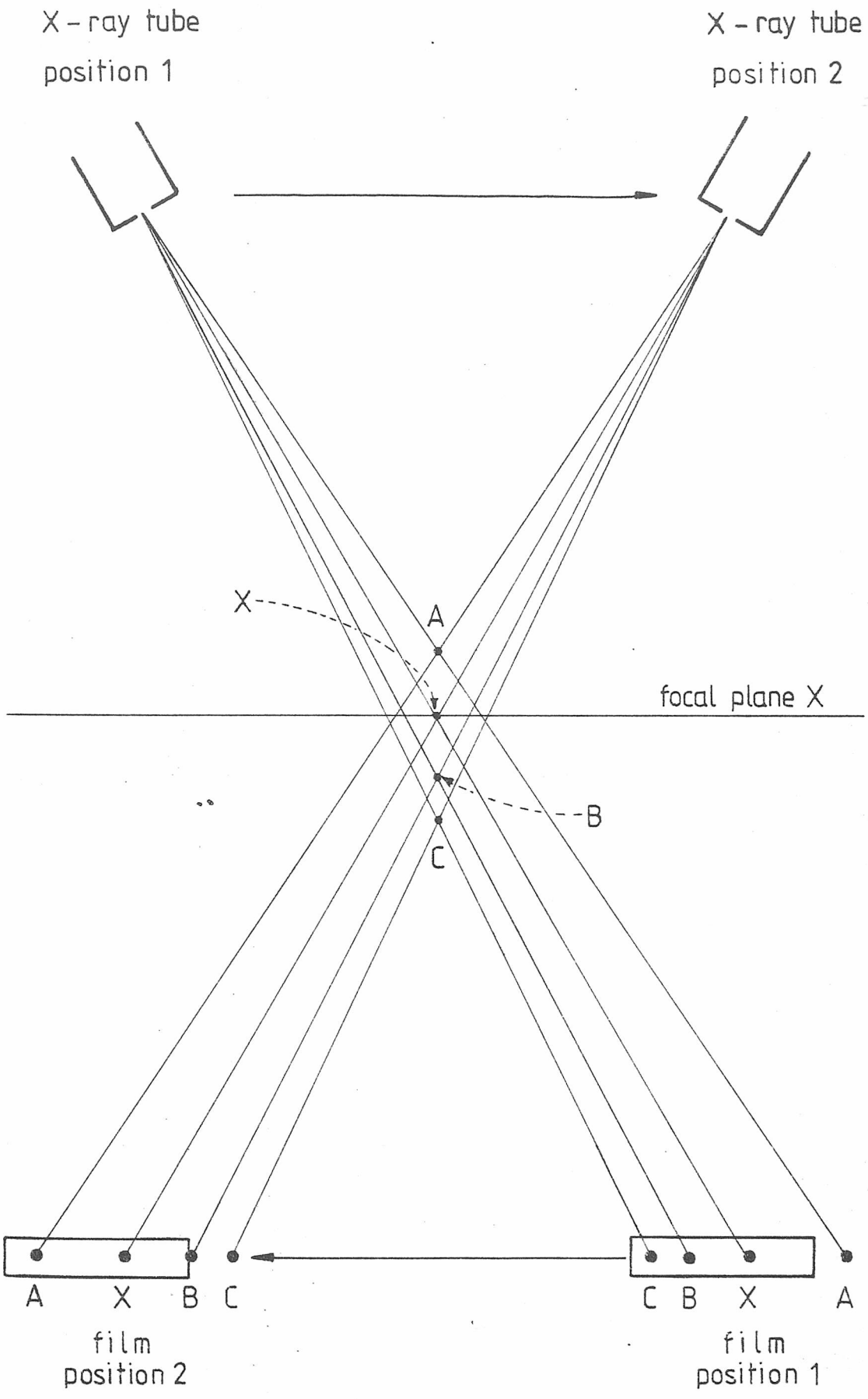

Figure 1.1 Moving source and photographic plate

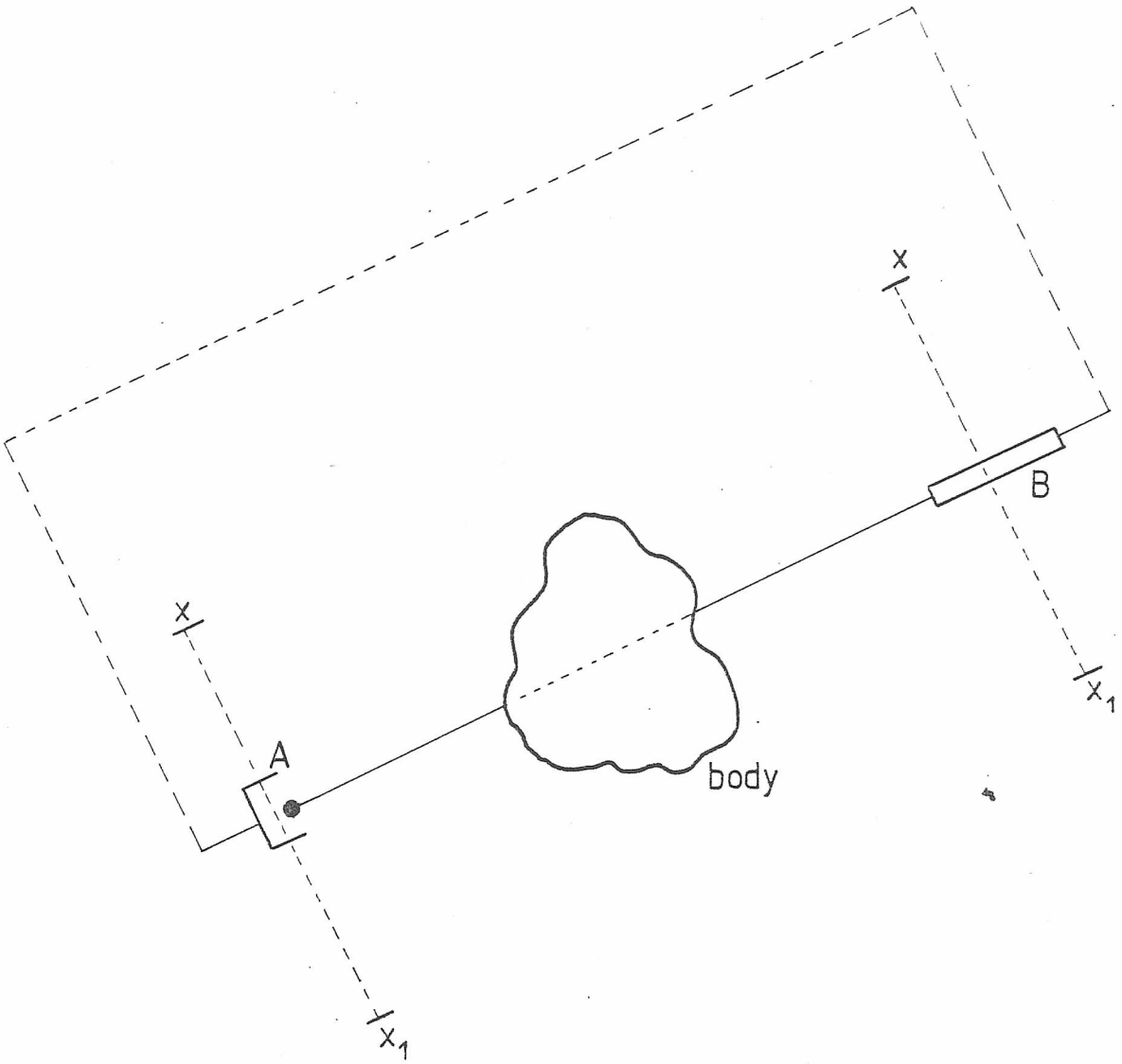

Figure 1.2 Basic construction of a transmission type of body scanner

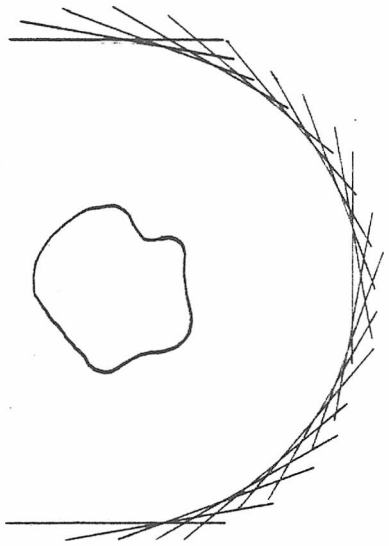

Figure 1.3 Scanning pattern for a transmission type of body scanner

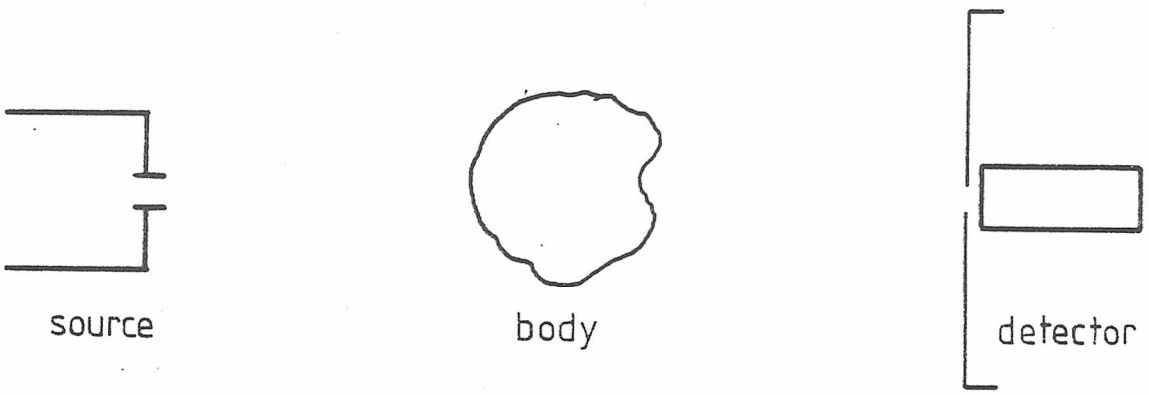

Figure 1.4 Single detector type of body scanner

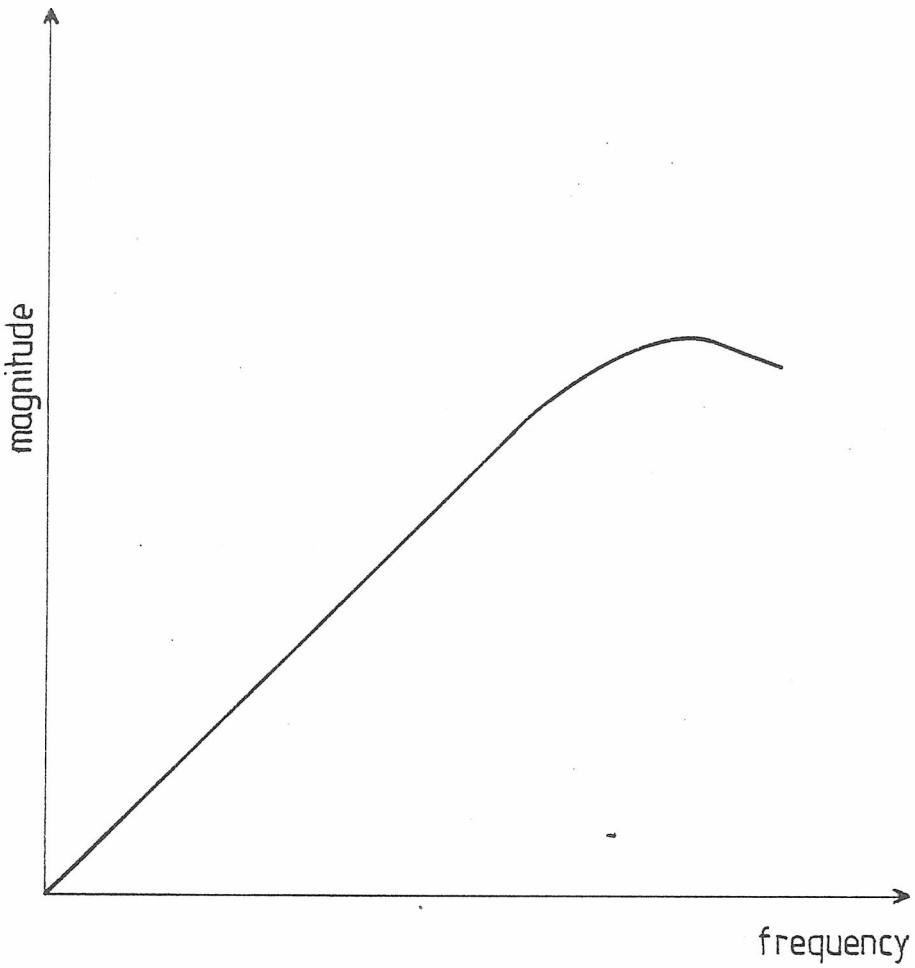

Figure 1.5 Mathematical filter used to modify the profile

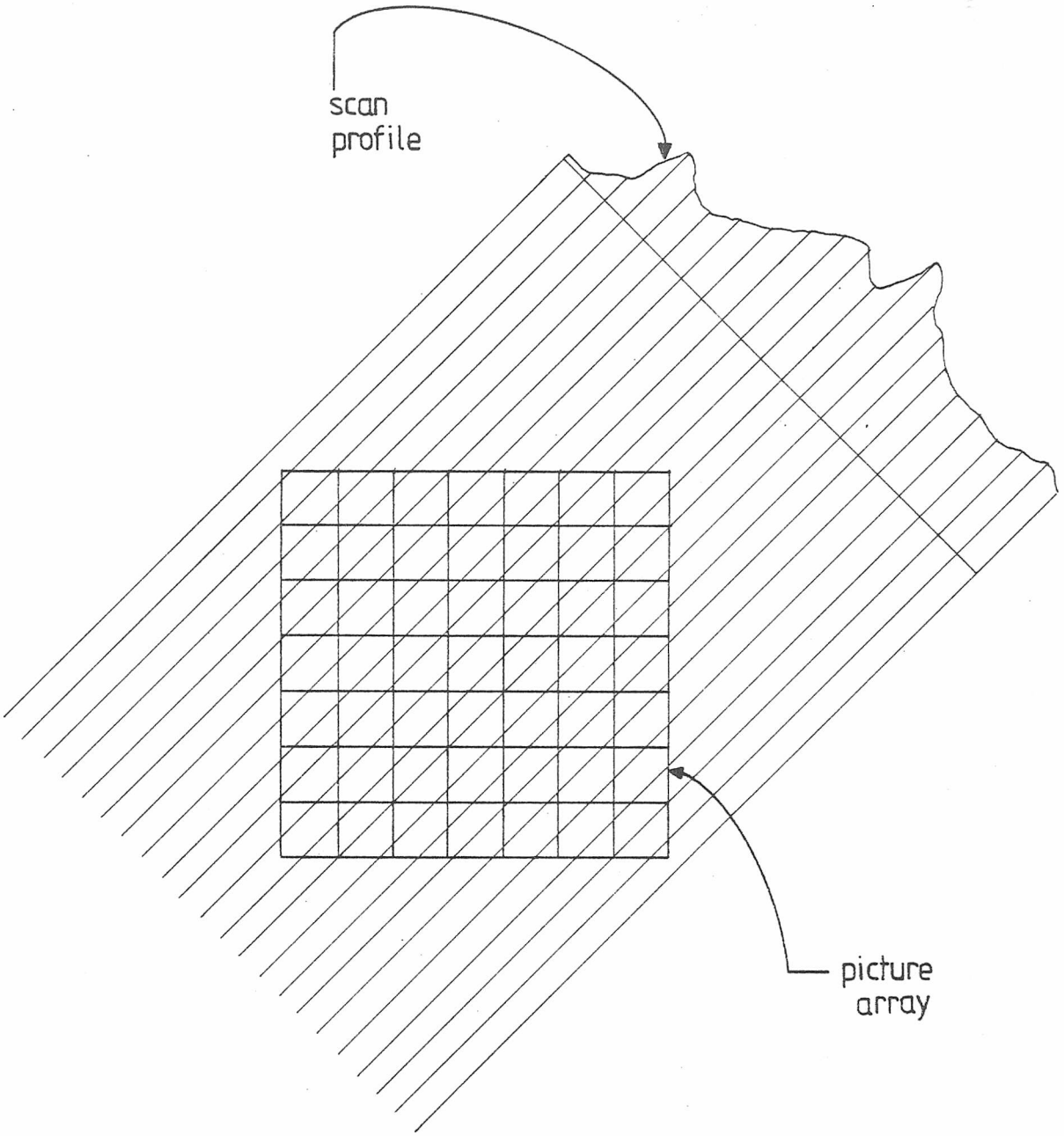

Figure 1.6 The application of the profile to the array

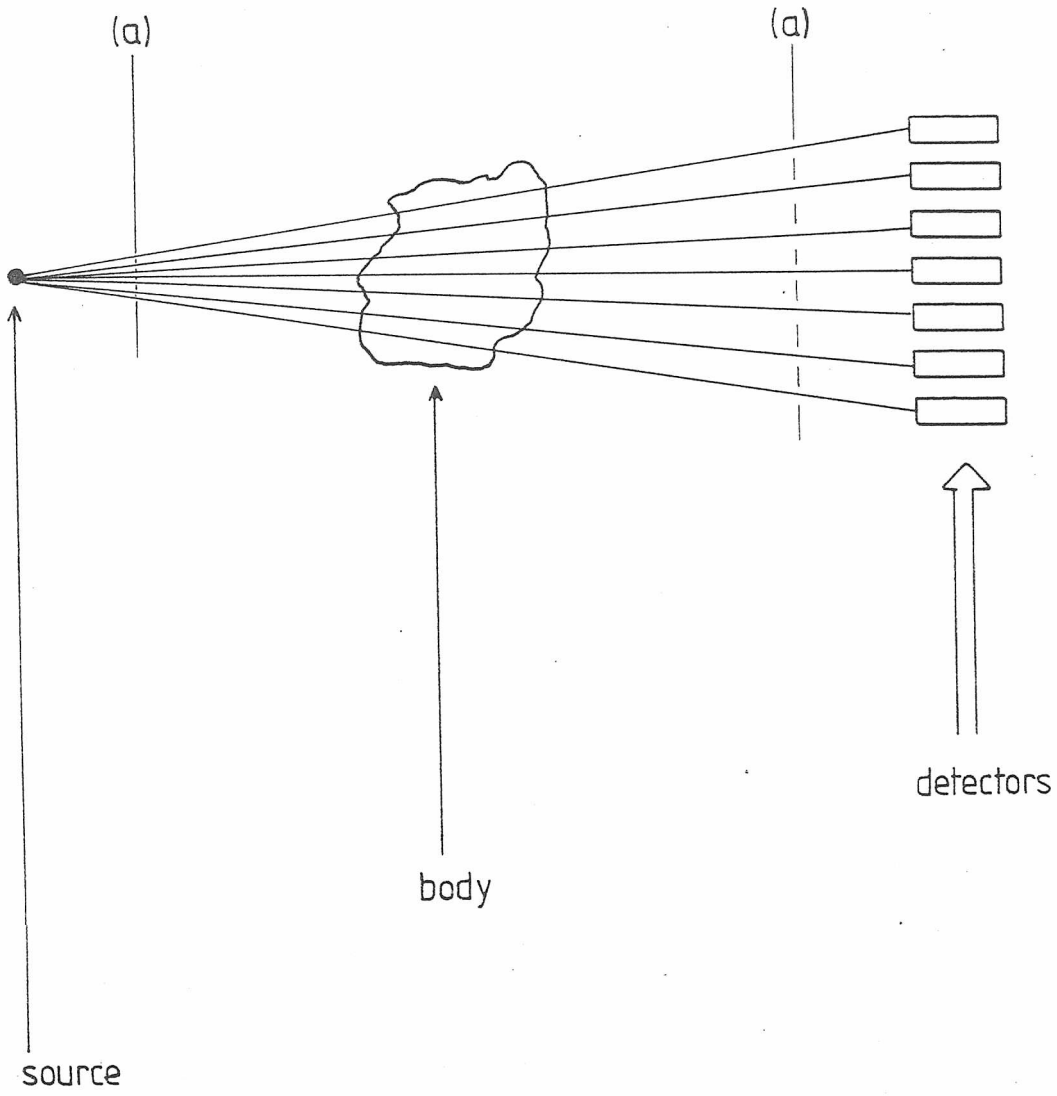

(a) - collimator

Figure 1.7 An array of scintillation detector type of body scanner

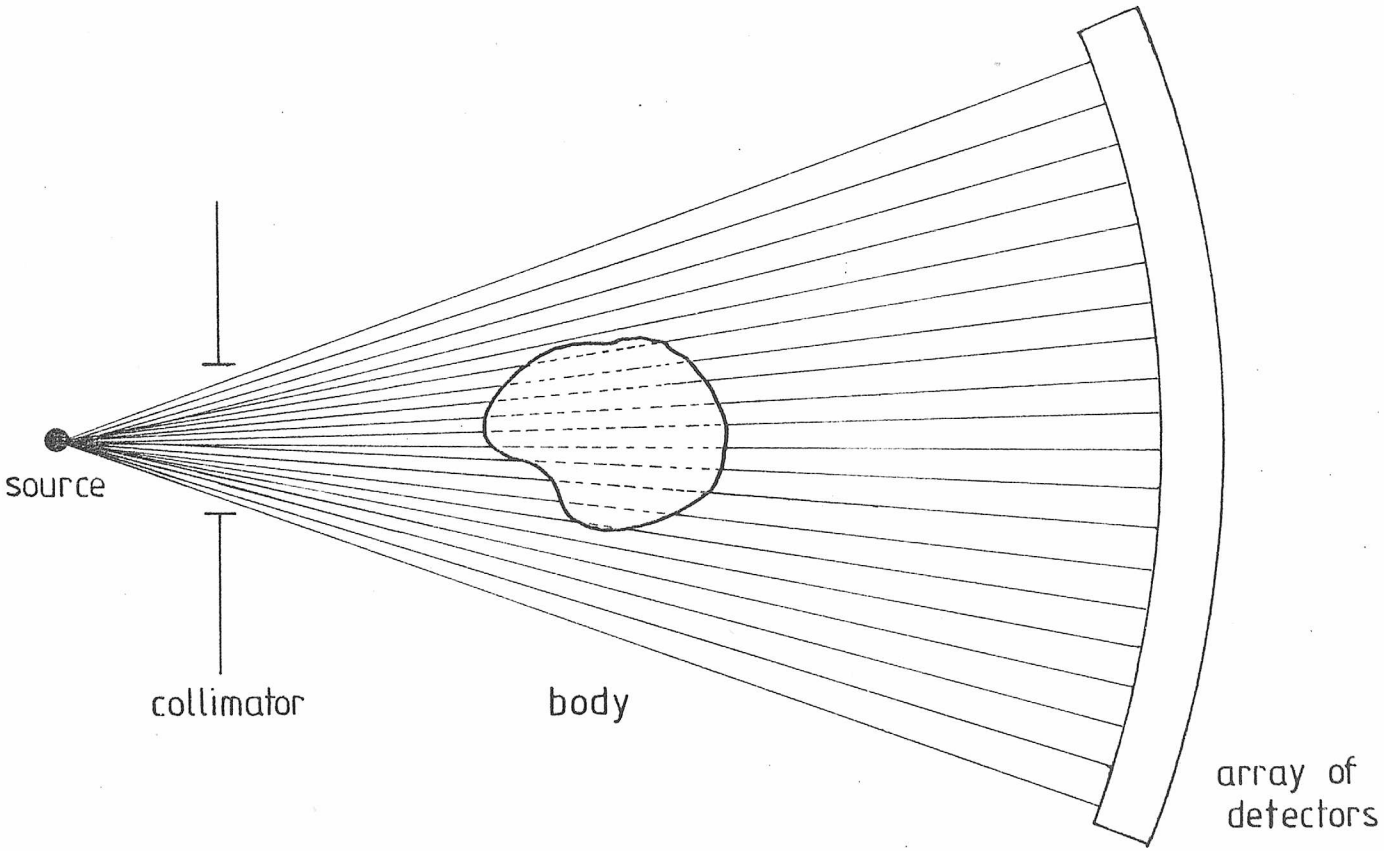

Figure 1·8 "Fan beam" type of body scanner

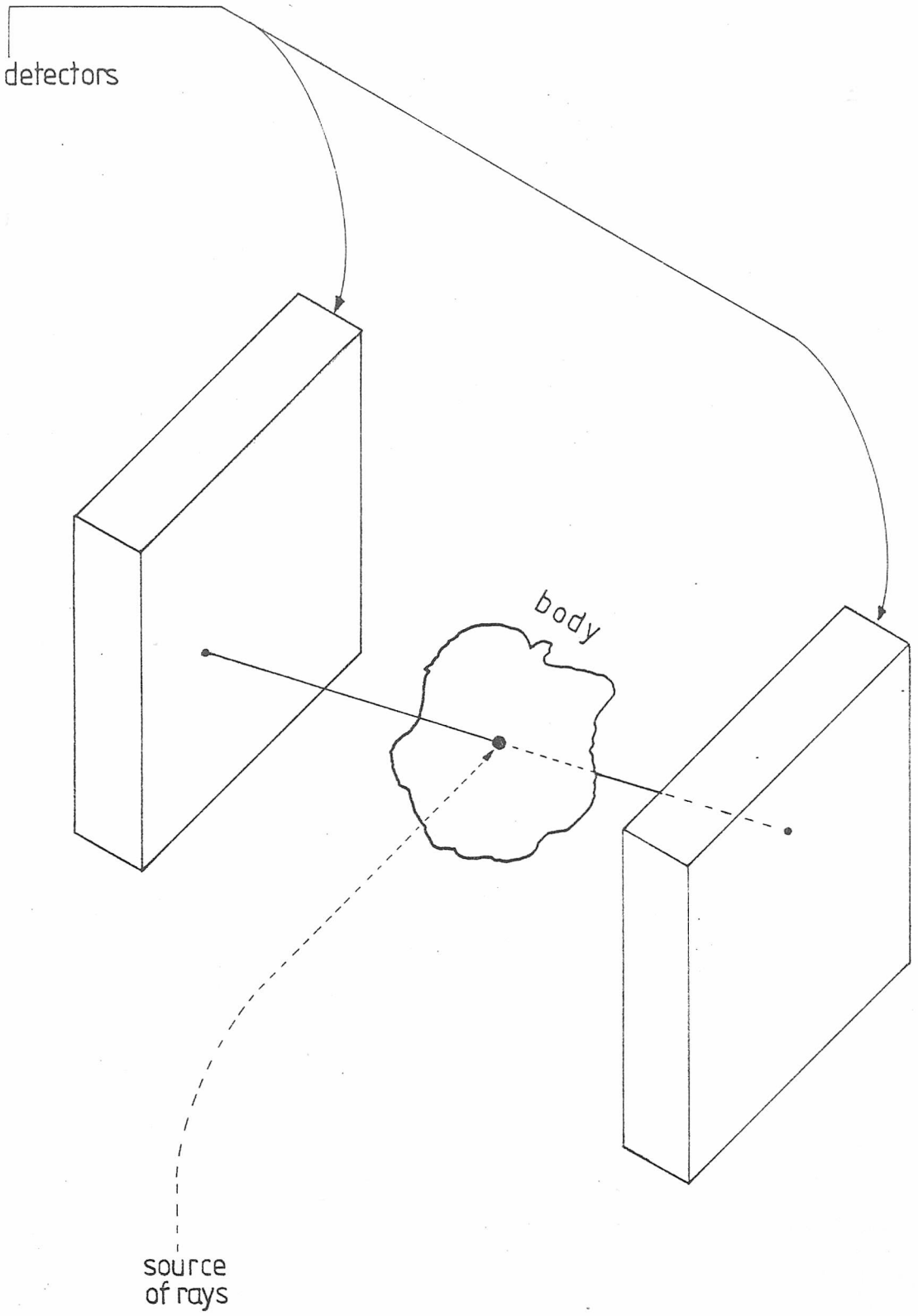

Figure 1·9 A pair of large area gamma ray detectors

CHAPTER TWO

THE BATEMAN CAMERA

This chapter sets out to describe the Bateman camera [2.1,2.2]. It begins with details of the camera construction and then goes on to outline its operation. The description of the camera presented here is based on the information received from the Bateman research team, and is not intended as a report on camera operation, but as an outline of the device to be used.

2.1 General Description of Device

The Bateman camera is a device which can detect pairs of gamma rays, produced by the annihilation of pairs of positrons and electrons. The prototype camera consisted of a pair of large area detectors sensitive to gamma rays. These detectors were placed on either side of the body, facing each other as shown in Figure 1.9.

The prototype detectors were designed, not so much with reference to the optimal specification, as to the availability of materials for a rapid test. These detectors were made up by using several layers of gamma ray detecting sections. The internal arrangement of one of these sections is shown in Figure 2.1. Each section consisted of alternate planes of anodes and cathodes, surrounded by a dense gas. The anodes in each section were constructed from gold plated tungsten wires of 20um diameter, placed at 2mm intervals. The cathodes, on the other hand, were fabricated by taking two 125um thick tin foils and laminating them on either side of a layer of 12.5um thick plastic, as shown in Figure

2.2(a). These layers of plastic and tin composite, were stretched on frames, and etched to produce a series of tracks seen in Figure 2.2(b). These tracks were the cathodes for the appropriate anode wires. The plastic used was kapton, due to its strength and its relative transparency to the movement of electrons.

The size of the cathode-cathode gap affected the imaging ability of the system. An 8mm gap was found to give a good quality image.

The easily ionised gas maintained between the anodes and cathodes was used to increase the number of electrons that manage to escape from the foil. The escaping electrons caused an avalanche effect on the anode wires. Therefore, the density of the filling gas also effected the imaging capability of a detector. The denser the gas the better the image became. The gas used was isobutane due to its high density and reasonable cost.

The efficiency that could be attained by a single anode-cathode detection section, was found by the Bateman team to be about 1%.

To generate a reasonable detection efficiency, of about 10%, twenty sections were necessary. These sections were stacked such that alternate cathode sections have their tracks orthogonal. The total configuration of a detector formed a multiple stack of multiwire proportional counters [2.3]. The total length of each prototype detector was 300mm, and the depth was about 104mm. The separation between the two detectors used in the prototype camera was variable.

2.2 Principle of Operation

These sections within the detector operated on the same principle as a multiwire proportional counter. The planes of cathodes within the detectors, acted as convertors of gamma rays to fast moving electrons. These electrons were found by the Bateman team, to have about a 50%

chance of escaping the cathode foils, with enough energy to register on the anode wires.

The effect of the cathode tracks being orthogonal, was that of constructing a grid. This operated on the principle that when an electron was detected by one of the anode wires, a pulse of current was produced. The next cathode track, which was orthogonal, had a current pulse induced in it due to the current flowing in the anode wire. This pulse proceeded along the cathode to a delay line. Computation of the X and Y co-ordinates was achieved by timing the arrival, at the ends of the delay lines, of the pulses induced in the X and Y delay lines with respect to a 'prompt' signal. The 'prompt' signal was generated at the origin of the avalanche on the anode wire. Within each detector, each plane of anode provided an independent output, so that a third co-ordinate Z could also be generated. This enabled a more accurate three dimensional position of where the gamma ray was detected, to be generated.

Large signals detected by the anodes, tended to correspond to wide angle knock-on electrons. Image quality could be improved by using pulse-height selection on the anode signals. Therefore the selection of small pulse heights on the anode signals, gave considerable enhancement in spatial resolution.

The radiation emanating from the body of the patient was in the form of two gamma rays on the same trajectory, but in opposite directions, resulting from the annihilation of a positron. As these gamma rays were travelling at the speed of light, they were detected within a short time of each other. It was found that "99% of all events lie within the 40ns interval", this was set by the intrinisic time resolution of the multiwire proportional counter detectors.

The two co-ordinates of where the gamma rays were detected, were recorded and stored on either disc or magnetic tape for processing offline by a computer at a later date. To increase the quality of the data produced by the detector system, the detection acceptance angle for the detector was decreased [2.4].

2.3 Further Developments

To increase the sensitivity of the camera and produce a better geometric convergence, additional pairs of detectors could be introduced. However, the addition of more pairs of detectors was limited by two factors. These were the increased cost of the additional detectors, and the increased complexity introduced into the control system. A possible economic system was that using three pairs of detectors at 120 degree intervals, forming a regular hexagon as shown in Figure 2.3. This was the configuration that was used used throughout this work.

2.4 Conclusion

A system to be used for clinical purposes, should be robust, reliable and not have any safety problems. This device fulfilled these requirements and could compare favourably with the cost of a convential system. The cost of a square metre gamma 'camera' was comparable with that of a 30cm diameter transmission scanner.

The rate at which this device took in information from the body was about 10kHz. It was limited to this value due to the increase in corruption of the data at higher rates by simultaneous emission. Simultaneous emission occured when more than one pair of gamma rays were emitted at the same time. The camera took the information from two of them and produced one detection. In this case the result bears no

relation to what existed within the body (see section 3.6.4 for more details of this phenomenon).

To produce a reasonably accurate picture of the section of the body, a sample size of about ten million was needed. However the time taken for this amount of data to be collected, meant that the body had to be immobilised for about 17min. This length of time may seem long, but during this time ALL the information about the section under study was gathered. The information gathered by the camera was true three dimensional information. The data stored could then be considered at leisure. In general it is claimed that the Bateman camera has a better spatial resolution and a higher sensitivity than the devices presently being used.

The description of the 'camera' presented in this Chapter, is based on the information received from the Bateman research team.

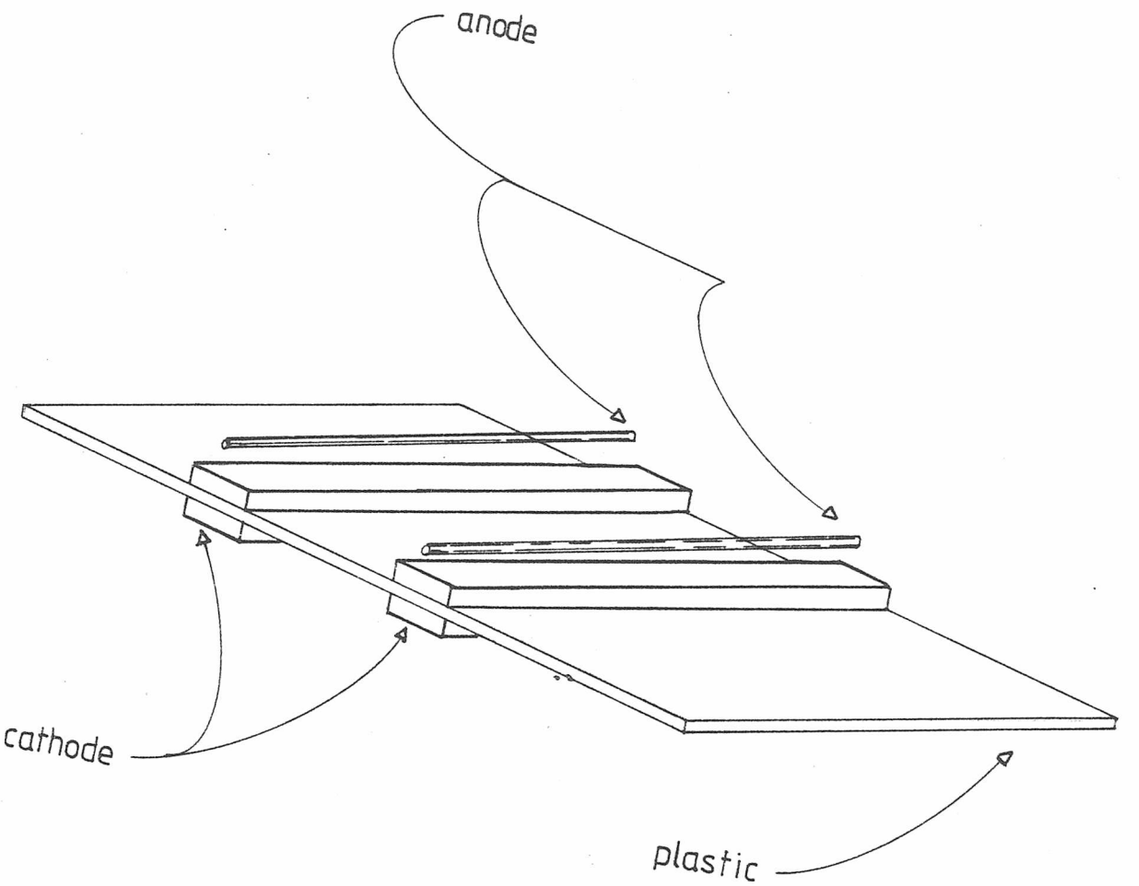

Figure 2.1 The internal arrangement of a section of a large area detector

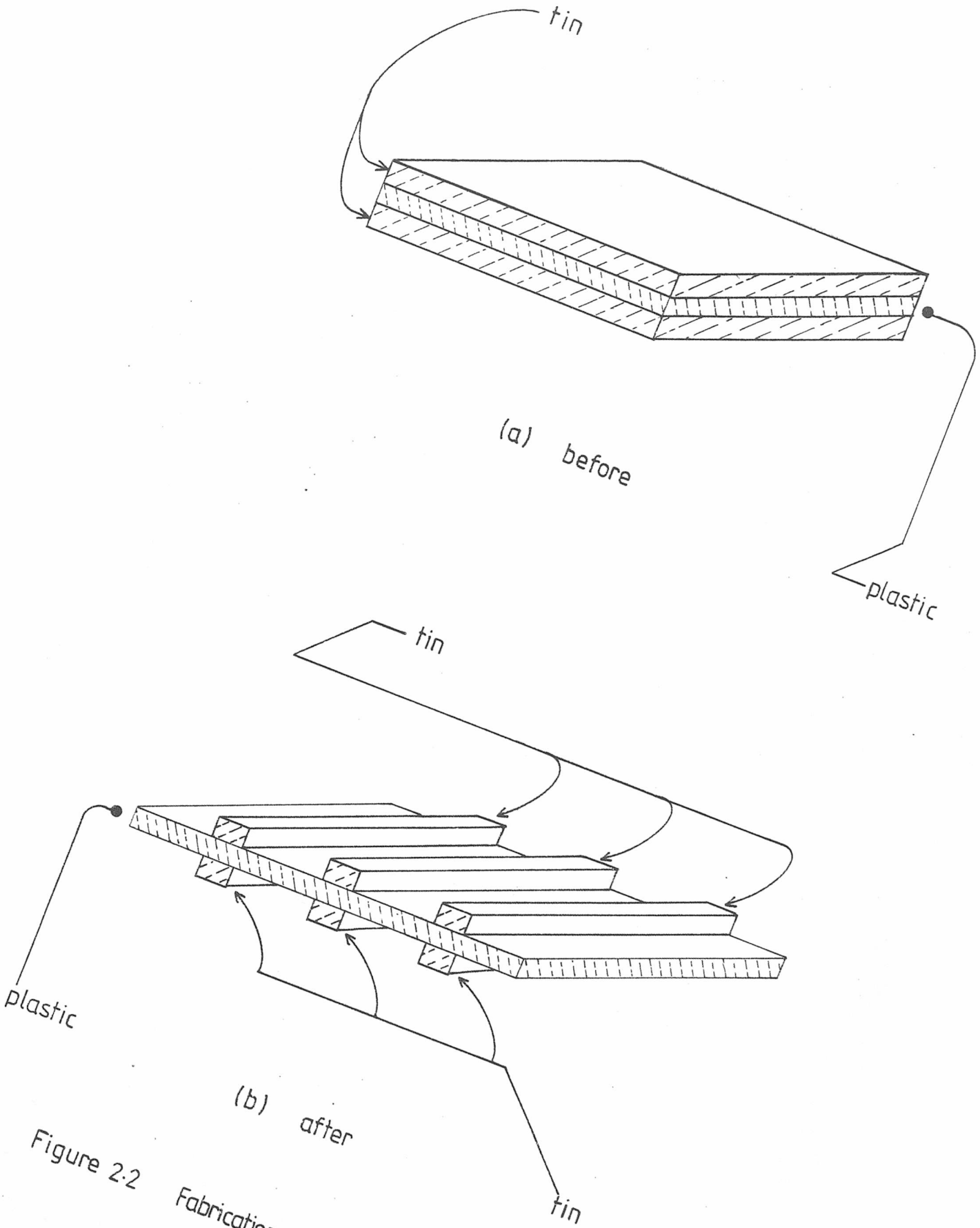

Figure 2.2 Fabrication of a section of a large area detector

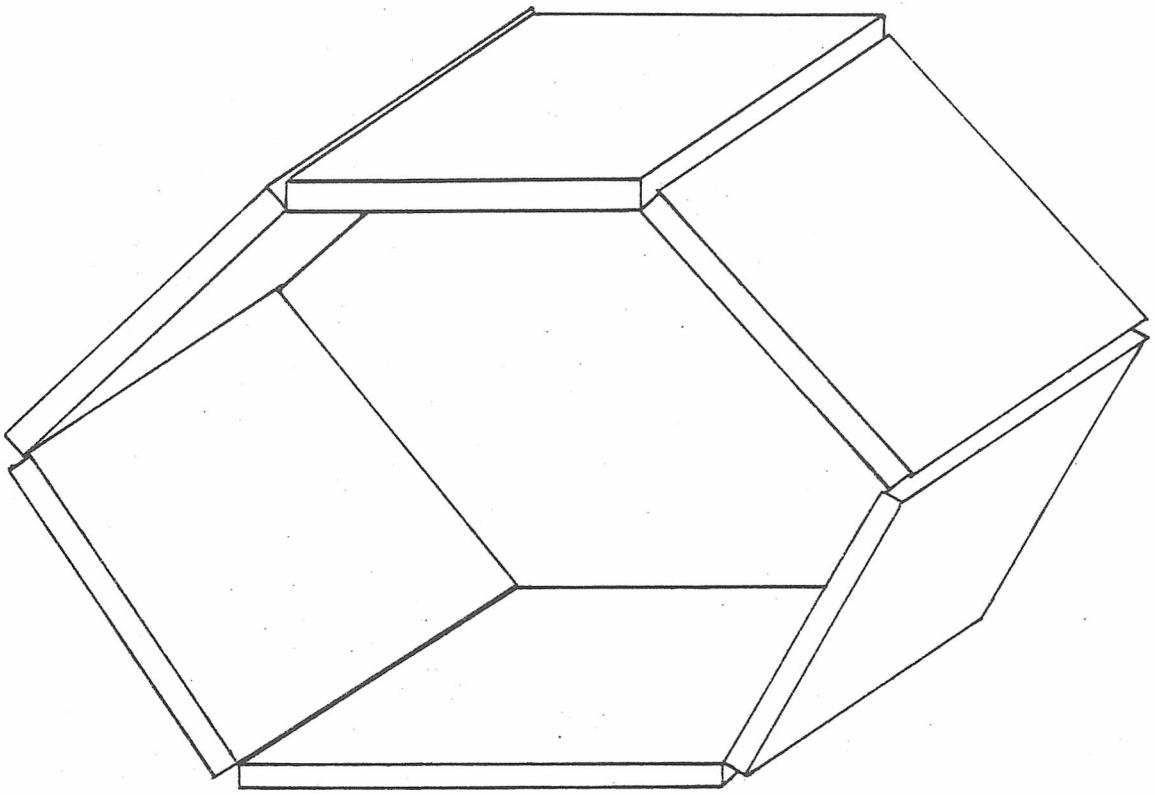

Figure 2.3 Possible economic camera

CHAPTER THREE

GENERATION OF SIMULATED INFORMATION

When a new system is developed, it has to be tested to prove that it can operate correctly. The system is usually tested by applying input conditions that produce a known result. In the case of a whole body scanner, the known input of data is produced from exactly defined objects called 'phantoms'. Phantoms are three dimensional shapes, which are filled with radioactive material which emit radiation exactly defining its shape. Several of these phantoms can then be arranged to simulate conditions associated with parts of the body. These groups of phantoms are placed within the detector system, and generate data which represents their three dimensional configuration.

The requirement for analysis software had already been met on most of the devices described in Chapter One. It was decided to construct a computer analysis package specifically for the 'positron camera', being developed and evaluated by Dr J E Bateman's team at Rutherford and Appleton Laboratories.

At the beginning of this work however, the Bateman camera had not been developed to such a level that it could produce any data. Therefore all the data used to test the new process of filtering, had to be generated independently of the camera. A computer program was developed to fulfil this requirement. This chapter describes how simulated phantoms were generated, and also how limitations of the camera were introduced into the data generated.

CHAPTER THREE

3.1 Method of Producing Simulated 'Phantoms'

The generation of simulated phantoms by a computer program required a random variable, which was used to model the random nature of the radiation emitted by the radioactive materials. Using this variable, random positions in space could be formed within the boundaries of any specified phantom.

To model a specific part of a body, a suitable arrangement of the phantoms had to be decided upon. The next stage was to generate the randomly placed points within the boundaries of these phantoms. The positions generated were those where the positron annihilations would have occurred in a real set of phantoms. To produce pairs of gamma rays emitted from these points, their directions in three dimensional space have to be generated to make the trajectories of the gamma rays unique. The direction of the pair of gamma rays was established by randomly generating a second point, such that it lay on the surface of a sphere, centred at the previously generated point.

The equation of the straight line describing the trajectory of the pair of gamma rays could be generated, since there now exists two points which lay upon it. Solving the mathematical description of the positions of the detectors in the camera with the equation of the line, produced the detector label numbers and the corresponding (X,Y) co-ordinates where the pair of gamma rays were detected. These values were stored to be used later in the analysis program. If in the course of solving the equation of the line with the detector system, however, only one detector was found to have been struck, that pair of gamma rays was discarded as would happen in the real camera.

The particular simulated phantoms produced were cuboids and spheres, as these were the easiest to describe and to handle. Point and line sources could be generated by producing cuboids with zero dimensions.

These simulated phantoms could also be solid or hollow. The hollow type of phantom was more difficult to analyse, due to there being a volume where there was no activity, completely surrounded by a layer of activity.

The simulated gamma ray was created by producing a point within the phantom and then generating its direction. The following two sections describe how the production of a point within two particular simulated phantoms, cuboids and spheres, was achieved. The third section describes how the trajectory of the ray was established, by using a second point which had been generated on the ray.

3.2 Generation of a Point within a Cuboid

The generation of a random three dimensional position within a cuboid was achieved by using the following method. Considering only the X dimension of the three, the X co-ordinate of a point within the cuboid was generated randomly by the following equation:

$$X = Xmin + (Xmax - Xmin) * RAN$$

where: Xmin - minimum X boundary of the phantom
Xmax - maximum X boundary of the phantom
RAN - random number generator ($0.0 < RAN < 1.0$)
('*' represents multiplication)

The Y and Z co-ordinates of the point were generated by similar equations. These equations produced a uniformly distributed set of points within the volume of the cuboid. An example of the distribution of points through the cuboid is shown in Figure 3.1.

To produce a hollow cuboid, an inner limit was set on the data produced by the equations for a solid cuboid, within which no radiation could be present. The implementation of this, was by simply taking the co-ordinates generated for the solid case, and checking whether they lay within this inner limit. If they did lie within the limit set, they were rejected.

3.3 Generation of a Point within a Sphere

The generation of a randomly placed point within a sphere was achieved after trying several different methods. The main reason for having any difficulty in implementing this, was due to the induced bias that some of the techniques introduced. These methods and their problems are described in detail in the following sections.

3.3.1 Method 1 - Polar Co-ordinates

The most obvious method for generating random points within a sphere, was by considering the three dimensional polar co-ordinates (R,Phi,Theta), to describe the position of the new point with respect to the centre of the sphere. Each of these quantities was set to have a uniform random distribution throughout their whole range. The values of these variables were randomly generated within their respective limits using the following equations:

$$R = Radius * RAN$$

$$Phi = PI * RAN$$

$$Theta = 2 * PI * RAN$$

where: Radius - radius of sphere which is the source
PI - constant (ie 3.14...)

The position of the randomly generated point was converted from polar to cartesian co-ordinates (X,Y,Z), with respect to the absolute origin, using the following equations:

$$X = R * \sin(Phi) * \cos(Theta) + Xc$$

$$Y = R * \sin(Phi) * \sin(Theta) + Yc$$

$$Z = R * \cos(Phi) + Zc$$

(where (Xc,Yc,Zc) is the centre position of the sphere)

On evaluation of this method for a uniform distribution of random numbers, it was found to produce a bias in the X and Z directions as shown in Figure 3.2. The mathematical proof why there should be a bias is given in Appendix C.

3.3.2 Method 2 - Modified Polar Co-ordinates

A modified version of the first method was constructed by considering the element cos(Phi) to be a uniform random variable, rather than the angle Phi itself. The value of sin(Phi) was then be evaluated by simple manipulation of a standard equation. The equations used were:

$$\cos(Phi) = 2 * RAN - 1$$

$$\Rightarrow \sin(Phi) = \sqrt{1 - \cos(Phi) * \cos(Phi)}$$

The position of the point in cartesian co-ordinates (X,Y,Z) was again generated by the polar to cartesian equations given in 3.3.1. On

evaluation of this method for a uniform distribution of random numbers, it also produced a bias. However, the only distribution affected by the bias was that of the radius R, as shown in Figure 3.3. But there was no bias in the distribution of the angles.

When random variables are combined together by arithmetic operations other than just addition and subtraction, the distribution of the result is usually different from the distributions of the operands. For example, if both operands have a uniform distribution, the result of multiplying them will produce a non-uniform distribution. Thus a bias is introduced.

3.3.3 Method 3 - Cube and Discard

The third method tried was by using the method described in 3.2, to generate a point within a cube. The length of the edge of the cube was set at two times the radius of the sphere to be generated, and was positioned such that the centres of the sphere and the cube were positioned at the same point in space. The co-ordinates of the point generated within the cube were checked to determine whether they lie within the boundaries of the sphere, by applying the following rule.

If (R^2 < X^2 + Y^2 + Z^2) accept gamma ray, otherwise reject

(^ is used in programming to denote 'to the power of').

As gamma rays could be rejected, this introduced the need for more processing per unit volume of a sphere, than that of a cuboid. The theoretical extra amount of processing time involved is now evaluated:

$$\text{Extra Time} = \frac{\text{Cube Volume - Sphere Volume}}{\text{Cube Volume (equivalent to sphere)}}$$

$$= \frac{(2 * R)^3 - (4 * PI * R^3) / 3}{(4 * PI * R^3) / 3}$$

$$= \frac{R^3 * (8 - (4 * PI) / 3)}{R^3 * (4 * PI) / 3}$$

Extra Time = 0.9099

As can be seen 90.99 % more time was needed to generate a sphere of equivalent volume to that of the cuboid. An experiment to demonstrate this effect was devised using the program. The following two sets of data were implemented and the times taken for the production of each of the phantoms were noted. (For computer details see Appendix D).

Consider:

```
NUMBER OF SAMPLES.... 100000
RANDOM SEED....          1
ROUNDING FACTOR....      1
SIZE OF DETECTORS ARE      1000.0  BY       4000.0
% SIMULTANEOUS EMISSIONS...             0.00%
DETECTION BOUNDARY OF DETECTOR IS       0.0 IN FROM THE EDGE
LIMITING ANGLE OF DETECTION...        0.00 DEGREES
NUMBER OF PHANTOMS...    1
PHANTOM  1
OBJECT:  CUBOID
TYPE:  SOLID
WEIGHTING FACTOR...  1.000
XMIN...            950.0       XMAX...          1050.0
YMIN...           1950.0       YMAX...          2050.0
ZMIN...            500.0       ZMAX...           600.0
TOTAL CPU USED TO CREATE THIS PHANTOM WAS  187.1 SECONDS
```

and

```
NUMBER OF SAMPLES....   100000
RANDOM SEED....           1
ROUNDING FACTOR....       1
SIZE OF DETECTORS ARE      1000.0  BY       4000.0
% SIMULTANEOUS EMISSIONS...             0.00%
DETECTION BOUNDARY OF DETECTOR IS       0.0 IN FROM THE EDGE
LIMITING ANGLE OF DETECTION...        0.00 DEGREES
NUMBER OF PHANTOMS...    1
PHANTOM  1
OBJECT:  SPHERE
TYPE:  SOLID
WEIGHTING FACTOR...  1.000
```

```
CO-ORDINATES OF CENTRE ARE    1000.0      2000.0      550.0
RADIUS...      62.0
TOTAL CPU USED TO CREATE THIS PHANTOM WAS  216.2 SECONDS
```

The percentage difference between the two run times is now calculated:

$$\Rightarrow \quad \% \text{ DIFFERENCE} = \frac{(216.2 - 187.1)}{187.1} * 100$$

$$= 15.5\%$$

As can be seen, the difference between the two values was nowhere near the 90.99% that was previously calculated. The main reason for the discrepancy, was that the CPU time taken to access the disc was large compared to that of accessing main memory. Therefore, if the data was not being sent to disc, as was the case when it was rejected, the time taken was reduced.

An example of the distribution of the concentration of the radiation in a sphere is shown in Figure 3.4. Where the sphere was hollow, the (X,Y,Z) co-ordinates produced were checked to determine whether they lay within an inner boundary in the sphere. If so they were rejected.

This method of producing data for a spherical phantom, did not produce a bias in any of the three dimensions. The time taken for production of phantoms by this method would not be much longer than the previous methods mentioned. Therefore this was the technique used.

3.4 Generation of the Direction of the Gamma Ray

To produce a unique emission for the pair of gamma rays from having only one point, its direction in three dimensional space was also required. The method used to produce the direction, was by generating a second point in space and evaluating the equation of the straight line

passing through both points. For both cases of the cube (3.2) and the sphere (3.3.3), the second point was produced on the surface of a sphere, centred at the first point. The point was generated, from a mathematical description of the uniform distribution of positions on the surface of the sphere, using the method described in 3.3.2. As the radius was kept constant, no bias was introduced.

These two points constituted a straight line in space. The description of the position of the line in three dimensional space produced by the detector system, was found by solving the equation of this line with the equations of each detector in turn. This position was checked whether it was within the dimension of that particular detector. The detectors were arranged in opposite pairs, which meant that, when one gamma ray of the gamma ray pair was detected, the other gamma ray could only be detected if it passed through the other detector of the detector pair. If it did not, the pair of gamma rays were rejected and no more detectors needed to be checked.

If only one detector was found to have been struck, no unique line could be produced and therefore the pair of gamma rays were rejected. If on the other hand, two detectors have been struck, the position on the appropriate detector was found by the method shown in Appendix A, and along with the corresponding detector numbers were sent to a data file on disc. This was carried out for all the phantoms until the required number of samples have been generated.

3.5 Variation of Density of Phantoms

When phantoms were being produced, if each phantom was given an equal probability of producing gamma rays, small phantoms would finish with having a higher density of radiation, than that of large phantoms. An example showing this phenomena is shown in Figure 3.5. This

discrepancy was overcome by weighting the probability of a gamma ray emanating from a particular phantom in direct proportion to its volume. The same density of radiation was now produced regardless of the size of the phantom, as can be seen in Figure 3.6.

Using different types of radioisotopes, a wide range of densities of sources of radiation could be present within the body. An example of this phenomena, was where an iodine compound would tend to collect in the thyroid gland. A method of simulating these variations in concentration of radiation was needed. A weighting factor was introduced to allow different relative intensities of the phantoms to be set up.

The weighting factor was applied within the computer program, by simply adjusting the effective volume of the phantom. As the number of gamma rays produced by the phantom was in direct proportion to its effective volume, the modification of the size of the volume also affected the number of gamma rays produced.

3.6 Restrictions Placed on the Detectors

The actual detectors suffered from problems associated with the real world. Obviously these problems could be ignored in a theoretical study such as one carried out on a computer, but, if the results from the computer program were to be realistic, the restrictions found on the real detectors must be incorporated into the computer simulation. Some restrictions were implemented to observe the effect they would produce on the final result, and these were described in the following sections. The particular phantom used to demonstrate the effects of these restrictions was a hollow sphere of radii 210 and 180 with a solid sphere of radius 32 in the centre. The picture of the result of no restrictions could be seen in Figure 3.7.

3.6.1 Detector Boundary

As the detectors were basically planes of wires separated by sheets of plastic, a framework was needed for mechanical support. This gave the detector a finite depth, but also produced a section around the edge where there was only framework. The section of framework produced a dead area on the detector where no gamma rays could be detected and was modelled to show the effect it had on the final picture.

It was implemented within the computer program by simply checking whether the position generated on the detector lay outside this boundary, and if it did, the gamma ray was rejected. The effect on the data was to introduce a bias in one of the directions as shown in Figure 3.8.

3.6.2 Acceptance Angle

There may have been a limitation, due to the electronic detection system, on the angle of detection of the gamma rays. Variations of this angle were modelled to observe the effect on the final picture.

The effect of limiting the angle was achieved by using vector operations. Firstly, the normal to the detector was generated by using the cross product on the two edges of the detector. The angle between the normal and the gamma ray was found by applying the dot product and hence the angle between the plane and the gamma ray was found. This angle was checked whether it was less than the angle specified, if so the gamma ray was rejected.

The smaller the acceptance angle, the more gamma rays were rejected and this added to the time taken to produce the phantoms. The increase in time taken could be quite large. However, the reduction of the acceptance angle made the statistics of the detections better [2.4], and this in turn, made the final picture clearer, as could be seen in Figure

3.9.

3.6.3 Finite Number of Detecting Elements

The detector could only have a finite number of detecting wires per centimetre. The density of wires depended on the cost and the complexity of the electronics. There was obviously a need to show, without constructing the actual device, the effect of different numbers of detecting elements. This would show whether it was economically justifiable to have a higher density of detection elements.

The simulation of different numbers of detecting wires was achieved, by applying a grid to the face of the detector. The positions of the gamma rays on the detectors, were rounded to the nearest grid point. The coarser the grid, the more the gamma ray deviated from its true position. Two pictures of the same phantom were shown, Figure 3.10(a) with the grid size of 1 unit and Figure 3.10(b) the grid size of 10 units. As can be seen from Figure 3.10(b), a regular pattern has been superimposed on the picture. The overall effect of reducing the number of detecting elements was to reduce the resolution of the final picture.

3.6.4 Simultaneous Emission

For a sample to be accepted, both gamma rays have to be detected. Once one gamma ray has been detected by a detector, the 'camera' waits for another detection to occur within a set period of time. Any detection within that time, is regarded as the other gamma ray.

As the emission of the gamma rays is a random effect, there was a finite probability that more than one pair of gamma rays would be generated within the time window detecting one pair of gamma rays.

Consider Figure 3.11, the two gamma rays AB and CD, were the result of the positron annihilation at M and N respectively. Suppose the positron annihilation at M occurred first, this meant that the detection at A started the detection process. The camera electronics now waited for the second ray to be detected on the other detector. However, as there was a second positron annihilation at N shortly after the first, the detection at D occured after that of A, but BEFORE B. The camera then took the two detections A and D to be the actual pair of gamma rays that was emitted. Thus the gamma ray that was stored due to this effect, bore no relation to the source of radiation.

All the gamma rays produced in this manner only contributed more noise to the system. The effect of introducing more noise resulted in a lower signal to noise ratio value for the system, and was observed by there being a reduction of the intensity of the final picture, shown in Figure 3.12. However, this effect was reduced due to the detectors only acting in pairs.

The phenomena of simultaneous emission was simulated by generating a new set of data for one of the detectors, the detector number and (X,Y) co-ordinates and substituting that for one of the original positions.

3.7 Conclusion

The generation of simulated phantoms could be achieved and these could be placed anywhere in three dimensional space. The data produced from these simulated phantoms, could be made to contain erroneous information as well as correct signal. The erroneous information produced was to simulate different defects inherent in the design of the camera and also effects due to the nature of the radiation emission.

The whole process of generating these phantoms was dependent on how good the random number generator was. If the number of random numbers available was small, this would interfere with the statistical independence of each sample. The distribution of the random numbers was also important in the generation of the samples. The distribution needed for this application had to be uniform throughout the range 0 to 1. The random number generator used was the one based on the computer used. Each generated gamma ray used four random numbers to describe it fully.

A computer program was written to check the distribution of random numbers, produced by the computer's random number generator, empirically. This was carried out by dividing the number range 0 to 1 into 90000 elements. A large number of random numbers were then generated, and each number was checked to see which element it lay within. Those elements were each incremented by one. This distribution of the random numbers was given by the values of the elements, after all the random numbers were checked. The distribution obtained when this was done, was a fair approximation to a uniform distribution.

Any simulation of the body using these simulated phantoms, could only be an approximation due to the particular simulated phantoms available having regular shapes. These phantoms were not meant to be used to give an accurate representation of a body, but were only used for extensive checking of the process of reconstruction, considered in this work.

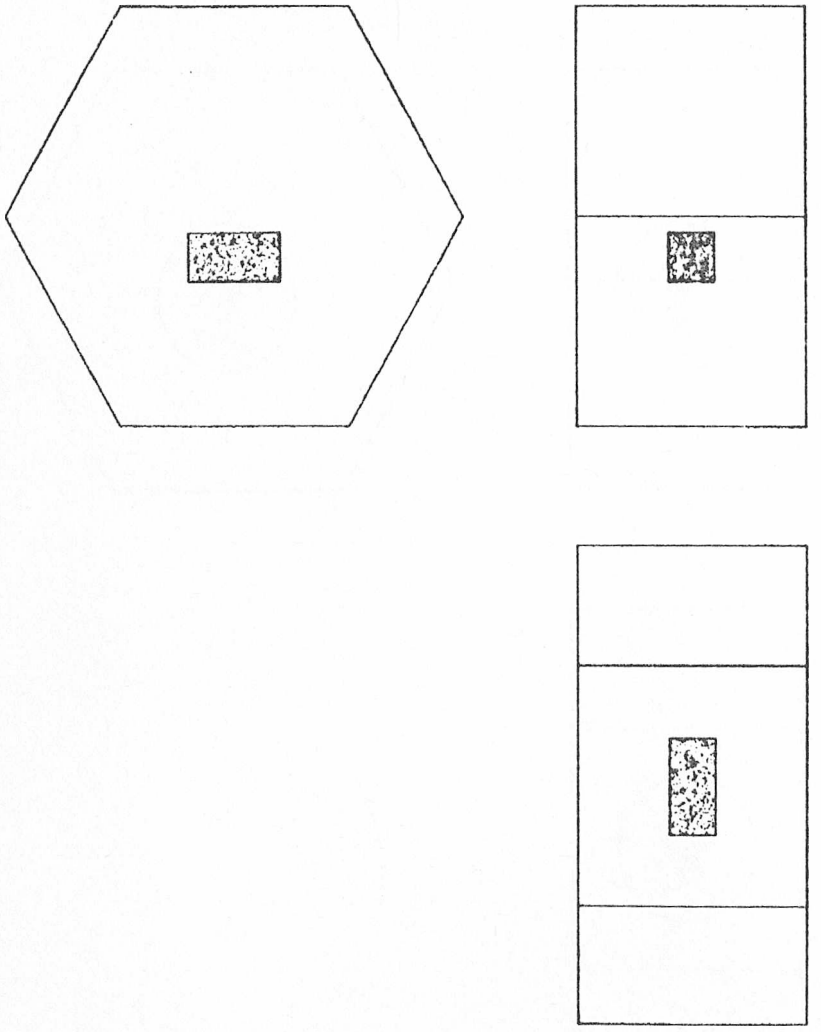

Figure 3·1 Distribution of randomly generated points within a cuboid.

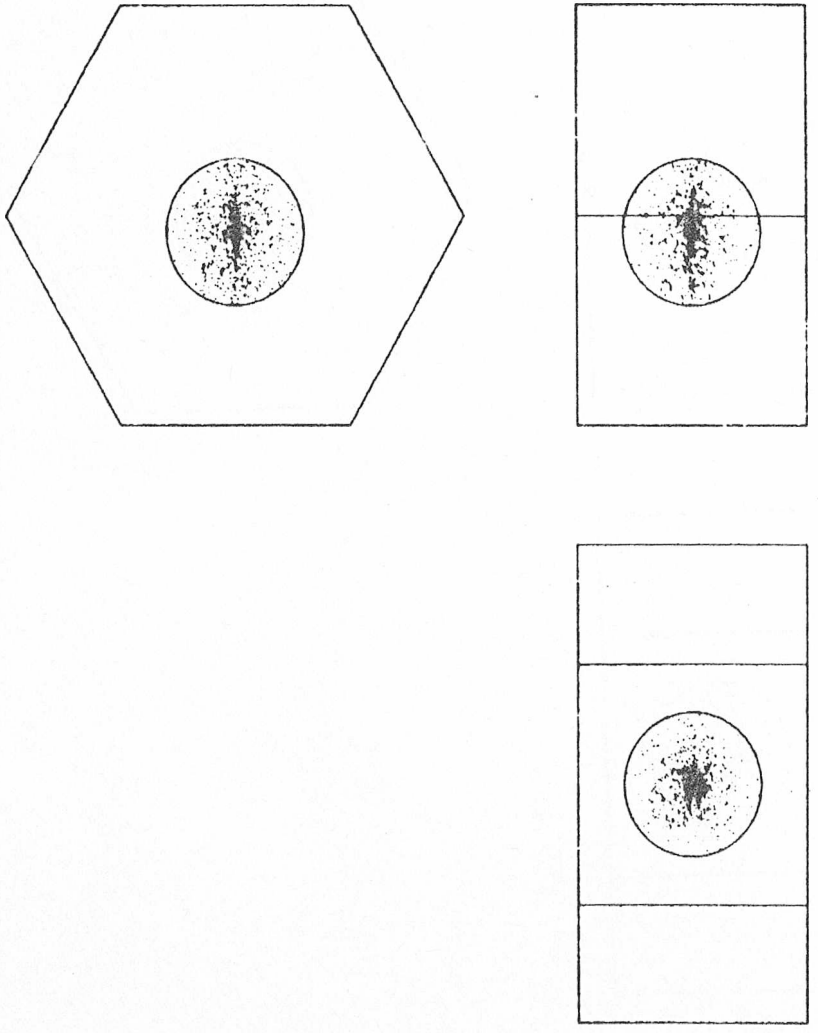

Figure 3·2 Bias in X and Z directions.

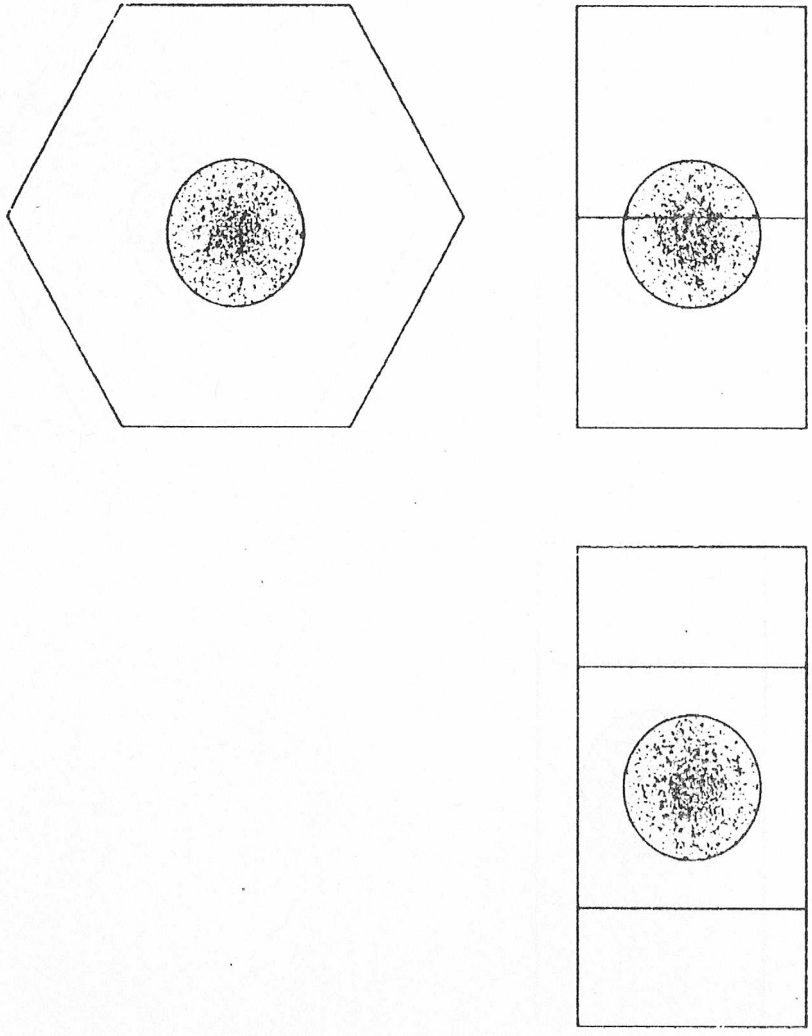

Figure 3.3 Bias on radius.

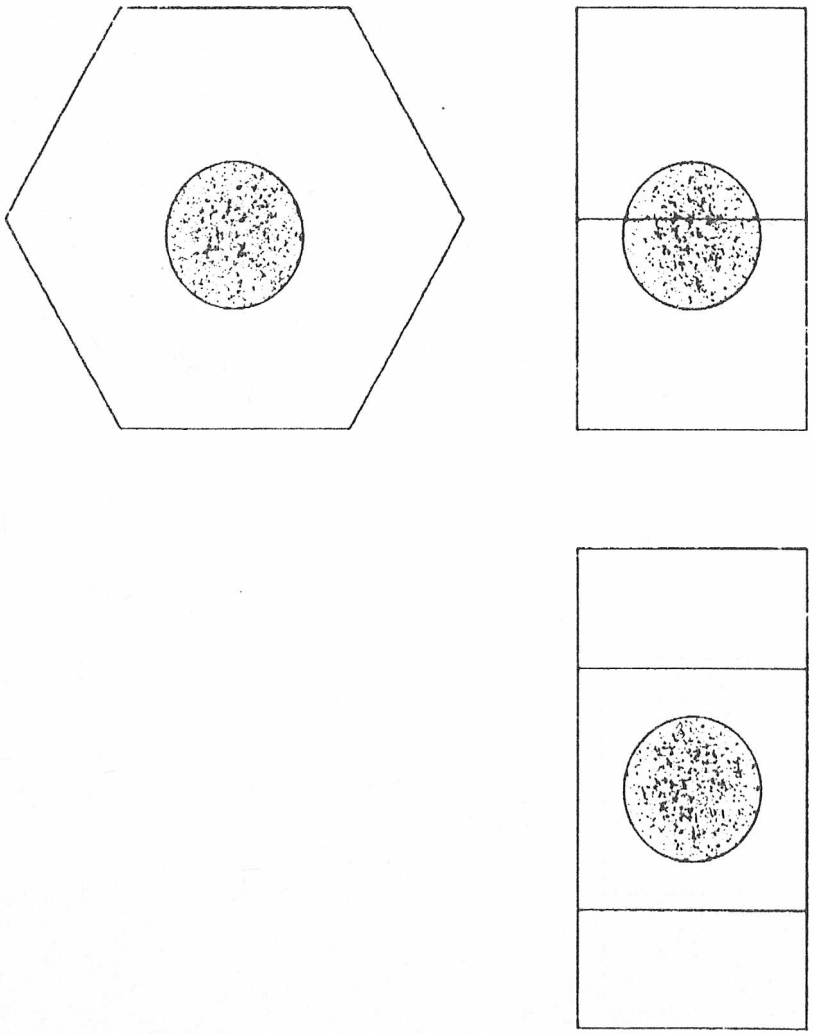

Figure 3.4 Distribution of randomly generated points within a sphere.

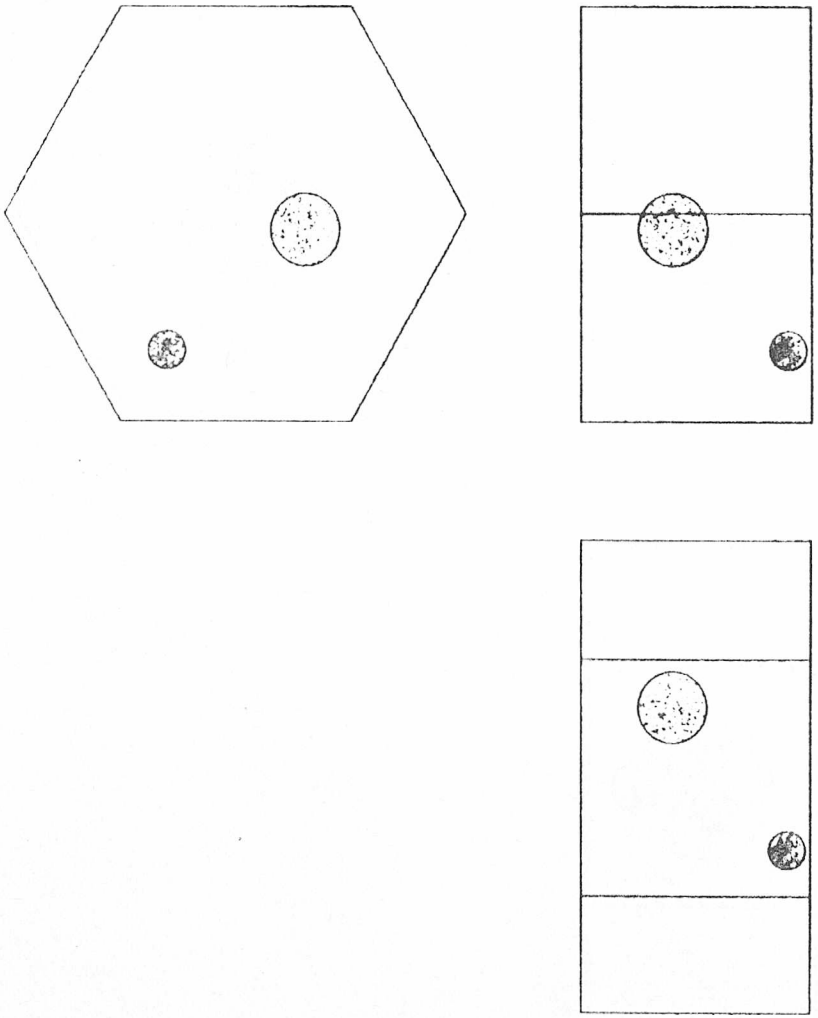

Figure 3.5 Example of density being dependent on the size of the phantom

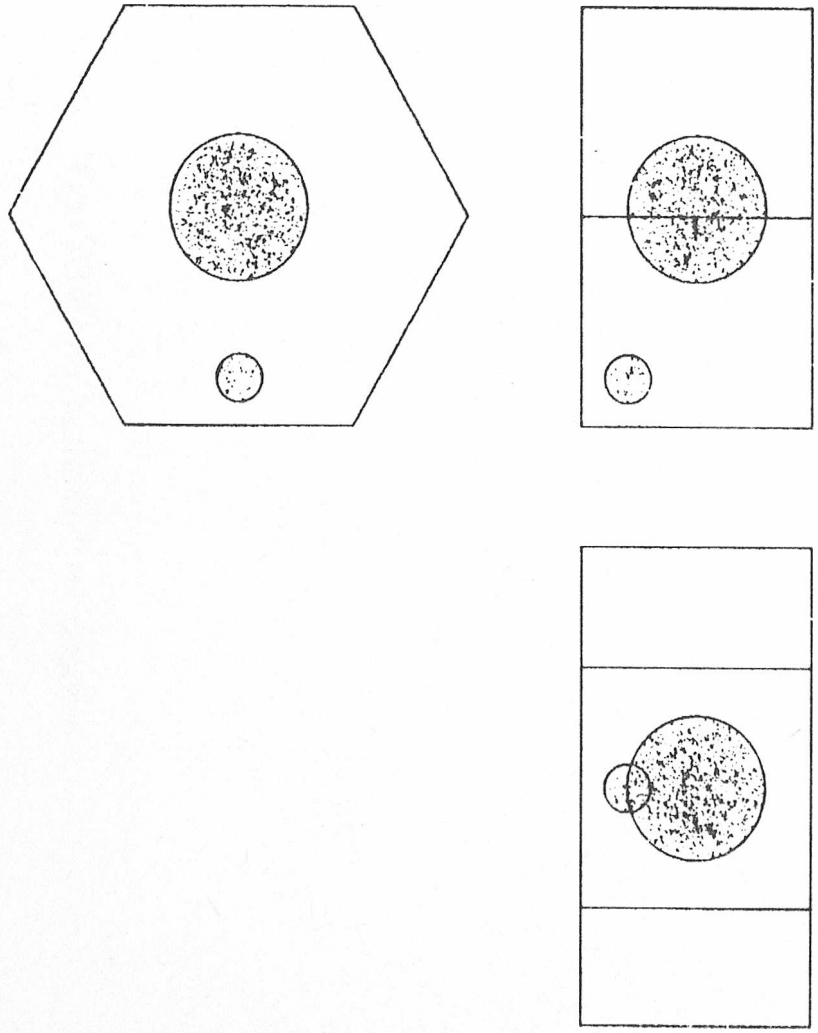

Figure 3.6 Example of density independent on the size of the phantom.

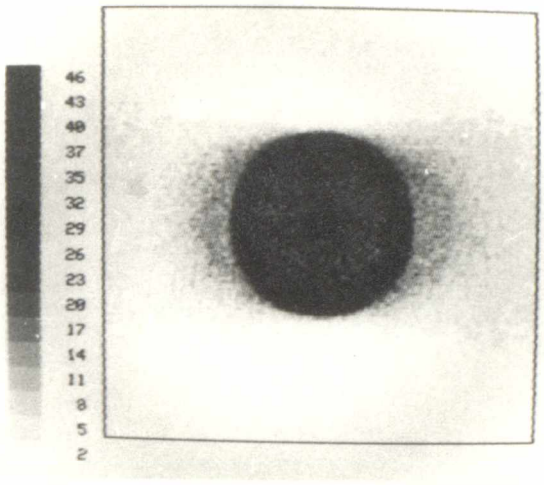

Figure 3.7 No restrictions on detectors

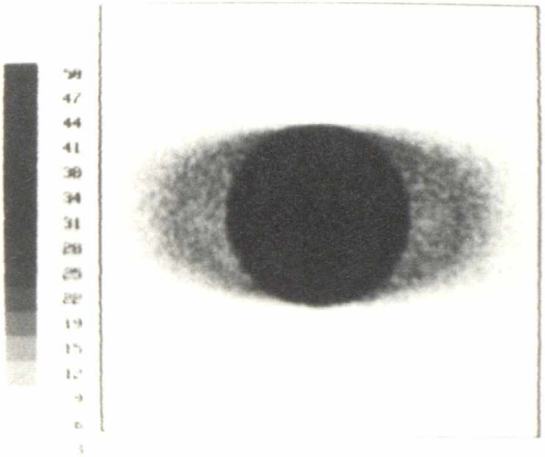

Figure 3.8 Non-detecting boundary set on detector

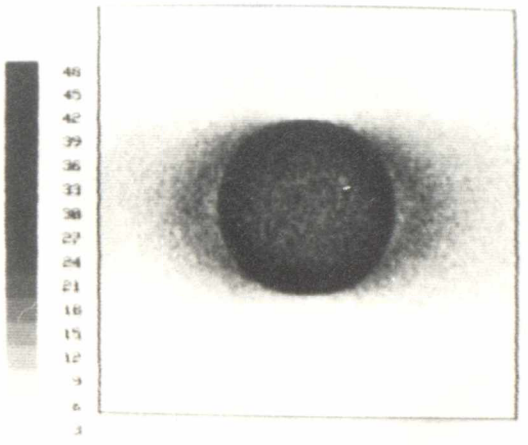

Figure 3.9 Limitation on angular acceptance of detector

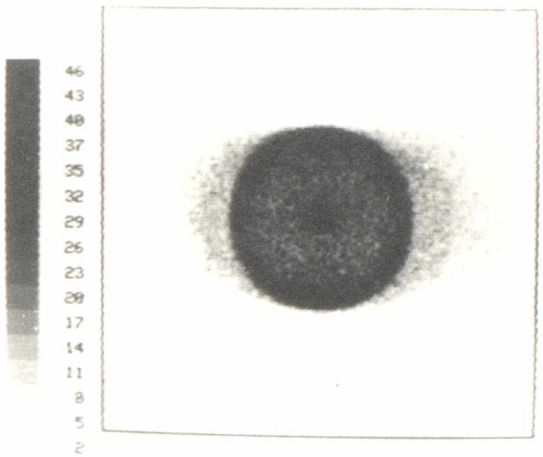

(a) Grid size = 1

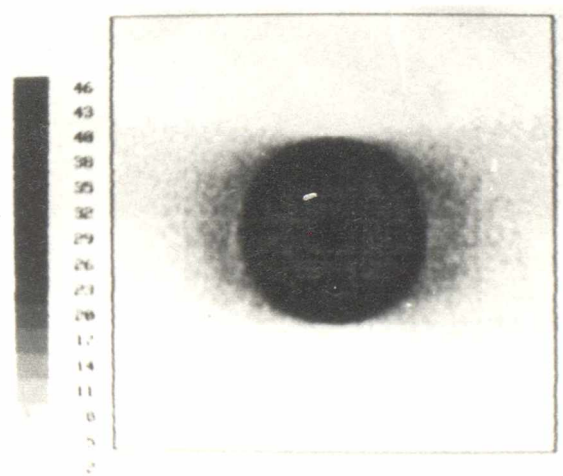

(b) Grid size = 10

Figure 3.10 Limitation on number of detecting elements within each detector

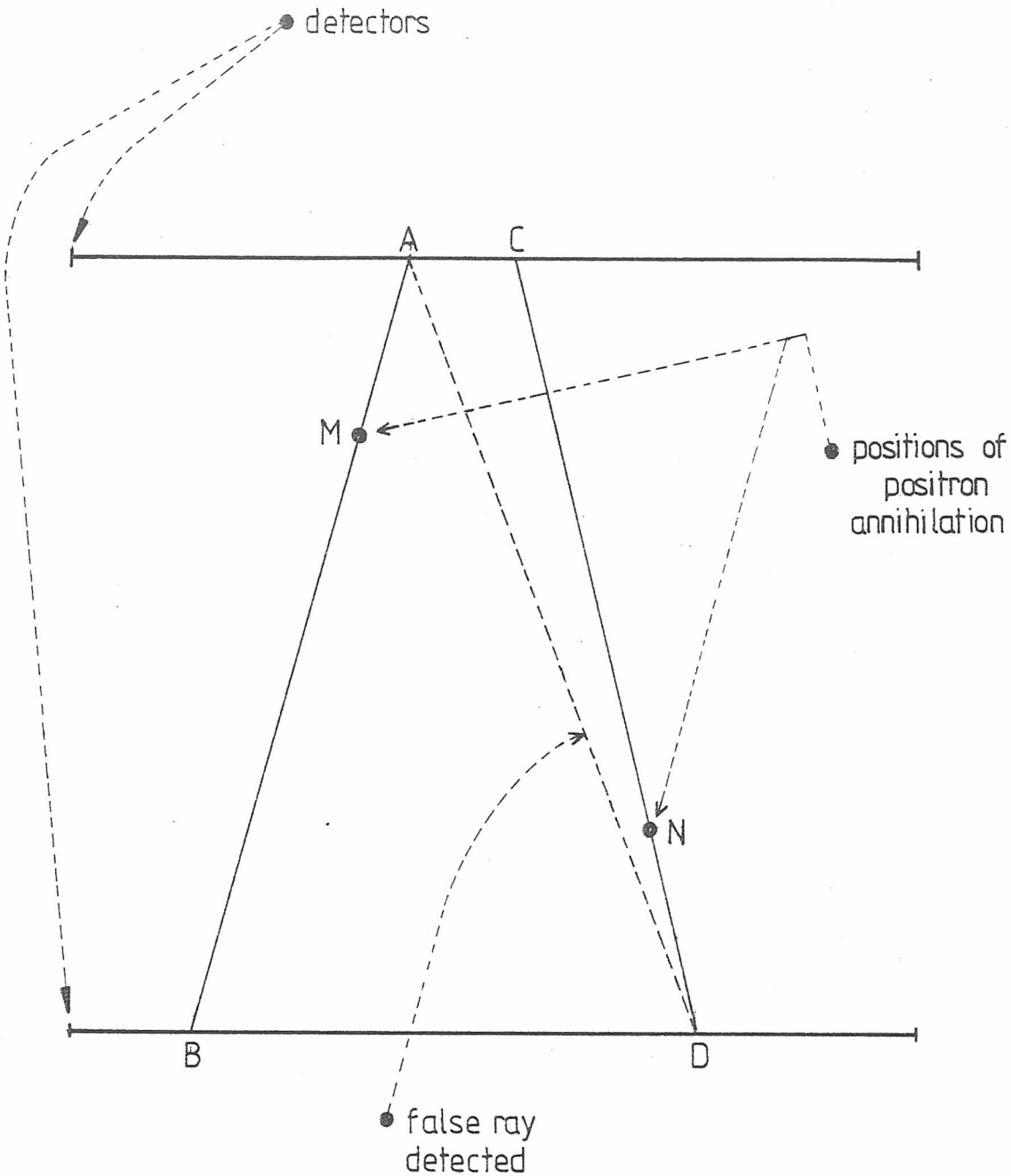

Figure 3.11 Simultaneous emission

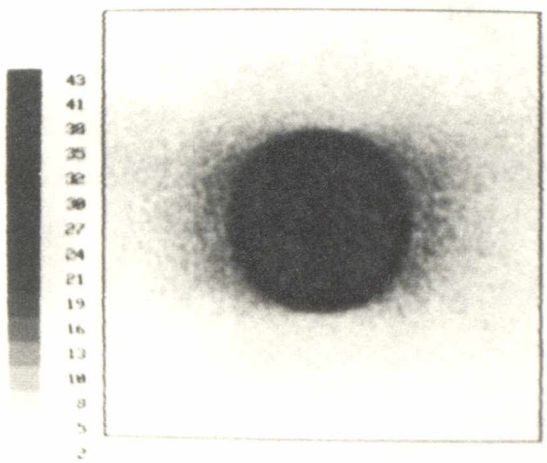

Figure 3.12 An example of 50% simultaneous emission

CHAPTER FOUR

DESCRIPTION OF THE NEW PROCESSES

A picture of a section through the body, was generated using the information produced by the Bateman camera. This was achieved by selecting the particular section to be viewed, and noting the position where each of the rays passed through it. These were then displayed by placing a dot on a screen at each of these positions. Figure 4.1 shows an example of this. The picture produced however, suffered from interference from signal emitted from sources of radiation, that were valid, but did not lie in that plane. Consider Figure 4.2, the source of radiation at A is in the plane of interest P, and should be shown on the final picture. The source of radiation at B, on the other hand, is also a valid source contributing radiation to the plane P, but should not appear on the final picture.

As can be seen, there was a need for processing the information received from the detector system. However, to enable the picture produced to be processed the area to be viewed had to be divided up into regular sections, which were squares. The number of rays passing through each square was 'counted', and the value was associated with that particular square. When all the rays have been processed, the picture information is contained in the array of squares. As the picture was now represented by an array of numbers, it could be manipulated using precise mathematics, rather than by a subjective technique.

A radically new method of processing the information will be described in this chapter. The modifications that are necessary to the basic concept, to improve the quality of the reproduction, will also be outlined and demonstrated.

The different methods of handling the information that were tried, were the following:

1. 'unprocessed'
2. 'three faced cube' method
3. 'six faced cube' method
4. 'three faced cube with raised base' method
5. 'three faced cube with all faces shifted' method
6. corrective technique using the above types
7. modification of the minimum

These processes are described in detail in the following sections.

4.1 'Unprocessed' Picture Generation

The information about the trajectories of the gamma rays was obtained from the Bateman camera in the form:

Pa Xa Ya Pb Xb Yb

where Pa and Pb indicated the particular detectors that were struck and the co-ordinates on the detectors were given by (Xa,Ya) and (Xb,Yb) respectively. These two positions were converted to their (X,Y,Z) coordinates which were with reference to an absolute origin positioned as shown in Figure 4.3. Note that these were two distinct co-ordinate systems that were being used.

The two points (Xa,Ya) and (Xb,Yb) lay on the line in space along which the pair of gamma rays passed. The equations describing the position of where this line was in space, were generated from these two positions using the equations in Appendix A.

Consider a surface parallel to the X-Y plane and adjustable in the Z direction, with detector 1 being the zero position. The position where the pair of gamma rays passed through this surface, was found by solving simultaneously the equation of the line with that of the surface. As the area to be displayed was a defined section of this surface, the (X,Y) position was checked to determine whether it lay within this area. A picture was formed by simply producing a dot on the screen at the position the ray passed through the surface, as shown in Figure 4.1. This picture however, had added signal from other layers of the body degrading the image.

To enable the added signal to be removed, the picture had to be quantised into defined areas, which were squares. Each gamma ray passing through the area was associated with one of these squares. The particular square was found and the value of the number of gamma rays passing through that square was incremented by one. This procedure continued until all the gamma rays that were detected have been processed. The final picture produced was that generated by using the values contained in the array of squares. The flowchart of the algorithm used in the computer program to carry out this procedure, is shown in Figure 4.4.

4.2 New Process

Previous methods of processing the data produced by an emission type scanner, concentrated on mathematically manipulating the final picture array, with either matrix or Fourier filtering techniques. Examples of these are described in Chapter 7. However, the strategy inherent in all the methods of processing described in this chapter, aimed to use more of the three dimensional information detected by the gamma 'camera'. This involved applying a process directly to the radiation paths before they were used to generate the picture array. To demonstrate the concept, and to simplify the explanation, the basic process will be described in two dimensional space.

Consider a flat array of squares, as shown in Figure 4.5, lying in the area of interest between the detectors of the gamma 'camera'. Each of these squares has two orthogonal edges which can 'count' gamma rays passing through them. Consider a source of gamma radiation at S, emitting radiation equally in all directions. The radiation being emitted by S will affect all the 'counting' edges of the squares in the array.

Two particular squares, 4 and 5, are now highlighted to show the effect the process has on squares which do, and do not, contain sources of radiation. In square 5 the 'counting' edges A and B will receive equal amounts of radiation, which means that the number of gamma rays 'counted' by these edges, will be approximately the same. This can be shown by both angles a and b being equal. Square 4, on the other hand, will have less radiation passing through edge D than C, shown by the smaller angle d compared to c. Therefore, the amount of gamma rays 'counted' by these two edges will be different.

The two 'counted' values associated with each square, can now be

used to try and improve the final picture, compared to that produced by the 'unprocessed' method described in 4.1. This is done by setting the value, of the number of rays passing through each square, to be the lower of the two 'counted' values. When the source is within the square, as in square 5, the minimum value does not deviate much from the 'unprocessed' value, as the two 'counted' values are approximately the same. However, when the source is outside the square, as in square 4, the value will be reduced due to the two 'counted' values being different.

The overall effect of this process, is to leave the value stored in the squares containing sources of radiation, unaffected, while reducing the value stored in those squares which do not.

4.2.1 'Three Faced Cube' method

The basic technique described in 4.2 was applied to three dimensional space, the flat array of squares became a flat array of cubes as only two dimensional pictures were to be produced. The information from the camera was used to produce the equation of the line taken by the pair of gamma rays, as described in 4.1 . In this process, the area of squares on the surface, used for the display, was then

considered as an area of cubes. However, only the three orthogonal faces of each cube, nearest the system origin, were used for the processing. As there was now a Z dimension involved in the processing of the gamma rays, these cubes were positioned on the surface, such that the specified height passed through the centre of the cube.

The positions where the pair of gamma rays cut the top and bottom surfaces of the array of cubes, were found by solving simultaneously the equation of the line with that of the two surfaces in turn. However, the positions found need not lie within the array of cubes as can be seen in Figure 4.6. The ray AB passes through the array of cubes but does not cut the top or bottom surfaces within the array, as in the case of EF. The first position(s) CD within the area, along the line are found and substituted for the actual values AB. The routine written to do this was a basic clipping routine. To find the faces of the CUBES that have been cut by the pair of gamma rays, between these two points, involved searching along the gamma ray and these faces then had their counts, for that face, incremented by one.

Once all the gamma rays have been processed in this manner, the three counts associated with each cube were compared, and the lowest value was placed into the array of squares used for the final display. The flowchart of the algorithm used for the computer program is shown in Figure 4.7.

Demonstration of Method

Consider a point source at the centre of one of the cubes. The probability of hitting any of the three surfaces is equal, since the source is assumed to be isotropic.

e.g. The counts through each face may be as follows:

Face 1	200
Face 2	197
Face 3	204

Now consider a point source above this surface. The face of the cube, which lies parallel to the surface, will have a higher probability of being struck by gamma rays from the point source. The other two faces are practically edge on to the source of radiation, and will have a low probability of being struck.

e.g. The counts through each face may be as follows:

Face 1	160
Face 2	23
Face 3	16

If the data had been displayed, after using the process described in 4.1, the counts through the faces would have been that of Face 1. In the above examples, this would have given the impression that there was a source of radiation in both squares. However, if this new process is used, the minimum face count of each cube, would then have been used for that square. In the first case, the value would be 197 instead of 200, still giving a strong indication that there was a source of radiation there. But for the second case, the value would be 16 instead of 160, indicating that there was very little possibility of any source of radiation being in that square.

4.2.2 'Six Faced Cube' Method

To try and improve on the process described in 4.2.1, the number of faces used to 'count' the gamma rays, was increased to six. This was used to try and utilise those rays that passed through one of the 3-faced cube 'non counting' faces, but did not occur on the opposite 'counting' one. The process used the same overall technique as that described in 4.2.1, except that it used all six faces of the cube. The flowchart of the algorithm used for the computer program is shown in Figure 4.8.

4.2.3 'Three Faced Cube With Raised Base Face' Method

The process described in 4.2.1 had the required surface passing through the centre of the cube. This arrangement was not symmetrical due to the face, parallel to the surface, being lower than the surface. To try and improve upon this arrangement, this face was raised such that it was in the same plane as the surface. The flowchart of the algorithm used for the computer program is shown in Figure 4.9.

4.2.4 'Three Faced Cube With All Faces Shifted' Method

The idea described in 4.2.3 was applied to all three faces to produce a shape as shown in Figure 4.10. The idea was to make the system completely symmetrical. The flowchart of the algorithm used for the computer program is shown in Figure 4.11.

4.3 Corrective Techniques

In each of the processes described, there was an effect which interfered with the general theory of operation. The 'three faced cube' method will be used as an example to highlight this.

Consider a line at 45 degrees to the three faces which passes through the point where these three faces meet. At any position on this line, the solid angle to each of the faces is the same. This means that there is an equal probability of the radiation being 'counted' on each of the faces. Therefore, if a large valued source of radiation is placed on this line, but outside the dimensions of the three faced cube, the result will imply that there is a smaller valued source within the cube. The smaller value of the imaginary source, is due to the solid angle of the actual source to the 'counting' faces, being smaller than if the actual source was inside the cube.

A graph showing the value of the contribution of a point source at each position on this line is shown on Figure 4.12. The values for this curve were calculated using the equation given in C.2. As can been seen from this graph, about 80% of the contribution is from within the cube. For the other processes, there exists similar lines in space where the probability of being 'counted' on the 'counting' faces, is the same. The other processes each have more than one such line.

The next logical step was to remove the 20% contribution from outside the cube. As about 18%, of the 20% outside the cube, was contained within the dimensions of the immediate layers of cubes above and below, only the effect of these needed to be considered. However, as both the upper and lower surfaces have to be processed to provide these values, not only was the contribution from the cubes on the 45 degree line removed but also that of the other surrounding cubes. This removed the need to find all such lines for each type of processing

'cube'.

The problem now arose as to how much of each cube was removed, from the total count of the cube in the centre. The method used to gauge the amount that was contributed from each cube in turn, was calculated using the solid angle of the centre of radiation, of the cube to be removed, to the three surfaces of the cube to be corrected. To evaluate these multipliers, the centre of radiation for each of the 'counting' cubes had to be calculated using the following method. A cube of source had to be represented by a point source at a position within the cube. The position within a cube where a point source could produce the same overall effect had to be found. This position was dependent on the location and the description of the 'counting' cube. The procedure involved, for each position throughout the cube, the calculation of the solid angle to the 'counting' faces. The minimum value of the solid angles obtained was used in the following equation to produce an equivalent position for a point source.

$$X = \frac{\sum mx}{\sum m}$$

x - position within cube
m - minimum solid angle from the three faces

Similarly for Y and Z.

This is similar to finding the centre of gravity of the cube. For the 'three faced cube' method, the centre of gravity was calculated to be at the position (4.677,4.677,4.677), on a cube of side 10 units. Using this position, each cube that surrounded the cube under consideration, had the minimum solid angle to the 'counting' faces evaluated. The minimum solid angle was then divided by the total solid angle of an isotropic emission, 4*PI, to produce the portion of the

total radiation emitted. The value produced was then used as the multiplier.

For the 'three faced cube' method, the positions of each of the surrounding cubes are represented by three dimensional co-ordinates with the position (0,0,0) being the cube to be corrected. The solid angles to the 'counting' faces are given. The minimum value of the three solid angles is also given. These values have been corrected by the division of 4*PI, and are therefore the multipliers.

X	Y	Z	SOL X	SOL Y	SOL Z	SOL (min)
-1	-1	-1	0.013	0.013	0.013	0.013
0	-1	-1	0.031	0.031	0.012	0.012
1	-1	-1	0.014	0.014	0.013	0.013
-1	0	-1	0.031	0.012	0.031	0.012
0	0	-1	0.155	0.031	0.031	0.031
1	0	-1	0.037	0.013	0.020	0.013
-1	1	-1	0.014	0.013	0.014	0.013
0	1	-1	0.037	0.020	0.013	0.013
1	1	-1	0.016	0.014	0.014	0.014
-1	-1	0	0.012	0.031	0.031	0.012
0	-1	0	0.031	0.155	0.031	0.031
1	-1	0	0.013	0.037	0.020	0.013
-1	0	0	0.031	0.031	0.155	0.031
1	0	0	0.036	0.036	0.033	0.033
-1	1	0	0.013	0.020	0.037	0.013
0	1	0	0.036	0.033	0.036	0.033
1	1	0	0.015	0.021	0.021	0.015
-1	-1	1	0.013	0.014	0.014	0.013
0	-1	1	0.020	0.037	0.013	0.013
1	-1	1	0.014	0.016	0.014	0.014
-1	0	1	0.020	0.013	0.037	0.013
0	0	1	0.033	0.036	0.036	0.033
1	0	1	0.021	0.015	0.021	0.015
-1	1	1	0.014	0.014	0.016	0.014
0	1	1	0.021	0.021	0.015	0.015
1	1	1	0.015	0.015	0.015	0.015

SOL X - multiplier in x direction
SOL Y - multiplier in y direction
SOL Z - multiplier in z direction
SOL (min) - minimum value of [SOL X, SOL Y, SOL Z]

The centre of radiation was calculated for the 'three faced cube with the shifted base' method, and on a cube of side 10, the position was found to be (5.0,5.0,5.0). For this method the multipliers were:

X	Y	Z	SOL X	SOL Y	SOL Z	SOL (min)
-1	-1	-1	0.016	0.014	0.014	0.014
0	-1	-1	0.029	0.034	0.014	0.014
1	-1	-1	0.016	0.014	0.014	0.014
-1	0	-1	0.029	0.014	0.034	0.014
0	0	-1	0.064	0.034	0.034	0.034
1	0	-1	0.029	0.014	0.020	0.014
-1	1	-1	0.016	0.014	0.014	0.014
0	1	-1	0.029	0.020	0.014	0.014
1	1	-1	0.016	0.014	0.014	0.014
-1	-1	1	0.016	0.014	0.014	0.014
0	-1	1	0.029	0.034	0.014	0.014
1	-1	1	0.016	0.014	0.014	0.014
-1	0	1	0.029	0.014	0.034	0.014
0	0	1	0.064	0.034	0.034	0.034
1	0	1	0.029	0.014	0.020	0.014
-1	1	1	0.016	0.014	0.014	0.014
0	1	1	0.029	0.020	0.014	0.014
1	1	1	0.016	0.014	0.014	0.014

The centre of radiation was calculated for the 'three sided cube with all faces shifted' method, and on a cube of side 10, the position was found to be (5.0,5.0,5.0). For this method the multipliers were:

X	Y	Z	SOL X	SOL Y	SOL Z	SOL (min)
-1	-1	-1	0.016	0.016	0.016	0.016
1	-1	-1	0.016	0.016	0.016	0.016
-1	1	-1	0.016	0.016	0.016	0.016
1	1	-1	0.016	0.016	0.016	0.016
-1	-1	1	0.016	0.016	0.016	0.016
1	-1	1	0.016	0.016	0.016	0.016
-1	1	1	0.016	0.016	0.016	0.016
1	1	1	0.016	0.016	0.016	0.016

The minimum value of each set of multipliers were used to modify the value of radiation 'counts' contained in the surrounding cubes, before being subtracted from the cube under consideration.

4.4 Modification of Minimum

The main criterion involved in the processes described in the preceeding sections, was that of using the minimum of the 'counted' values associated with the faces of the cube. However, more information could still be gained from these 'counted' values. To try and utilise this information, the following equation was applied instead of just using the minimum.

$$Ifin = Imin * \frac{Imin}{Iav}$$

Ifin - final value for the cube
Imin - the minimum of the 'counted' values
Iav - the average of the 'counted' values

The idea behind the equation was as follows. If all the values on the three faces were the same, as in the case when the source of radiation was within the bounds of the cube, the minimum and the average of these values would be approximately the same. This meant that the multiplying factor (Imin/Iav) had the value one. If however, the values were all different, as in the case when the radiation was outside the bounds of the cube, the minimum would be smaller than the average. Therefore the value of the multiplying factor would be less than one. If this technique was applied to the example shown in 4.2.1, the values become 194 and 4. As can be seen the first value did not alter much, whereas the second value reduced even more. In fact, the greater the difference between the three numbers the smaller the multipling factor, and in turn a smaller value for the final answer.

4.5 Conclusion

All the processes described in this chapter have a cube as their basic structure. The original concept of these new methods come from the 'three faced cube' method. To try an improve on this technique, various modifications were applied. These included moving certain 'counting' faces or applying corrective techniques. In this chapter, the need for processing the picture was also described.

The results of applying these processes to the simulated data are shown in Chapter Six. They are also compared to test if one was consistently better than the others.

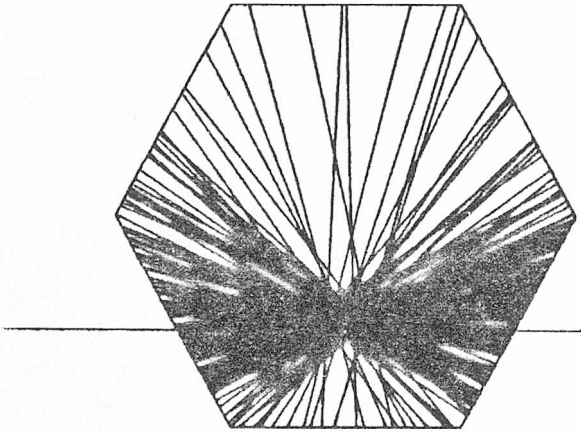

Figure 4.1

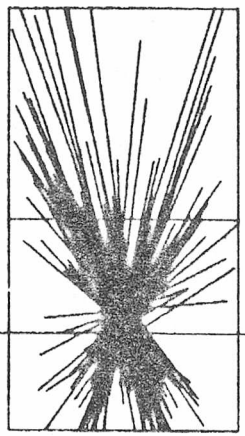

Exact data from camera.

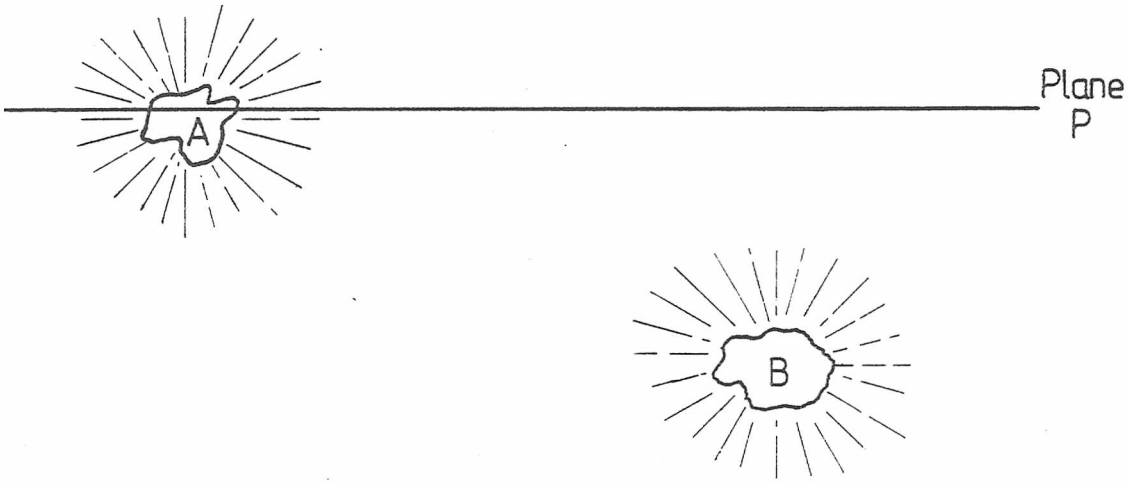

Figure 4.2 Typical arrangement of sources contributing radiation to the viewing plane P

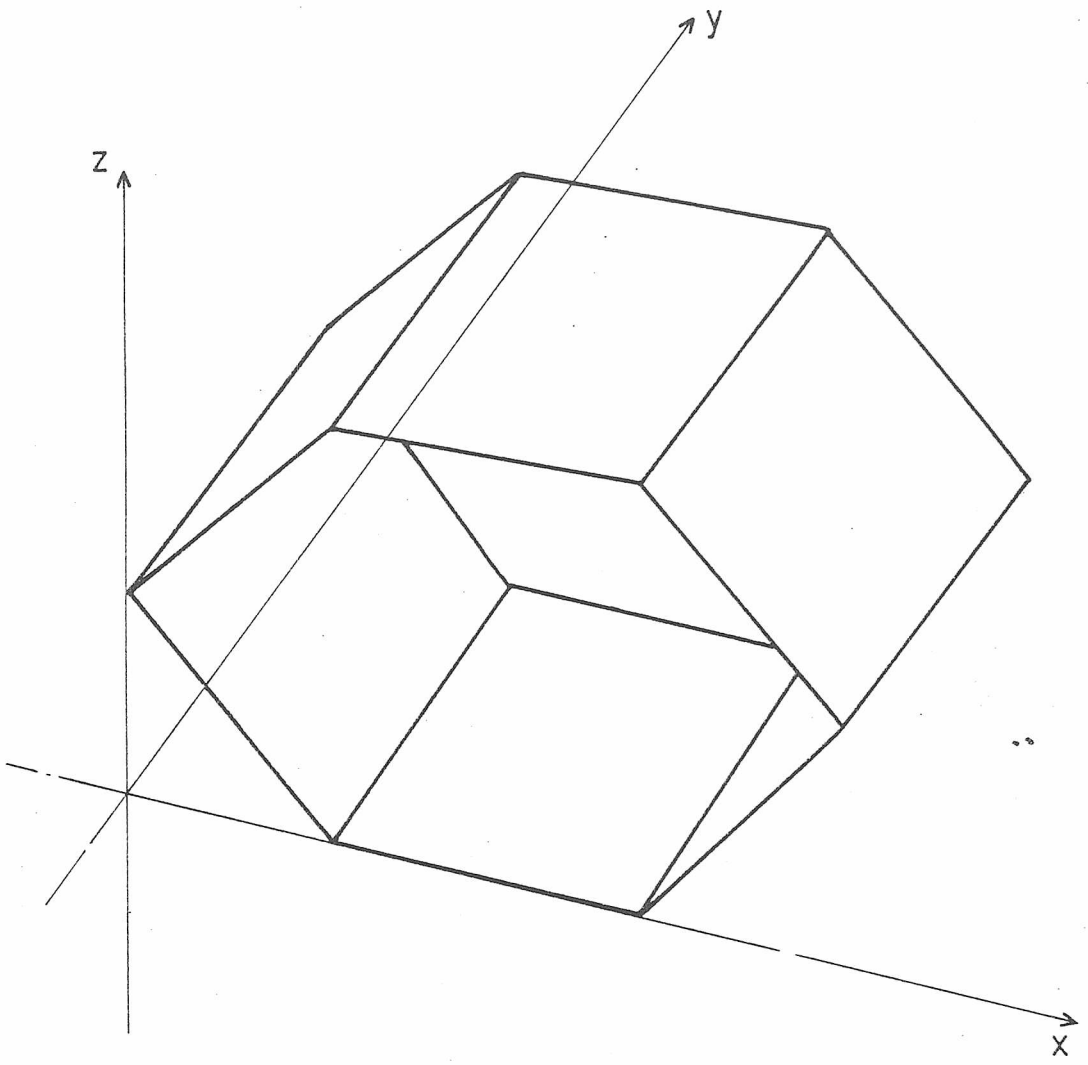

Figure 4.3 Position of the Absolute Origin

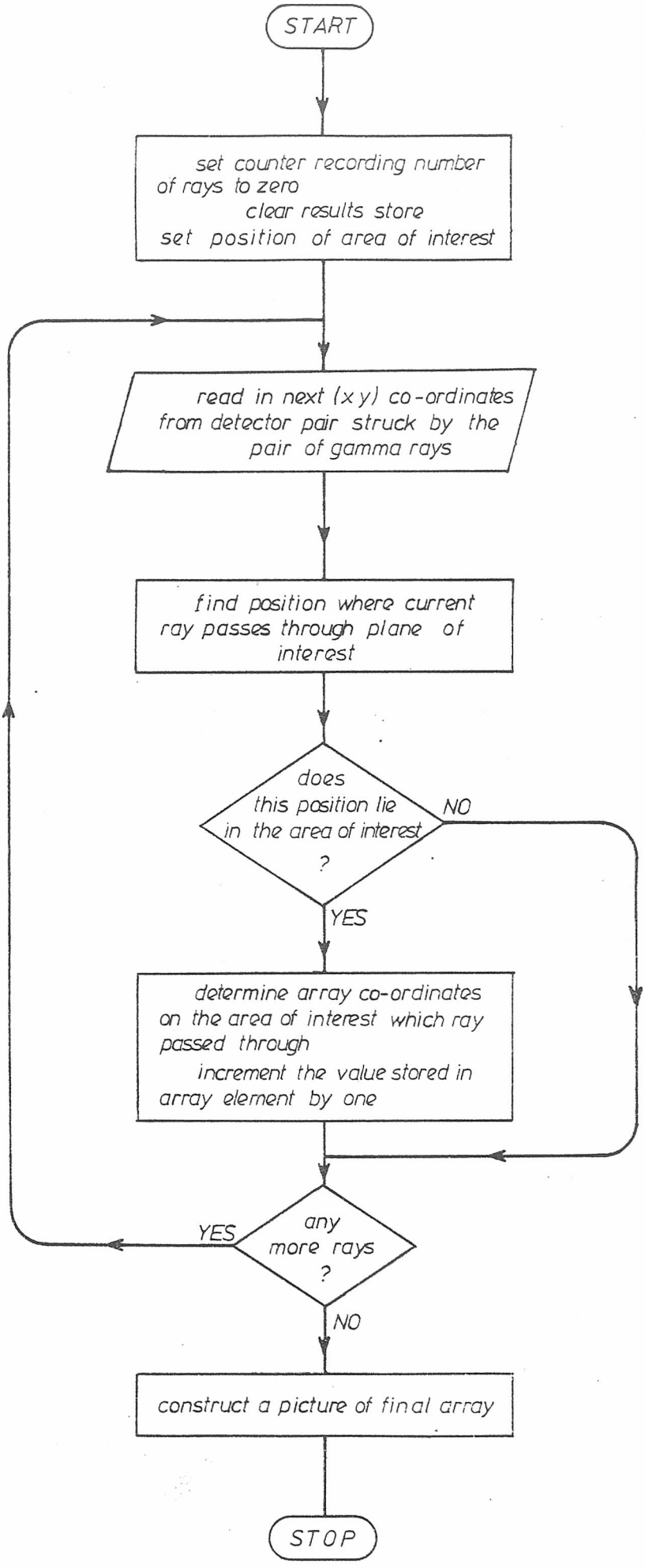

Figure 4.4 Flowchart of unprocessed method

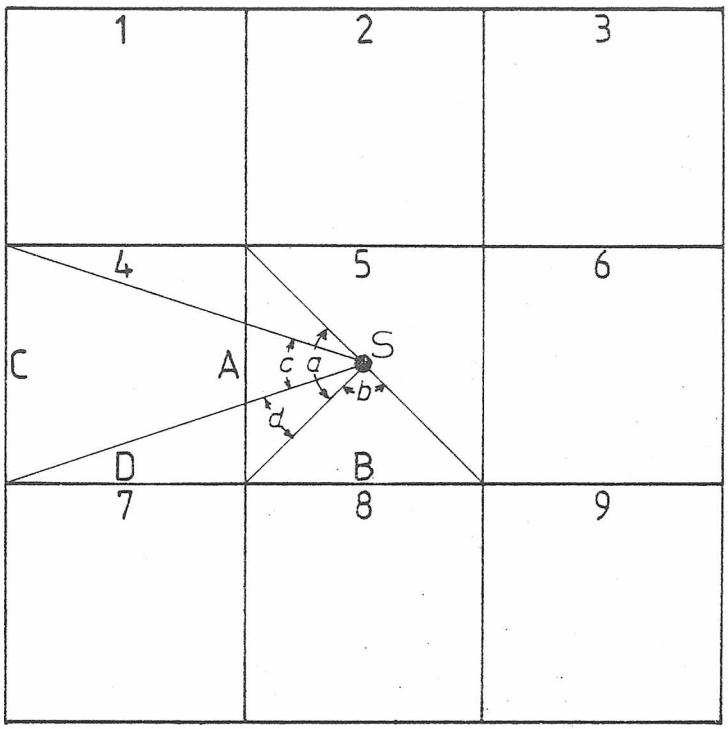

Figure 4.5 Two dimensional "Counting" system

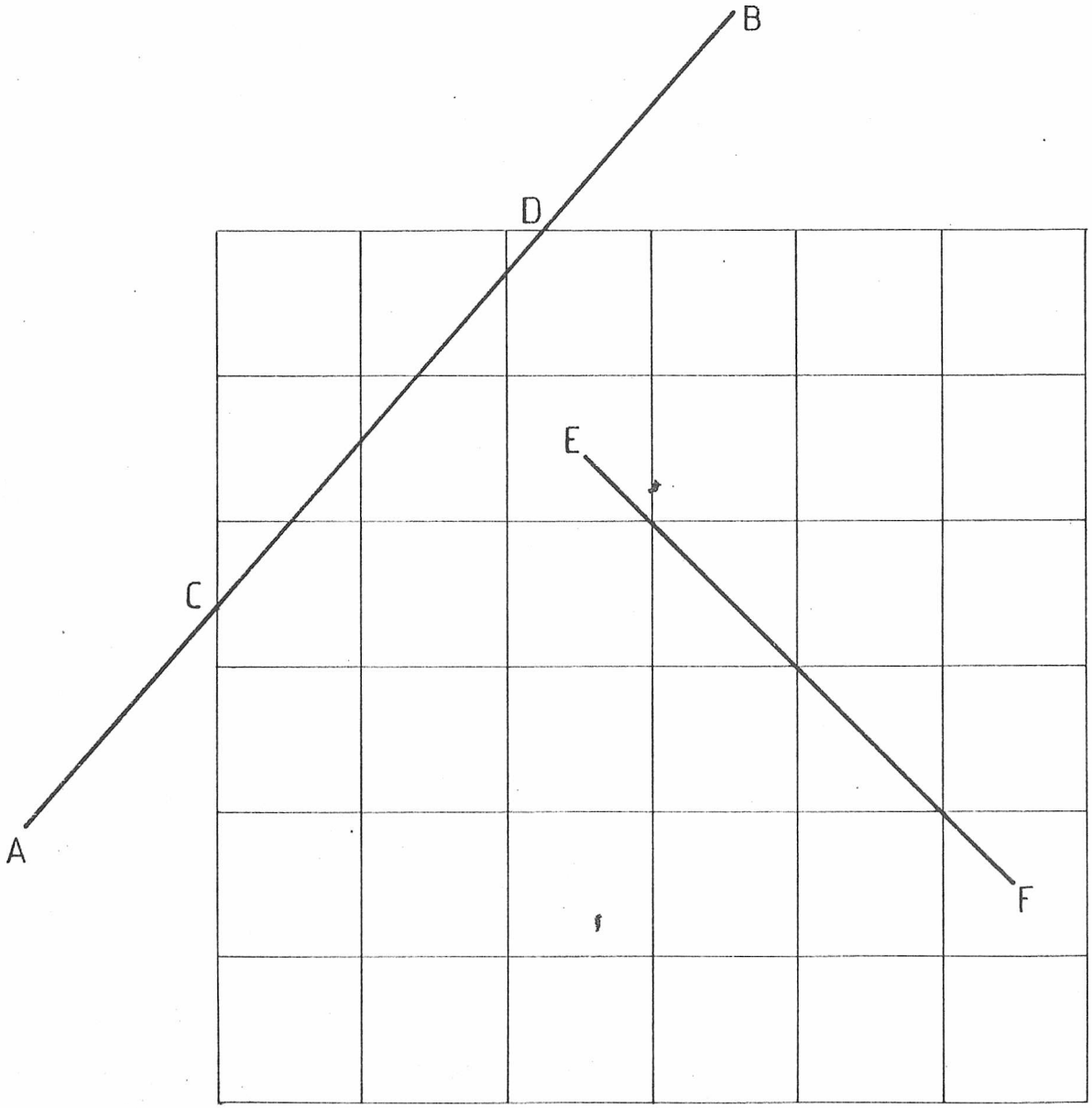

Figure 4.6 A clipping technique

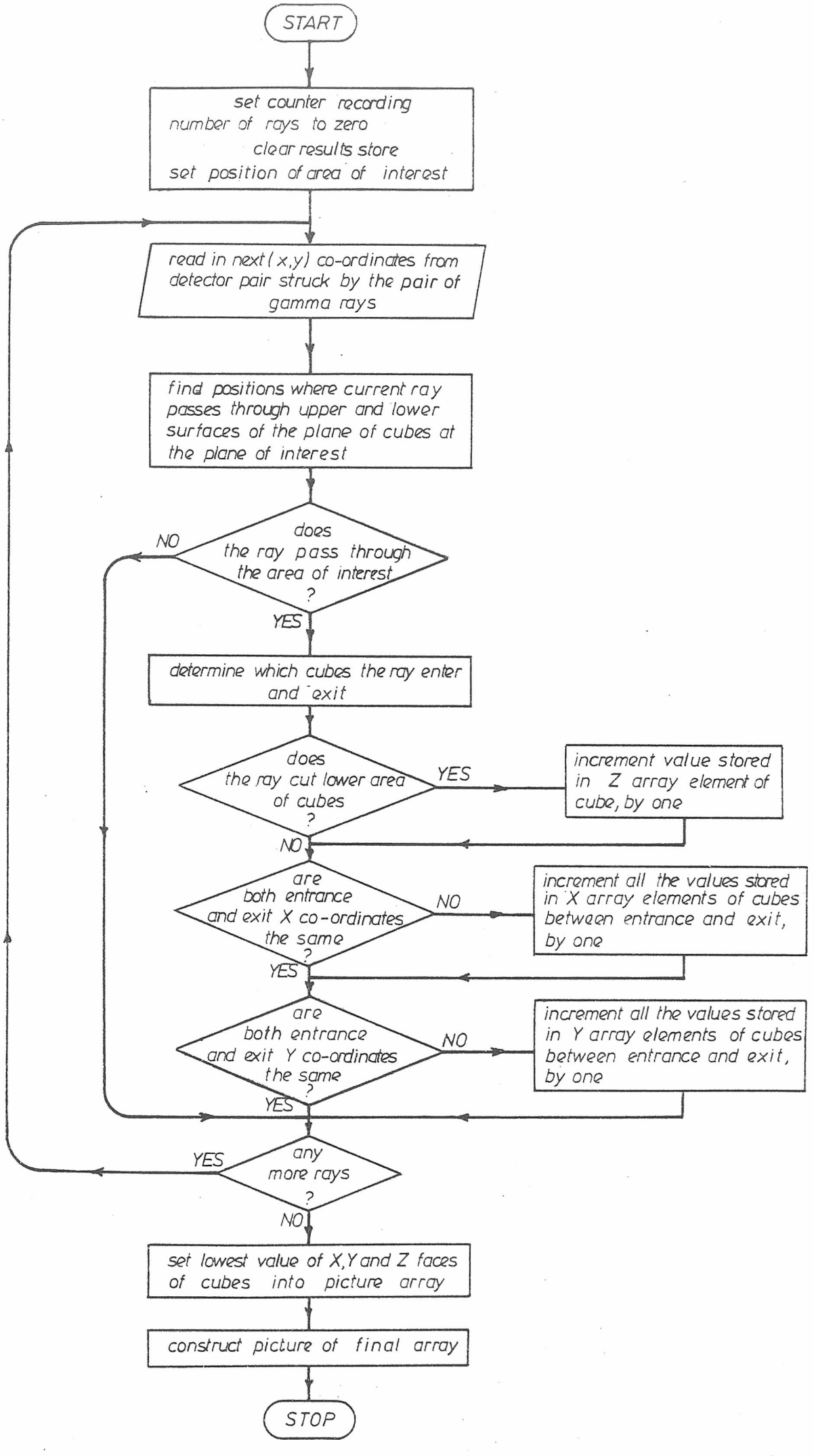

Figure 4-7 Flowchart of "3-faced cube" method

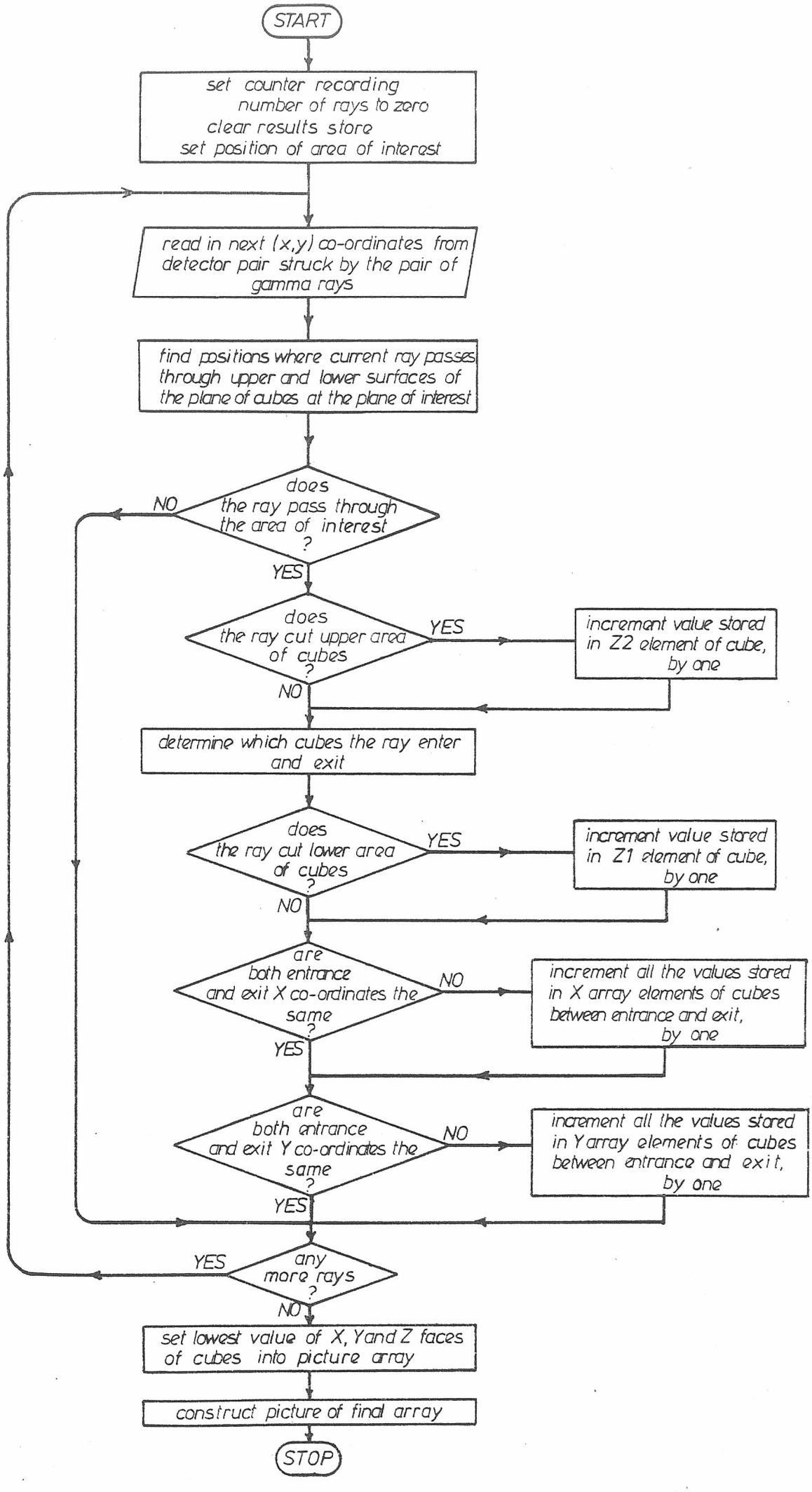

Figure 4.8 Flowchart of "6-faced cube" method

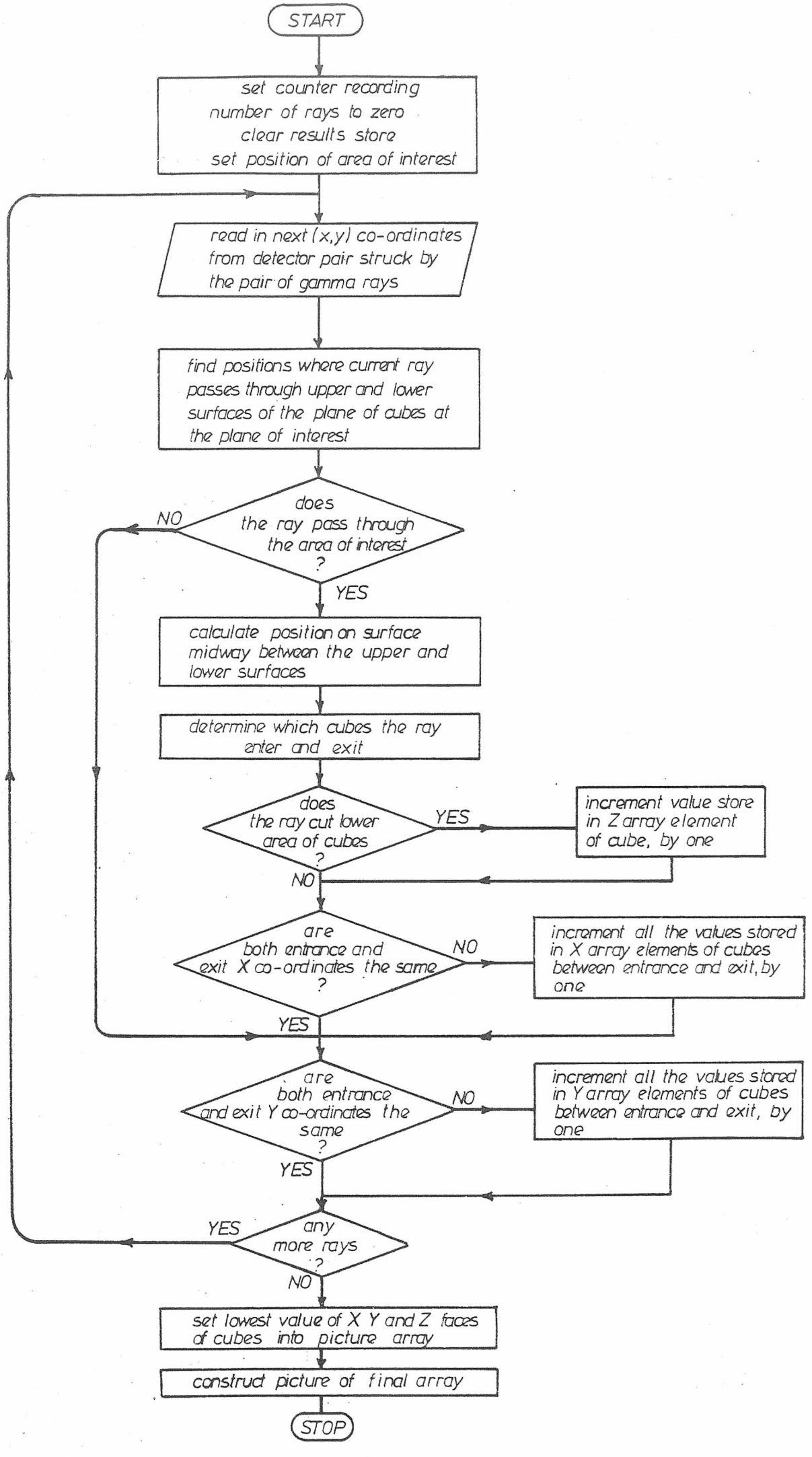

Figure 4.9 Flowchart of "3-faced cube with raised base" method

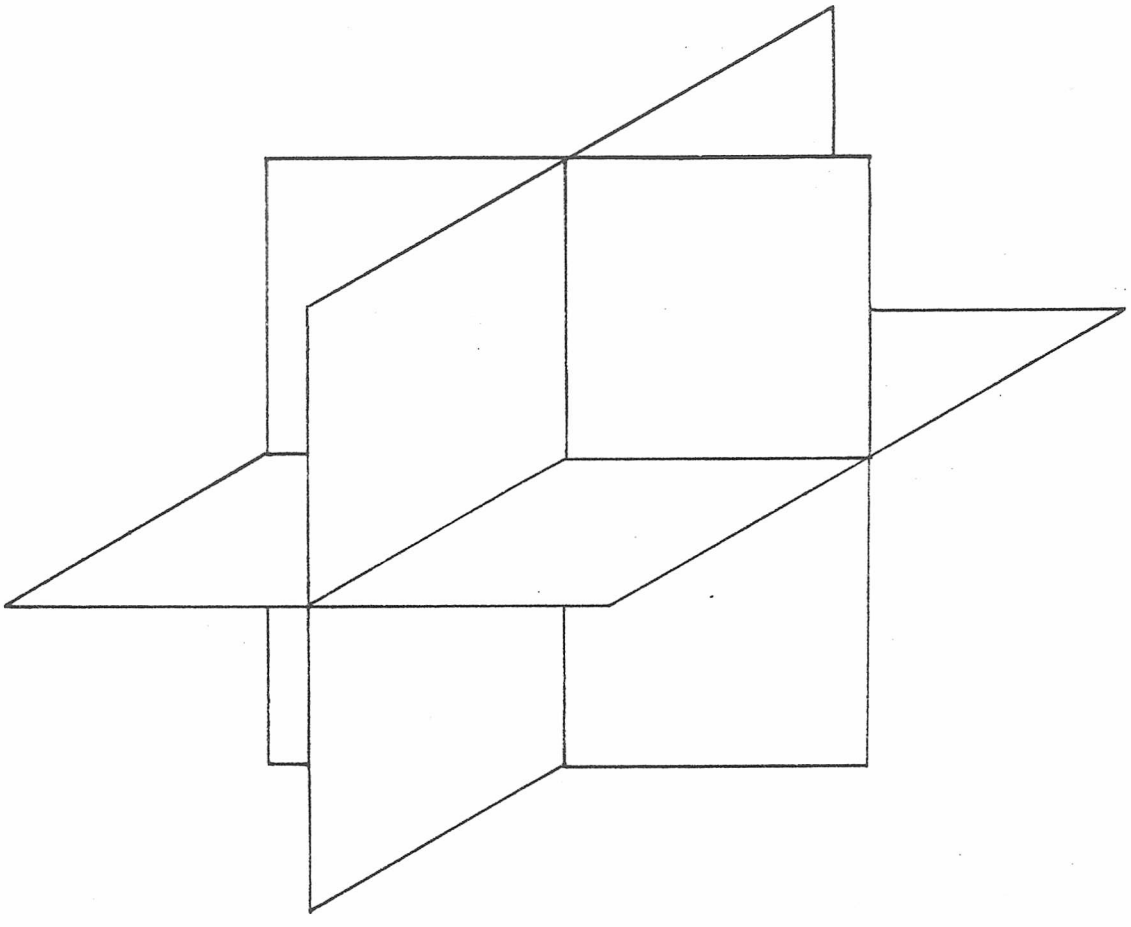

Figure 4.10 Configuration of a "three faced cube with all the faces shifted"

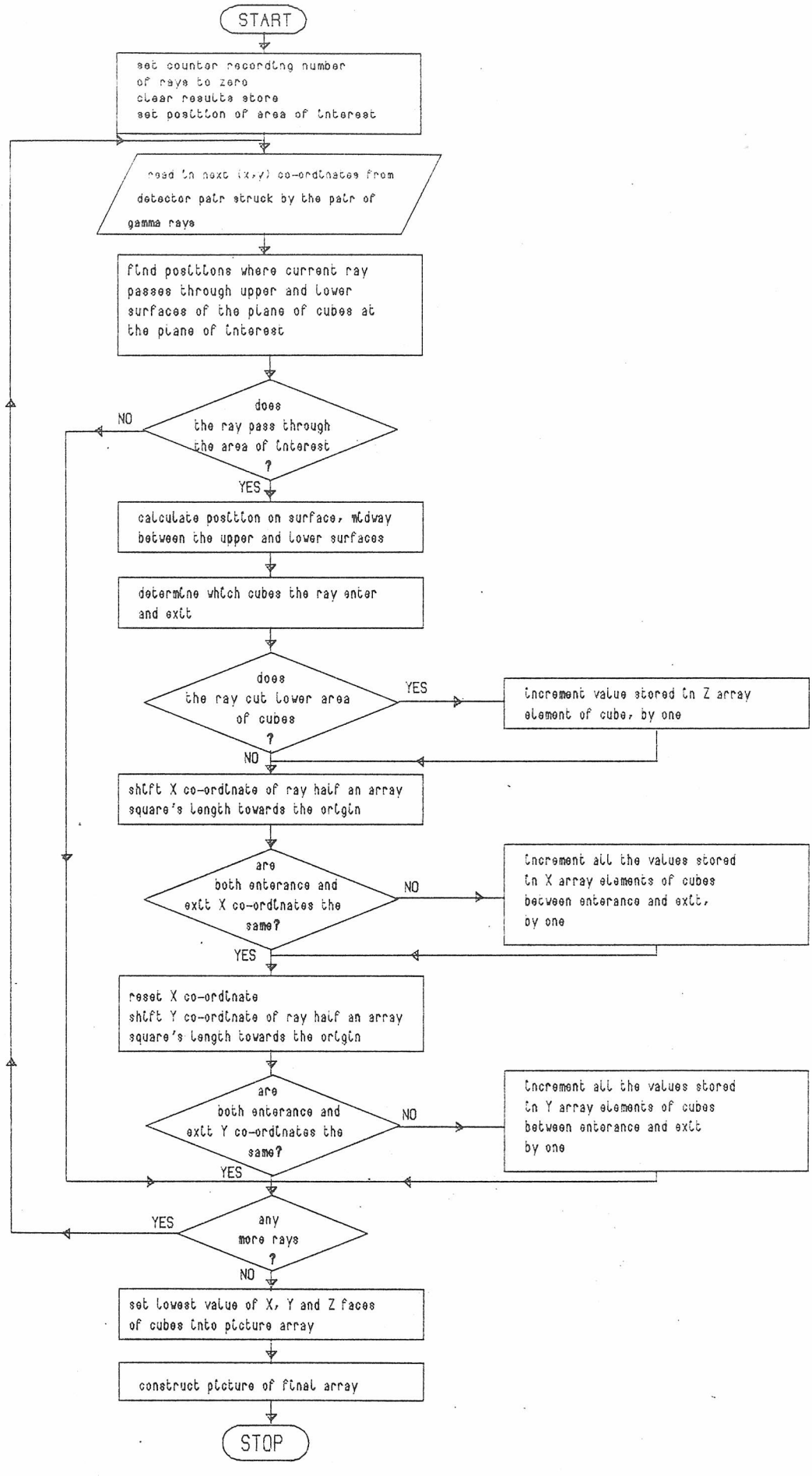

Figure 4.11 Flowchart of '3-faced cube with all faces shifted' method

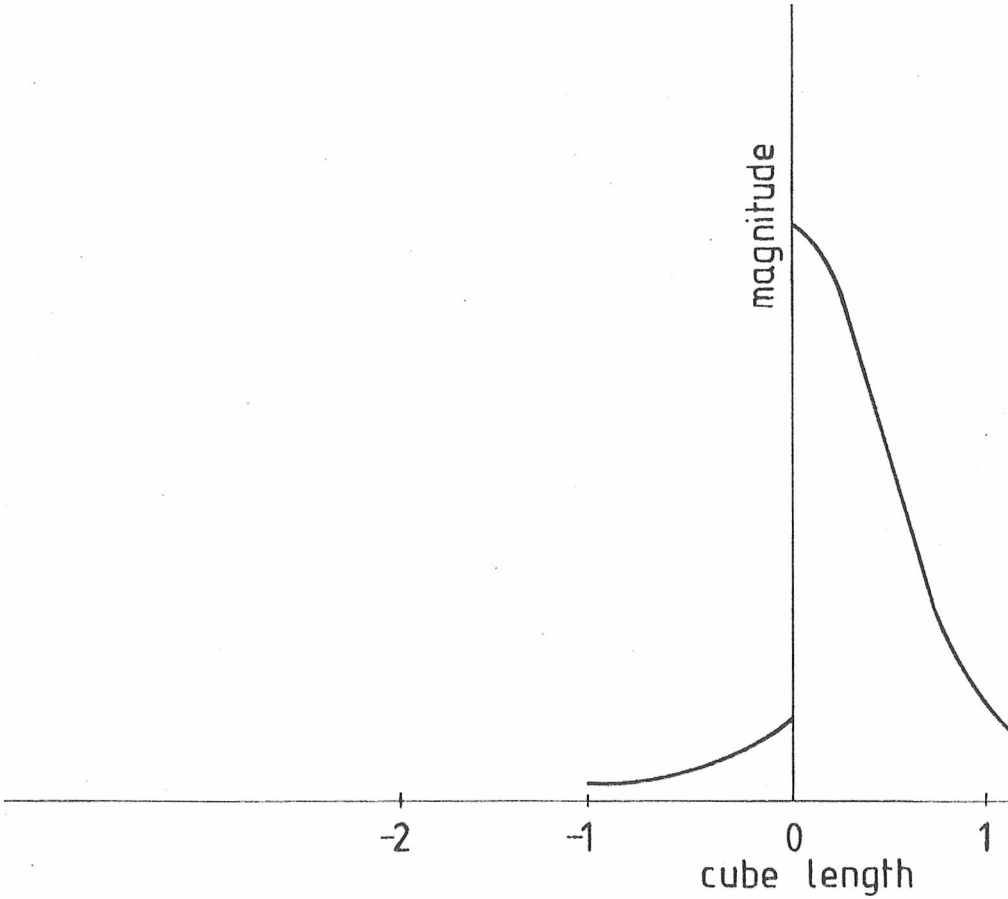

Figure 4.12 Contribution of a point source to "Three faced cube" method

on a 45° line

CHAPTER FIVE

PICTURE GENERATION

The final output produced by the processes described in Chapter Four, is a picture of a particular section through the patient. The drawing of these pictures involved the need for a graphics output device. This chapter describes three such devices.

5.1 Method of Producing a Picture

The information representing the section through the body was stored in a two dimensional array. The numeric values stored in the elements of this array, representing the number of rays and hence the intensity, may vary from zero to several thousand. However the devices that display the final pictures were only capable of a finite number of variations of intensity. Therefore, the whole picture had to be quantised to be within these levels of intensity.

The values contained in the elements in the array, varied according to which section through the patient was being considered. If the section passed through an area of high concentrations of radiation, the variation of the value of each element, was larger than when the section was in an area of low concentrations.

To enable a picture of any level of radiation to be viewed, a software brightness control was introduced. The brightness control adjusted the quantised levels of brightness within the picture, but always left the zero position at zero. Thus the incremental value

between two levels in the scale increased or decreased according to the magnitude of the brightness. An example of two possible brightness values is shown in Figure 5.1. Varying the brightness enables local maxima to be highlighted, as is shown at point Z. Using scale A shows the overall effect, while scale B limits the high values and shows some lower level variation.

As the values in the elements of the array were integer values, the same intensity of radiation could result in a difference of one in adjacent elements. To prevent this difference being magnified, the zero position of the scales was always kept fixed at zero.

It was realised that there are various techniques of scaling which can be used to highlight different features within a picture [5.1]. However, as the aim of this project was to investigate a new process of enhancing the final picture, only one of these was implemented to show the effect. An example of this is shown in Figure 5.2.

5.2 Output Devices Used

Three particular output devices were available to produce the final picture. These were a lineprinter, a Tektronix 4014 and a Sigma colour graphics terminal. To compare these systems, a standard format for the output had to be decided upon. The format chosen, based on the restrictions of all the devices, was a grey scale using sixteen variations of intensity. A description of the three output devices and how they produced the final picture, is given in the following sections.

5.2.1 Lineprinter

A graded scale of shading for the lineprinter was devised, to to produce a gradual transition from light to dark, using the set of characters described in the following section. The main criterion considered in choosing the characters used, was that each shading character had to be symmetrical with a broken outside edge. This enhanced the effect of merging with the background at the edge of a shape, as well as making it appear to "disappear" when out on its own. Characters fulfilling these two criteria were chosen and tested.

The following arrangement was used to produce an order of intensity of the characters considered. A large array of each character was constructed, and illuminated from the back by a uniform density light source. The light source was of the type used for photographic reduction of masks for integrated circuits. The detector used with the light meter was positioned at the centre of the array, to reduce any effect from the edges. The light meter measures the light intensity emitted from the character arrays.

Several different characters were investigated for the production of a grey scale. However, there was only a small number of characters which fulfilled the above criteria, and these produced a similar value of intensity. A greater range of variation of intensity was needed. To achieve an expanded range of intensity, overprinting of characters was introduced. In the following list, where more than one character is specified, they were printed on the same place on the paper to produce one shading character. Using the following list of characters, the corresponding light powers were recorded:

Chars	mW
<SPACE>	4.59
.	4.08
^	4.02
+	3.94
-	3.94
:	3.90
I	3.83
#	3.81
H	3.78
*	3.76
S	3.73
8	3.72
%	3.71
X	3.70
$	3.67
^ V	3.48
\ -	3.48
N /	3.35
I -	3.33
7 4	3.28
N /	3.23
A B	3.19
I =	3.11
H I	3.10
Z =	2.97
< >	2.94
( ) =	2.91
H $:	2.81
X H Z	2.71

From the above list of characters, a scale of sixteen variations of intensity from light to dark can be formed. This scale was not exactly linear but was the best approximation to a straight line from the above list.

Number	Char	mW
0	<SPACE>	4.59
1	.	4.08
2	+	3.94
3	I	3.83
4	*	3.76
5	%	3.71
6	$	3.67
7	\ -	3.48
8	N /	3.35
9	7 4	3.28
10	A B	3.19
11	H I	3.10
12	Z =	2.97
13	) (=	2.91

14	H $:	2.81
15	X H Z	2.71

These characters produced quite a reasonable range of grey scale. The picture shown in Figure 5.3 used this scale.

The two main advantages of this method of picture generation, were that each picture is automatically produced on paper and that most computers have a lineprinter. However, there were also disadvantages to this method of picture generation. The picture produced was not square as the characters used were themselves rectangular, which results in a distorted picture. Also the characters were of a fixed size, and therefore the dimensions of any picture produced could not be altered, except by using a photographic technique. The above list of characters may, however, vary from lineprinter to lineprinter, even within the same model. Thus a new set of character might have to be produced for a different lineprinter.

The picture produced was also dependent on the quality of reproduction of the ribbon used. Slightly different pictures would be produced if the ribbon was new to that when it was old. Therefore, any comparison of pictures produced at different times, has to take this factor into consideration.

5.2.2 Storage C.R.T. Terminal [5.2]

The operation of a storage cathode ray tube (C.R.T.) is similar to that of a normal C.R.T.. The main difference is the storage C.R.T. has an extra layer of special material on the screen, whose molecules can exist in two stable states, light emitting and non-light emitting, when bombarded by low velocity electrons. These low velocity electrons flood the whole screen, and are provided by means of an extra electron gun. The material can also be made to change state by being energised from

the electron beam produced by the normal electron gun. Therefore, the path traced out by the normal electron beam will leave a line of light emitting material on the screen. These lines that are produced, constitute the picture that the user has drawn on the screen. The material on the screen will remain in this light producing condition, until the screen is flooded with a burst of high velocity electrons. Unfortunately, as there is no mechanism available to selectively flood a part of the screen, the whole picture must be redrawn after the screen has been cleared.

The actual terminal used was a Tektronix 4014 [5.3]. The Tektronix 4014 terminal consists of a storage C.R.T., a keyboard, the associated electronic circuitry and an enhanced graphics module. This terminal has two basic modes of operation. The first is the alphanumeric mode where it can print lines of keyboard characters at four different sizes, and the second, the graphic mode, where it can draw line vectors on the screen. The enhanced graphics module extends the capability of the basic 4014 terminal by providing six extra facilities.

The facility in the enhanced graphics module for drawing variable intensity dots, was achieved by varing the size of the dots drawn according to an intensity value sent to the terminal. A grey scale was constructed using this facility, for use in producing the pictures. Each element of the picture array was made of a square matrix of sixteen dots. The intensity of each matrix of dots was set according to the value of the appropriate element in the picture array. Zero intensity was not drawn for consideration of drawing speed. The results of using this for the picture production are shown on Figure 5.4.

However, the criterion of disappearing when the character was out on its own, mentioned in 5.2.1, was not achieved due to each square having a solid outside edge. Also the values at the lower part of the intensity scale, could not be easily separated. As can be seen from the

picture, this does not produce a very satisfactory result.

Another method of generating a picture using this terminal, was by varying the intensity of the picture elements by altering the number of dots drawn per picture element. The combinations of dots used for each level of intensity is shown in Figure 5.5. These configurations were made to conform to the criteria mentioned in 5.2.1. Due to there being a variable number of dots, the picture took less time to draw than the method described previously, as less information had to be transferred to the terminal. The results using this method of scale generation can be be seen in Figure 5.6.

An advantage of using a storage C.R.T. terminal is that results of different brightness settings can be evaluated and the best one chosen within a matter of minutes, compared with the lineprinter. It also allows the capability of producing a variable size picture, by simple alteration of the computer software.

5.2.3 Raster Scan Terminal [5.4]

A raster scan terminal is basically a television monitor with a large memory which are controlled by a processor. The raster scan display has to be refreshed about every 1/50 of a second, which means that the information describing one frame of the picture, has to be produced at the same rate. To use this type of display with a multi-access computer, means that the information must be stored locally within the terminal. Therefore, the terminal must contain enough memory to store the complete picture (frame store) to be displayed on the screen.

The section of memory used for the picture is called the 'bit plane', which can store either 0 or 1 in each element. Using more than one bit-plane allows a greater variation of intensity within each element, by the arranging of the bit-planes into a binary word. For example, a system of three planes would have eight variations in intensity.

Multi-bit plane terminals also allow the introduction of colour information into the pictures. Each colour on the screen is stored, as specific amounts of red, green and blue, in a separate section of memory. Each combination of bit-planes is associated with one of these colours. For example, a terminal with three bit planes would have a maximum of eight colours shown at the same time.

To modify the information contained in the local memory, there is a need for a local processor. The processor allows the terminal to appear like a normal terminal, until special sequences of characters are sent which switch subsequent characters to the graphics section of the terminal.

The actual raster scan terminal used was a Sigma colour terminal [5.5]. The basic construction of this terminal was a normal V.D.U. connected to a microprocessor. The microprocessor was in direct contact with the main computer, local memory and the display screen via a vector generator. Under normal use the microprocessor controller was transparent to the characters being transmitted between the V.D.U. and the main computer. However, when the 'graphics control sequence' of characters was received, the microprocessor intercepted everything afterwards and used that as data for producing graphics. This process only stopped when a 'new line sequence' was received. The microprocessor had an internal buffer which allowed these sequences to be checked for, and the control data intercepted was acted upon by the microprocessor.

All the information which was concerned with the screen was controlled by the hardware vector generator. These include lines, dots, characters and blocks. These could be either written or erased by using the appropriate command.

The colour of any bit-plane could be changed interactively, and each of the three generator colours (red, green and blue) could have sixteen variations of intensity. This gave the possibility of 4096 different colours. However, as the system had four bit-planes, only 16 colours could be drawn on the screen at any one time. The colour numbered zero was defined as the background colour.

For drawing the output from the Bateman camera, several different colour representation were used to help operators evaluate a particular type of display. If the display was in a familiar scale, it would be easier for them to adapt to a new system, and to quickly evaluate whether it was an improvement over previous systems.

There were four scales implemented to observe the effect of each on the picture produced. These were not the only possible scales available, and if required an operator could specify his own colour scale. The scales produced were 'Grey', 'Reverse', 'Colour' and 'Aberdeen'.

The 'Grey' scale produced a grey scale from white through to black, with black being the maximum intensity of radiation in the picture. The 'Reverse' scale was the opposite of the 'Grey' scale, with white being the maximum intensity. The 'Colour' scale was a scale whose adjacent colours were markedly different, but when viewed in monochrome produced the 'Grey' scale. The scale was used to highlight small differences in a picture. The 'Aberdeen' scale was one that was used by the Department of Bio-Medical Physics and Bio-engineering of the University of Aberdeen [5.6]. This scale also had its adjacent colours different, but had no particular scale when viewed in monochrome. This scale only contained

ten variations of intensity, therefore the other six were set to be the background.

The following table gives the intensities of each primary colour (red, green and blue), for producing the colour scales that were used:

Colour no.	Grey	Reverse	Colour	Aberdeen
	R G B	R G B	R G B	R G B
0	F F F	0 0 0	F F F	0 0 0
1	E E E	1 1 1	F F 9	0 0 0
2	D D D	2 2 2	F B F	0 0 0
3	C C C	3 3 3	4 F F	0 0 0
4	B B B	4 4 4	F 9 A	0 0 0
5	A A A	5 5 5	A 9 F	0 0 0
6	9 9 9	6 6 6	B 7 B	0 8 0
7	8 8 8	7 7 7	4 9 8	0 B 0
8	7 7 7	8 8 8	8 6 6	0 A A
9	6 6 6	9 9 9	6 6 6	8 0 A
10	5 5 5	A A A	0 7 0	A 0 0
11	4 4 4	B B B	9 2 2	A 0 6
12	3 3 3	C C C	0 4 9	F 8 0
13	2 2 2	D D D	0 4 0	A 3 0
14	1 1 1	E E E	3 0 0	F F 0
15	0 0 0	F F F	0 0 0	F F F

(all values in Hexidecimal)

Using the same picture the effect of using the above scales is shown in Figure 5.7.

The advantages of the raster scan terminal was its that it could selectively erase sections of the picture, it has a reasonable range of colour and intensity, and had the ability to fill in shapes.

Due to the increase in the access speed and packing density of memories, the frame store was now totally solid state. The increase in the size of the memories, due to this greater packing density, allows a greater number of bit-planes to be stored per picture element. These two factors will mean that the cost of colour terminals will fall, while their performance will increase.

5.3 Conclusion

The quality of any system is governed by the quality of the final result. In this case, it is the final picture that has to compete with other whole body scanner systems, not the camera itself. All of the above devices produce an output, but each has its disadvantages. Every computer system has access to one of the above output devices, and therefore should be able to produce an output.

The best picture was produced by the Sigma colour graphics terminal, mainly due to this terminal being able to draw filled in squares, as one of its basic commands. Also its ability to change colour scales from within a program interactively, makes it vastly superior in the production of final output. The main disadvantage with it, was the lack of a hard-copy facility. Taking photographs of the screen was the only method available and was used for all the results shown in this thesis.

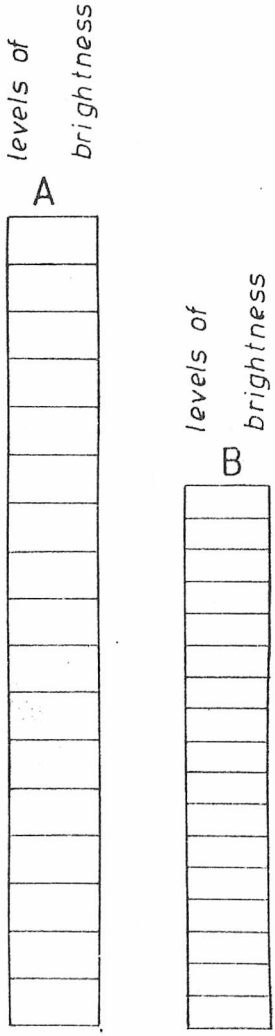

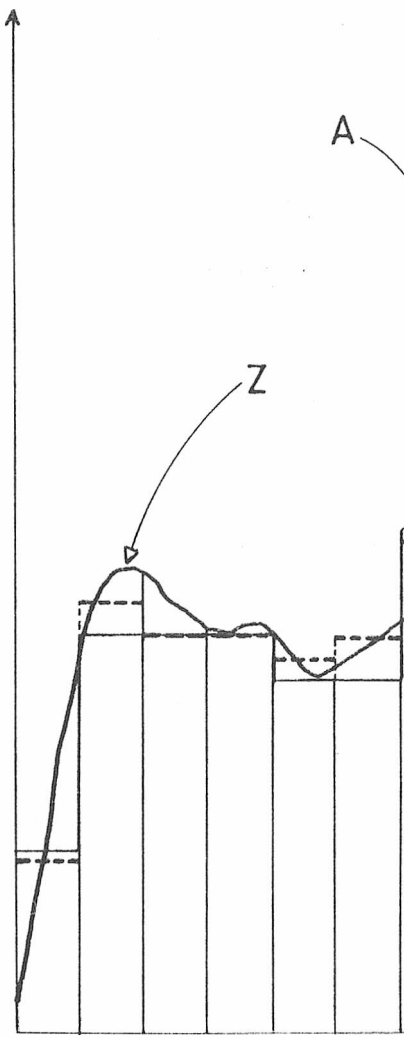

Figure 5.1 Effect

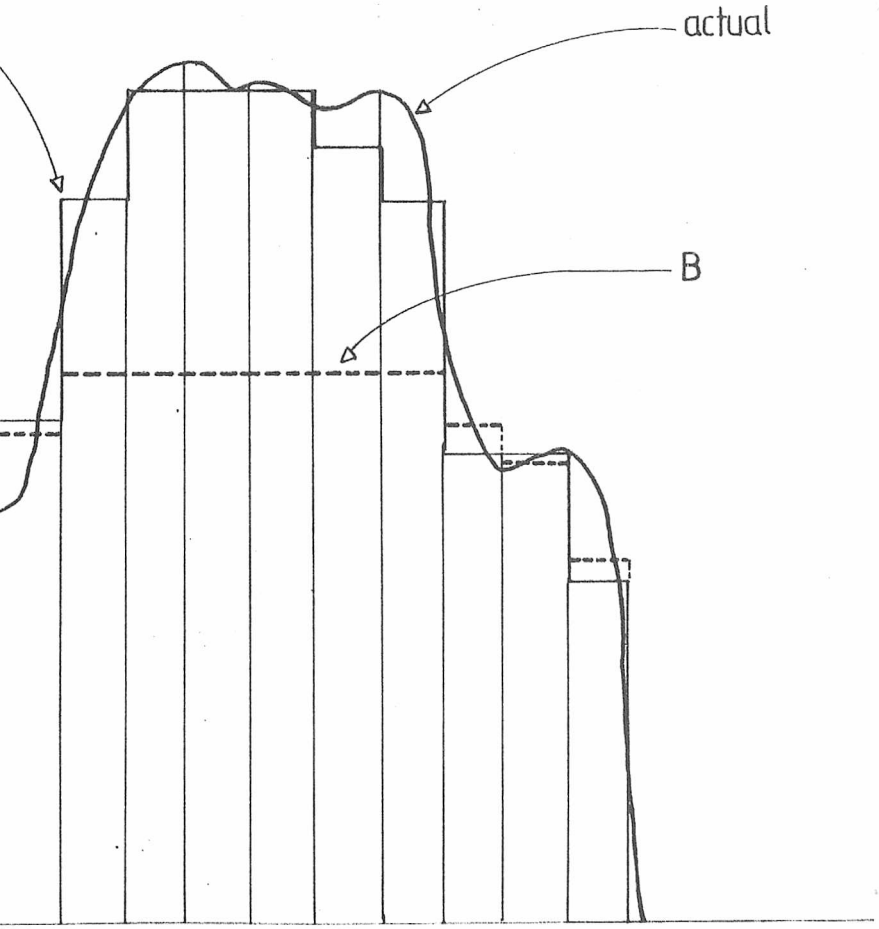

of varying brightness scales

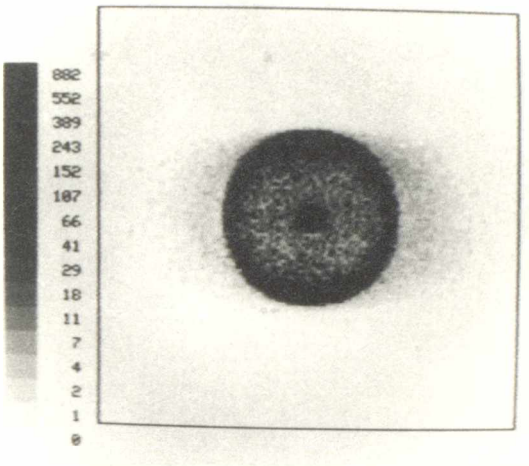

Figure 5.2 An example of exponential scaling

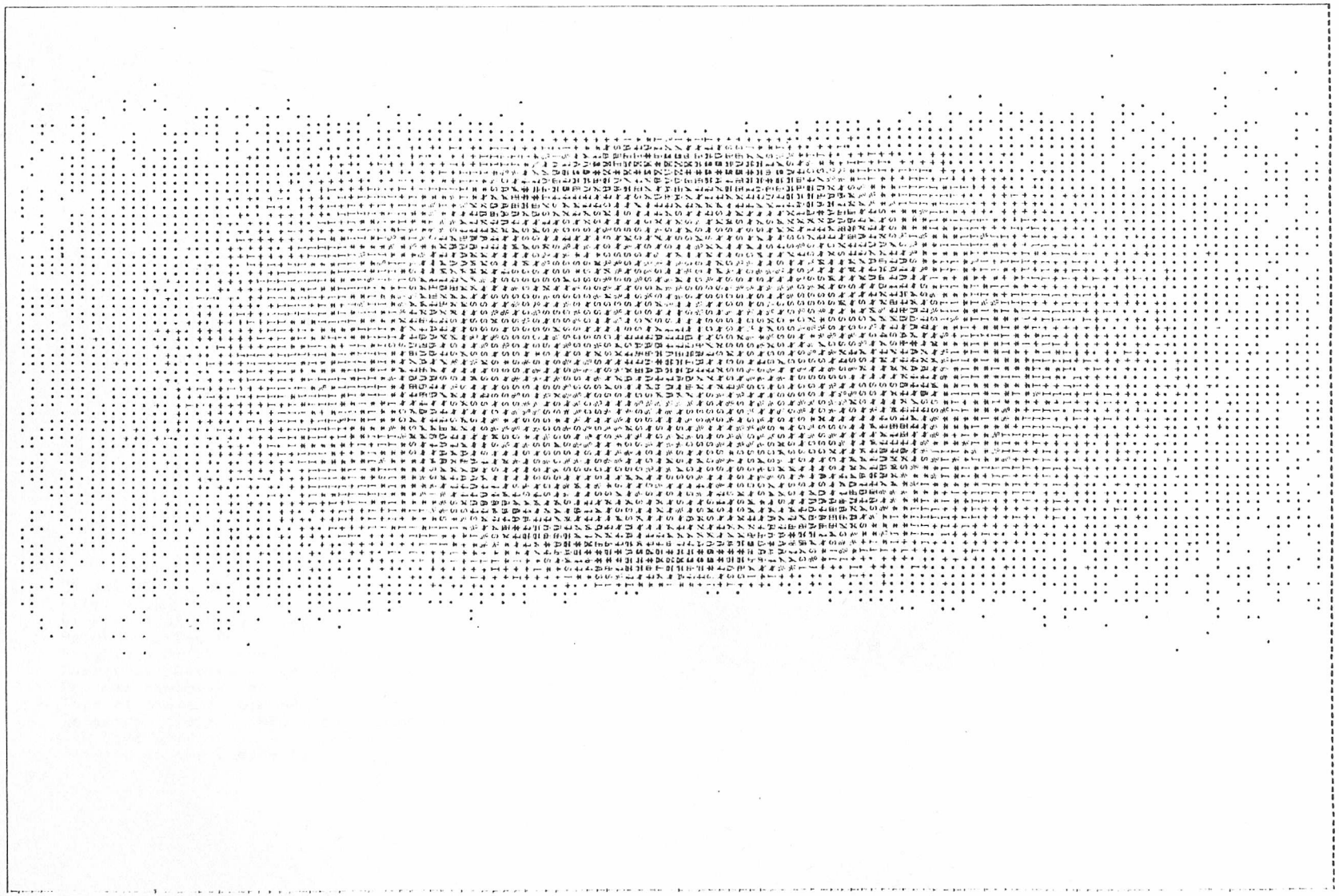

Figure 5.3 Example of using the lineprinter for output.

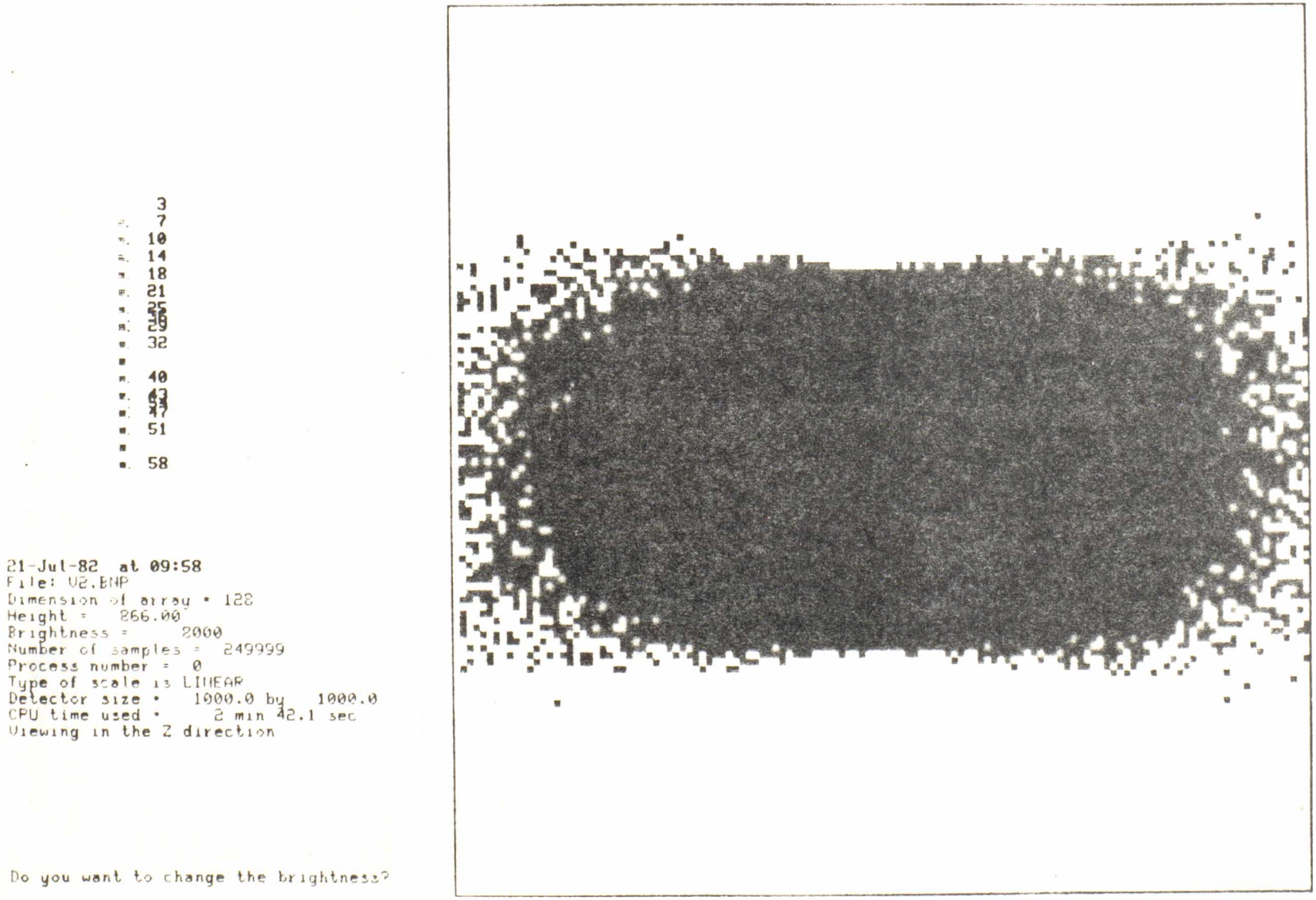

Figure 5.4 Tektronix output using variable intensity dots.

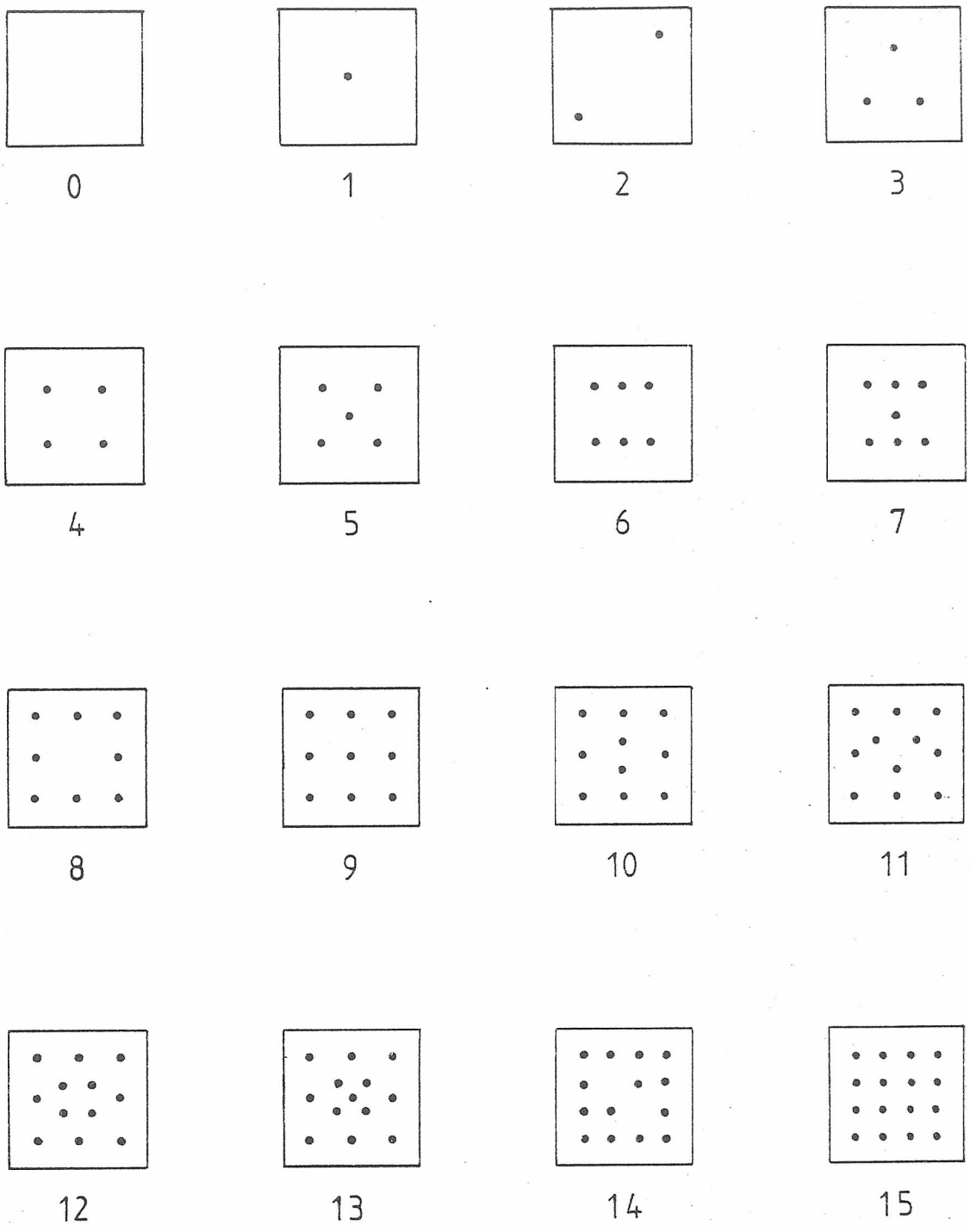

Figure 5.5 Configuration of elements of the grey scale used for the Tektronix

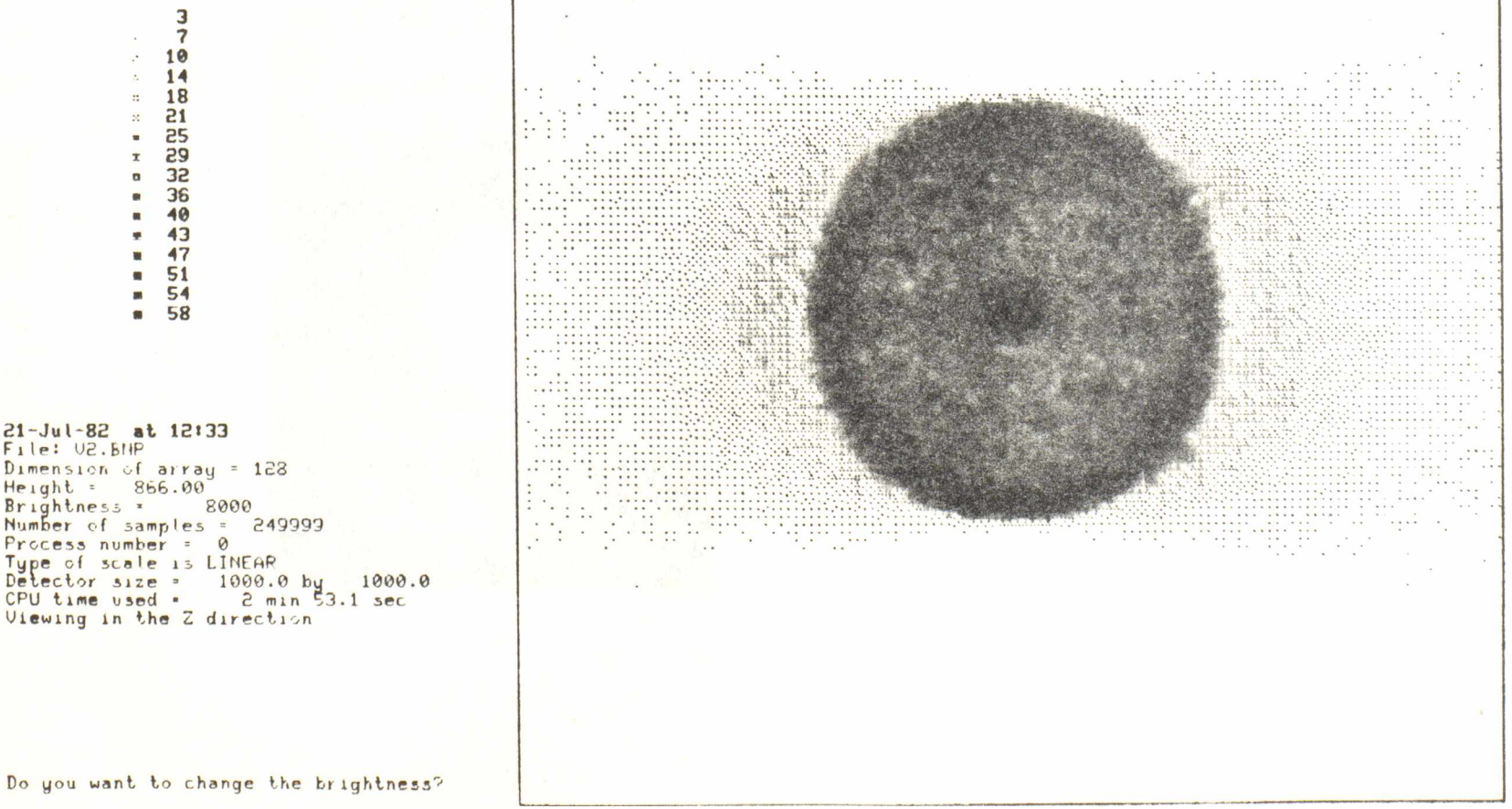

Figure 5.6 Tektronix output using variable number of dots for the intensity.

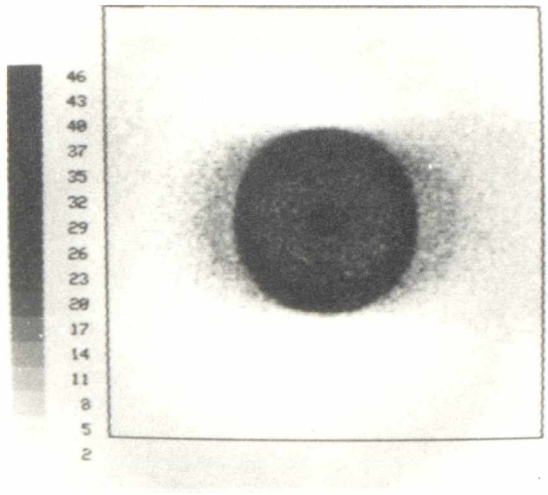

(1) "Grey" scaling

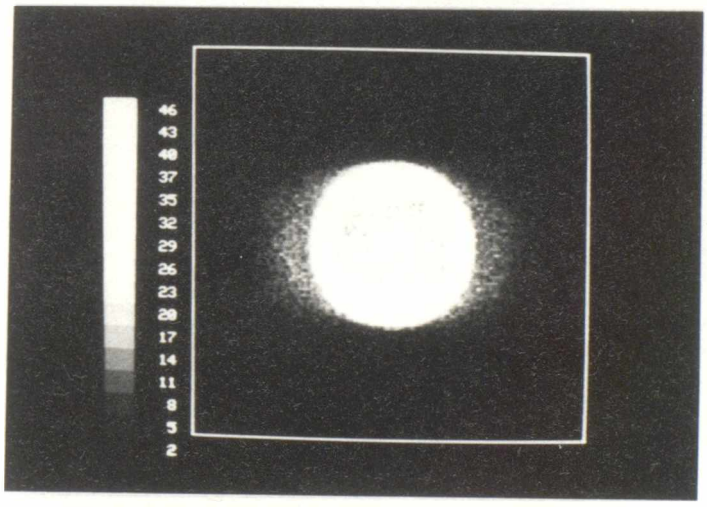

(2) "Reverse" scaling

Figure 5.7 Examples of different colour scaling

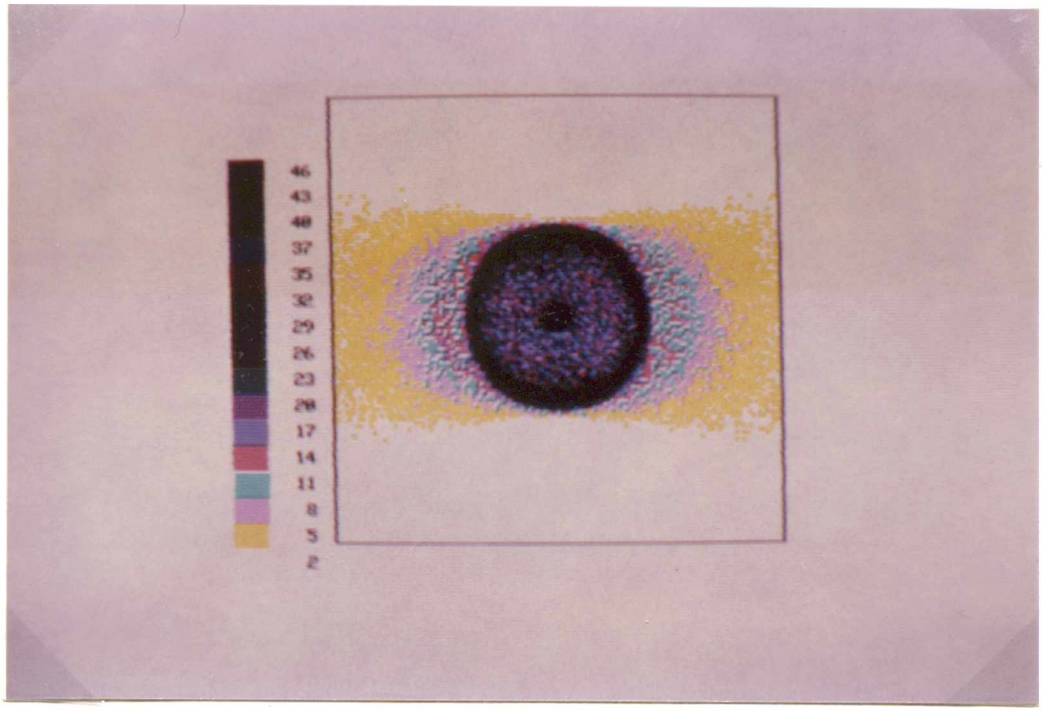

(3) "colour" scaling

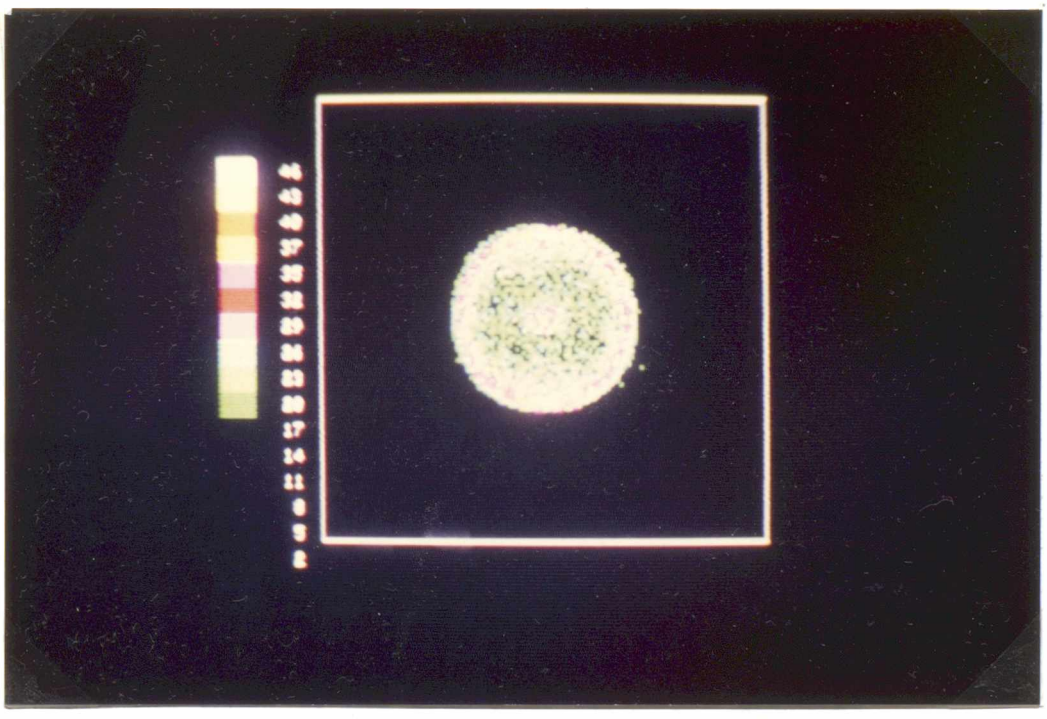

(4) "ABERDEEN" scaling

Figure 5.7 continued

CHAPTER SIX

COMPARISON OF PROCESSES

The comparison of all the processes described in Chapter Four, depends on the ability to set all the pictures produced on a scale of merit. However, there can be no technique which can be used to test pictures produced by real data obtained from a body, due to no-one knowing exactly what is contained within an individual body. As no two human bodies are precisely the same, only a general description of what they contain, in terms of its density and position, can be produced. This is however, not precise enough to be used as a quantative test. The only method by which the quality of the picture produced can be judged, is by obtaining the opinions of people, such as radiologists, who have experience at interpreting such pictures.

However, a comparison was made possible by the production of a standard reference picture, thus enabling any improvement or degradation to be visually observed. The standard reference picture was chosen to be that of the 'unprocessed' picture.

To permit a computer based test to be performed, as a measure of 'goodness of fit' between processed pictures and the ideal picture, a second reference picture was also produced. This second standard picture was known as the simulated reference picture.

These reference pictures, were used to test which of the processes described in Chapter Four was the best. The definition of best was one of consistency rather than occasional excellence.

The standard reference picture was the worst allowable picture, thus any processed picture had to be better than this, otherwise there was no purpose in carrying out any processing. As the simulated reference picture is the perfect picture (i.e. the desired result), all the pictures, including the standard reference picture, were compared to it. Therefore all the pictures were compared to an absolute reference.

In this work, two methods of assessing the final product of the two processes were implemented. The first of these two methods was to evaluate the transfer function of the surface produced by the processes. The second compares the actual picture with the simulated reference picture, and produced a value which represented how close they resembled each other.

6.1 Performance of Each Process

For a perfect imaging system, the transfer function, when viewed in the frequency domain, is a surface at a constant value in the Z dimension. Therefore the closer the result produced by the system is to this ideal, the better the performance. The transfer function of any system can be obtained by simply applying an impulse to the system. For the case of a whole body scanner, an impulse at the centre of the system will provide an overall transfer function. The impulse used was constructed by defining a cuboid of zero dimensions emitting a large quantity of radiation.

To obtain the system transfer function of the process at that position required the following procedure. The processed picture of the surface through the impulse was generated. The resultant two dimensional array was manipulated such that the position of the centre of the impulse was moved to the position (1,1) in the array. The array was then two dimensional Fourier transformed (see section 7.2.1). As the original input waveform was an impulse, the result was the transform of the transfer function of the detector system. As it was difficult to explain the operation of a two dimension surface, a line was chosen which highlighted the main features of the surface, and this was then used for the comparison.

6.1.1 Impulse Test on Each Process

The impulse test was applied to each of the processes described in Chapter Four. The waveforms that were produced are shown in Figure 6.1. These waveforms can be categorised into five sets corresponding to the type of process. Each different process group follows the same characteristic. The 'unprocessed' waveform has less magnitude at high frequencies, than at low frequencies, which reduces sharp edges. The '3-faced cube' group have a more linear form, but are also reducing high frequencies. The '6-faced cube' group have a shape similar to a damped oscillation. The lower of the two waveforms, however has a lower second maximum and tends to be more level from that point on. The '3-faced cube with shifted base' group are similar to the '3-faced cube' group but are at a steeper gradient. The '3-faced cube with all faces shifted' group have the same shape as the '6-faced cube' group except at a more reduced level.

The result of the impulse test was that none of the processes produced the ideal output. The process which had a large section of the waveform level was the lower of the 'six faced cube' group (i.e. 'six faced cube' method using the modified minimum technique).

6.2 Methods of Comparing Pictures

The array of values generated, are quantised before they are used for the picture, due to the output terminal only being able to provide a finite number of different levels of intensity (see section 5.1). The position where these levels of intensity were positioned, was controlled by a software brightness control, which affected the image of the surface produced. Due to the quality of the picture being determined by the brightness value, the number of pictures to be compared was rather large. As there was a limited amount of time available to study the

results, a faster method of assessing the content of the pictures was needed. A numeric test was implemented as a method of reducing the number of pictures to be viewed. Since the final picture is what is to be judged, the test had to compare the picture generated from the data, with the simulated reference picture. Using clinical data this would have been extremely difficult, but with the use of simulated phantoms it was relatively easy to construct this reference. The test was not considered as an ultimate measure of picture quality but as a guide to which pictures should be viewed.

The obvious method of comparing the two pictures, was by applying the following equation:

$$\text{Test} = \frac{\sum |A - E|}{\sum E}$$

where A - actual value in section
E - expected value for section

The test basically summed the difference of each element, and then normalised that value by the number of samples on the array. However, this proved to be more dependent on the number of samples, than the difference between the elements. Due to this, the test was not suitable for comparison of the processes, as they each contained different numbers of samples.

Several other tests were tried [6.1], but these did not give very fruitful results either. Of these tests tried, only the Chi Squared test produced any meaningful results.

6.2.1 Chi Squared Test [6.2]

The Chi Squared test involves comparing two sets of data, to determine how similar the distribution of their values are. The two distributions of data were the two pictures to be compared. To enable easy comparisons to be made, one of the pictures was always the simulated reference picture. The technique then involved a direct comparison of each corresponding element, using the following equation.

$$\text{Chi Squared} = \sum \frac{(A - E) * (A - E)}{E}$$

A - actual value in section
E - expected value for section

A difficulty arises when applying the equation for each element one at a time. If the expected value E is small and tending towards zero, the Chi Squared becomes equal to infinity. Thus producing a meaningless result for the test. To overcome this problem, the elements are grouped together to form larger squares, until E for the larger square is non-zero, preferably much larger than the advised minimum of five [6.2]. The grouping of these elements provide a means of comparing the two distributions of individual sections of the picture, to enable the detection of any major discrepancy. In this particular application the number of groups of squares was kept constant at thirty. Due to the large sample size, this usually kept the value of E much larger than five. On the few occasions that it was not, an error message would appear. The form of Chi Squared used was:

$$\text{Chi Squared} = \sum \frac{\sum (A - E) * (A - E)}{\sum E}$$

A - actual value in section
E - expected value for section

The value of the Chi Squared was a measure of how similar the two distribution of data were. The ideal case of where the two sets of data were identical, the value of Chi Squared was zero. When they deviated from this, the value of Chi Squared increased in size. So for a picture to become more like the ideal, meant a reduction in the value of Chi Squared.

The largest source of error inherent in the application of the Chi Squared test, is that of a constant level of background. When the picture is viewed, the shape of the object may be very clear, but if there is a constant background the value for the Chi Squared test will tend to indicate a bad correlation between the two sets of data.

6.2.2 Application of the Chi Squared test

The two pictures could be thought of as two long arrays of values, constructed by stacking the rows end to end. To remove the effect of the total number of rays used, the total number contained in the simulated picture array was arranged to be the same value as the amount in the picture to be compared. This enabled comparison of pictures generated using different numbers of samples. The final value of Chi Squared was rounded to the nearest ten, as a variation of ten could not be viewed in the final pictures.

6.3 Comparison of Processes using Chi Squared Test

Several different combinations of phantoms were constructed to observe the effectiveness of the new processes. The phantoms constructed will be described and their results given.

The phantoms produced had the following details the same. The number of samples used was 250000. The dimensions of the detectors were 1000 by 1000, with the positions being rounded to the nearest 1. There was no defects on the camera system.

The main phantom studied was a simulated head with a concentric tumour. This was basically a hollow sphere of outer radius of 210 and an inner radius of 180. The tumour was a solid sphere of radius 32 [7.13].

6.3.1 Three Dimensional Views

To check whether a process was consistently better than the rest, the phantom was viewed in the three dimensions X, Y and Z producing the following results.

Z Direction

	Chi * Chi			
	uncorrected		corrected	
Process	norm	mod	norm	mod
unprocessed	710	---	---	---
3-faced	830	740	950	940
6-faced	830	690	---	---
3-faced/base	830	740	800	810
3-faced/all	840	740	870	730

uncorrected - applying 4.2.1 to 4.2.4
corrected - applying 4.3
norm - using minimum
mod - applying 4.4

These Chi Squared values were used as a scale from the simulated reference picture, at position zero, to the standard reference picture. Any value greater than the standard reference picture value, meant that the process was reducing the quality of the final picture.

The values of Chi Squared produced were outside the tables for the probability of significance. This was mainly due to the problem with having a large sample size mentioned in 6.2 .

Y Direction

	Chi * Chi			
	uncorrected		corrected	
Process	norm	mod	norm	mod
unprocessed	1560	---	---	---
3-faced	1580	1520	1660	1570
6-faced	1510	1260	---	---
3-faced/base	1700	1590	1780	1810
3-faced/all	1720	1540	1730	1560

X Direction

	Chi * Chi			
	uncorrected		corrected	
Process	norm	mod	norm	mod
unprocessed	810	---	---	---
3-faced	740	770	790	600
6-faced	670	560	---	---
3-faced/base	750	740	920	1160
3-faced/all	750	730	810	800

As can be seen from the above tables, the results from the processes are consistent regardless which view is used. The resultant pictures viewed in the Z direction are shown in Figure 6.2.

Due to the number of photographs that would be needed to show all the processes, only the 'unprocessed' and the 'six faced cube' method using the modified minimum technique, which was consistently the best process, will be shown.

The unprocessed and the best processes for the X and Y directions are shown in Figures 6.3 and 6.4.

6.3.2 Different Levels Within a Phantom

The picture produced by the processes, as the surface of interest was moved through the phantom had to show that the best process was still consistently the best. Two other levels within the system were processed and are shown in Figures 6.5 and 6.6.

The second of these two surfaces passed through an area where there was no sources of radiation. This made the application of the Chi Squared test impossible, due the previously stated problem of zero expected values appearing on the bottom line of the equation (see section 6.2.1). However, when the pictures are viewed, it is obvious that the 'six faced cube' method using the modified minimum technique was better due it having less signal on the screen.

6.3.3 Rejected Information

Due to the nature of the processes, a large proportion of the detected rays were rejected. The percentage of the total rays left, after each process had produced the picture shown in Figure 6.2, is shown in the following table:

	% Left			
	uncorrected		corrected	
Process	norm	mod	norm	mod
unprocessed	48.2	---	---	---
3-faced	47.8	20.7	25.6	11.5
6-faced	38.9	13.8	---	---
3-faced/base	47.7	20.8	34.2	15.3
3-faced/all	47.5	20.8	41.8	18.7

As can be seen from the table there is a large amount of the information discarded, even 'unprocessed' has rejected 51.8% of the input data. The large scale of the rejection of data meant that the sample size gathered from the patient had to be large, otherwise most of the information would have been thrown away. The above values were also dependent on the concentration of the radiation in the plane considered, which meant that even more data could be rejected if the surface does not go through an area of radiation emission. When the modification of the minimum technique was used, even more of the input data was rejected.

6.3.4 Absolute Execution Time

Most of these processes involved different techniques of manipulating the detected information, therefore the subsequent times taken varied. The execution times for all these process when they produced the picture shown in Figure 6.2, are shown in the following table:

	Execution Time			
	uncorrected		corrected	
Process	norm	mod	norm	mod
unprocessed	168.3	---	---	---
3-faced	444.9	572.9	676.6	809.9
6-faced	592.7	721.6	---	---
3-faced/base	402.8	530.4	702.7	830.2
3-faced/all	421.3	555.4	733.1	866.8

time in CPU seconds

The time of execution was mainly due to two particular events in the computer programs used. These were the reading in of the data and the incrementing of an element in the array. The reading in time, however, was common to all the processes and was not a variable factor. The number of times an element in the array was incremented, depended on which process was used. As these processes considered three dimensions, two faces per cube could be incremented per ray, and also the ray could be 'counted' by more than one cube. Thus the time would vary according to the position of the sources of radiation. Obviously the corrected processes carried out this procedure for three sets of cubes. The modification of the minimum again added to the overall time but was not a variable time factor.

These times for processing were larger than in an operational package, as every routine was written in Fortran. If subroutines that were accessed frequently, were written in assembly code, the speed of operation would increase. Also the program used had a lot of built in

options, as it was a prototype program, and most of these had to be check within the process loops, thus slowing down speed of operation.

6.4 Test for Consistency

Three other phantoms were studied to test if the process that was found to be the best for the above phantom, would remain to be the best of any type of phantom.

(a) Study One

The first phantom studied was a solid sphere placed in the centre of the detector system, of radius 100. Applying each of the processes in turn gave:

	Chi * Chi			
	uncorrected		corrected	
Process	norm	mod	norm	mod
unprocessed	160	---	---	---
3-faced	160	60	990	530
6-faced	140	20	---	---
3-faced/base	150	60	660	240
3-faced/all	150	60	170	70

Figure 6.7 shows the 'unprocessed' and the '6-faced cube' using modified minimum technique pictures.

(b) Study Two

The second phantom to be studied was a solid cube, positioned in the centre of the detector system. The dimensions of the cube were 156.25 by 156.25 by 156.25. Applying each of the processes in turn gave:

	Chi * Chi			
	uncorrected		corrected	
Process	norm	mod	norm	mod
unprocessed	930	---	---	---
3-faced	920	750	1660	1930
6-faced	800	630	---	---
3-faced/base	930	750	1110	1110
3-faced/all	930	770	930	840

Figure 6.8 shows the 'unprocessed' and the '6-faced cube' using modified minimum technique pictures.

(c) Study Three

The third phantom studied was a simulation of a torso with three inner organs. The torso was a hollow sphere with radii 300 and 250, with a radiation level of 1. The largest organ was a solid sphere of radius 80 with a radiation level of 2. The middle size of organ was a solid sphere of radius 60 with a radiation level of 4. The smallest organ was a solid sphere of radius 40 with a radiation level of 3. These organs were arranged in a circle within the bounds of the torso, with their centres on a plane parallel to the Y-axis.

	Chi * Chi			
	uncorrected		corrected	
Process	norm	mod	norm	mod
unprocessed	1090	---	---	---
3-faced	1080	750	1960	1240
6-faced	950	630	---	---
3-faced/base	1100	790	1470	750
3-faced/all	1090	780	940	630

Figure 6.9 shows the 'unprocessed' and the '6-faced cube' using modified minimum technique pictures.

As can be seen from the tables the 'six faced cube' method using the modified minimum technique, still gave the lowest value for the Chi Squared test.

6.5 Defects in the Camera

The defects that were described in 3.6 are now introduced into the phantom representing a head with a tumour, described in 6.3.

(a) Detector Boundary

A boundary of 200 was set on all the detectors, to simulate such a boundary on a real camera. The results obtained are given in the following table.

	Chi * Chi			
	uncorrected		corrected	
Process	norm	mod	norm	mod
unprocessed	400	---	---	---
3-faced	300	240	610	240
6-faced	840	520	---	---
3-faced/base	230	200	240	210
3-faced/all	270	250	270	250

As can be seen the best process is the 'three faced cube with shifted base' method using the modified minimum technique. When viewed, see Figure 6.10, the 'six faced cube' method using the modified minimum technique produces a better picture. This discrepancy was due to the 'six faced cube' method having extra information on the picture which did not interfere with the main information content.

(b) Acceptance Angle

The acceptance angle of the detectors was set to 70 degrees. The results of this are shown in the following table.

	Chi * Chi			
	uncorrected		corrected	
Process	norm	mod	norm	mod
unprocessed	370	---	---	---
3-faced	420	500	560	530
6-faced	460	390	---	---
3-faced/base	420	490	400	640
3-faced/all	450	500	520	620

As can be seen the 'six faced cube' method using the modified minimum technique was the best. Limiting the acceptance angle should improve the quality of the data obtained from the whole body camera [2.4]. Figure 6.11 shows the results of this restriction on the detectors.

(c) Finite Number of Detecting Elements

The number of detecting elements (wires) was reduced by a factor of ten. The results of this are shown in the following table.

	Chi * Chi			
	uncorrected		corrected	
Process	norm	mod	norm	mod
unprocessed	390	---	---	---
3-faced	310	260	680	260
6-faced	280	200	---	---
3-faced/base	260	210	260	210
3-faced/all	310	250	310	250

As can be seen the 'six faced cube' method using the modified minimum technique was the best. Figure 6.12 shows the result of limiting the number of detector elements. The effect of reducing the number of detector elements means that the detectors themselves can be made cheaper, as less precis construction techniques need to be used.

(d) Simultaneous Emission

The proportion of erroneous data was set to be 50%. The results of this are shown in the following table.

	Chi * Chi			
	uncorrected		corrected	
Process	norm	mod	norm	mod
unprocessed	400	---	---	---
3-faced	300	240	610	240
6-faced	840	520	---	---
3-faced/base	230	200	240	210
3-faced/all	270	250	270	250

As can be seen the 'three faced cube with raised base' method using the modified minimum technique was the best. Simultaneous emission tends to produce more background signal and reduces the difference between that and the actual signal. As stated in section 6.2.1, if there is a large part of the picture at a constant value, this will tend to make the value produced by the Chi Squared test meaningless. Figure 6.13 shows that the 'six faced cube' method using the modified minimum technique was still the best.

6.6 Array size

The size of the array determines the detail that can be seen on the picture. This was varied to determine the differences in processing time between a range of sizes of picture array.

Process	32	64	128
unprocessed	12.0	11.9	12.1
3-faced	26.9	26.5	29.3
6-faced	32.2	32.6	35.0
3-faced/base	25.5	26.6	29.4
3-faced/all	25.9	27.3	29.0

There was a random effect acting on these results due to the random placement of the rays. But it can be seen that the variation of the size of the display array did not markedly alter the processing time.

As the resolution has decreased the sharpness of the picture also decreased. In Figure 6.14 two array sizes (64 and 128) are shown to demonstrate the effect.

6.7 Conclusion

The process that was consistently the best of the new processes, was the 'six faced cube' method using the modified minimum technique. There were two possible reasons for this fact. The first was that the 'six faced cube' method enclosed a volume of space, whereas the others did not. As the process used two 'counting' surfaces per dimension, this introduced an averaging effect into the process, which in turn tended to remove the effect of radiation from outside the bounds of the cube. The second was that the 'six faced cube' method is symmetrical, and is also in contact with neighbouring cubes by having common faces. This feature give each 'six faced cube' method a connection with its neighbour, which in turn induced a stabilising effect of each element.

The outcome of these two correcting functions was to smooth out any elemental deviation and to produce a self correcting array.

The corrective techniques used did not give as good results as expected. This may have been due to the wrong values of multiplication factors being used. However, if they had produced the best picture, they would have had a handicap due to the extremely long time that they take to process the information. The 'six faced cube' method, did not take substantially longer to carry out the processing, than simply using 'unprocessed'. Considering the transfer function described in 6.1.1, the waveform for this process is the most level in the mid to high frequency range.

In all the pictures produced, all the unwanted information appeared to be only in one axis. This is due to the detectors being a finite length and the camera having open ends, where a large proportion of the radiation could escape.

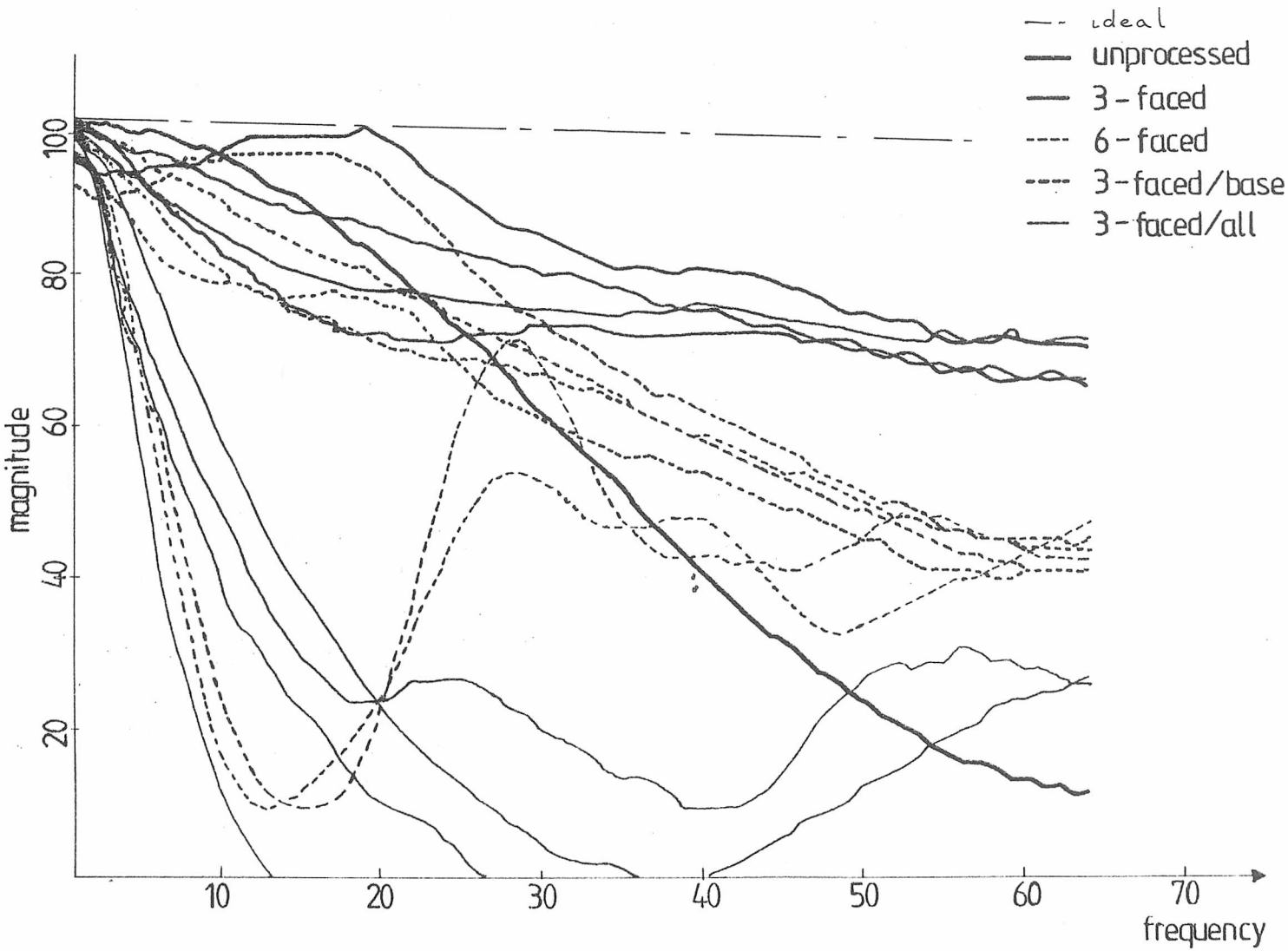

Figure 6.1 Impulse response of each process

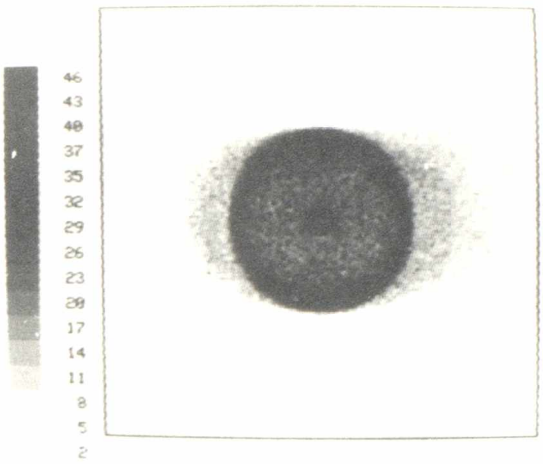

(1) " unprocessed "

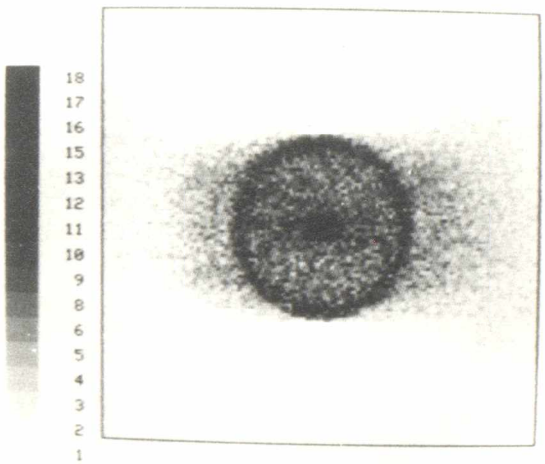

(2) " three faced cube "

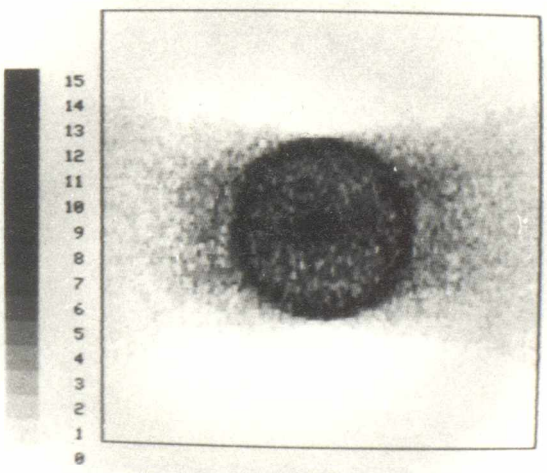

(3) " six faced cube "

Figure 6.2 Pictures of each process in Z direction

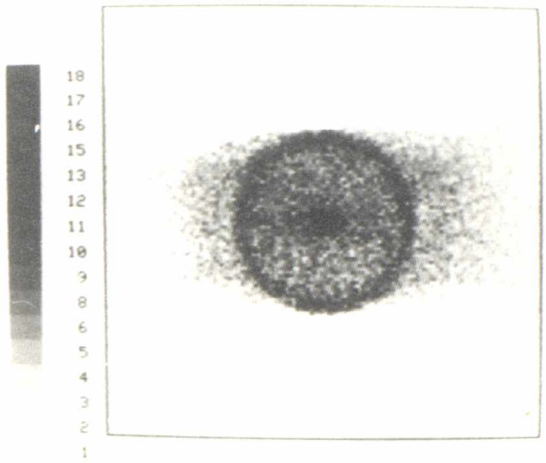

(4) "three faced cube with shifted base"

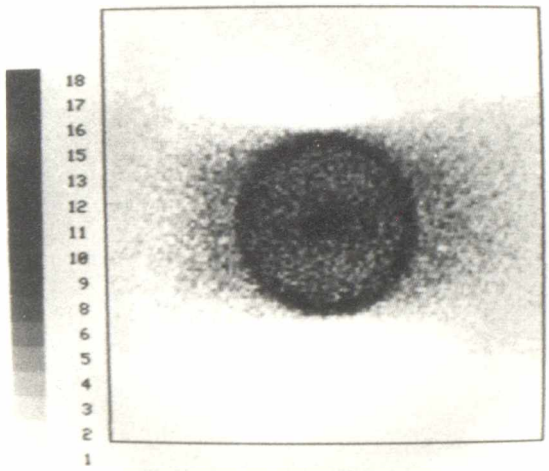

(5) "three faced cube with all faces shifted"

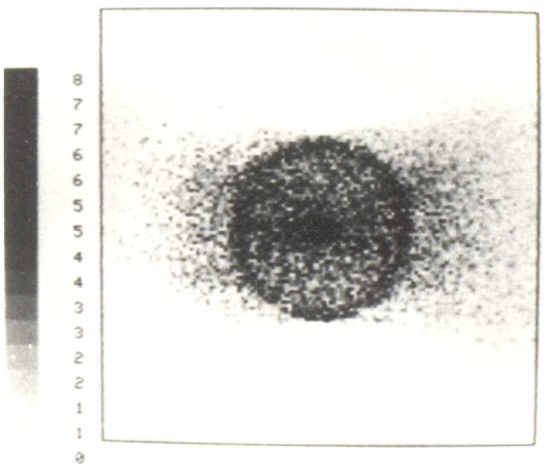

(6) "three faced cube" + modified minimum

Figure 6.2 continued

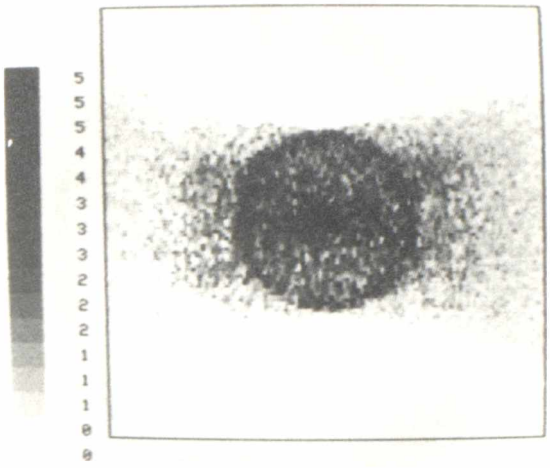

(7) " six faced cube" + modified minimum

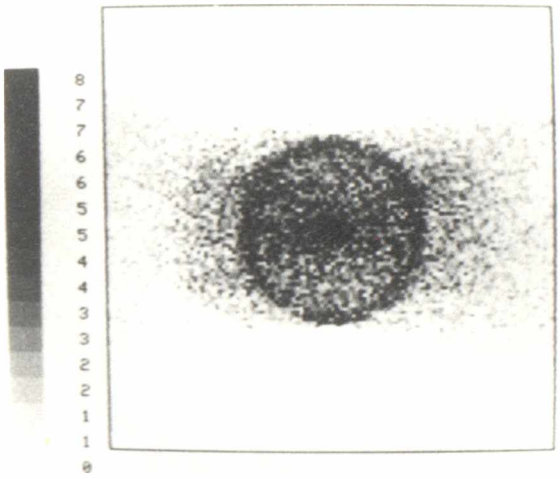

(8) "three faced cube with shifted base"+ modified minimum

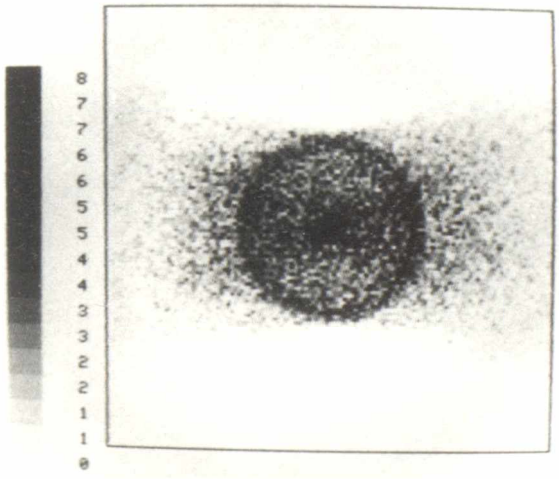

(9) "three faced cube with all faces shifted" + modified minimum

Figure 6.2 continued

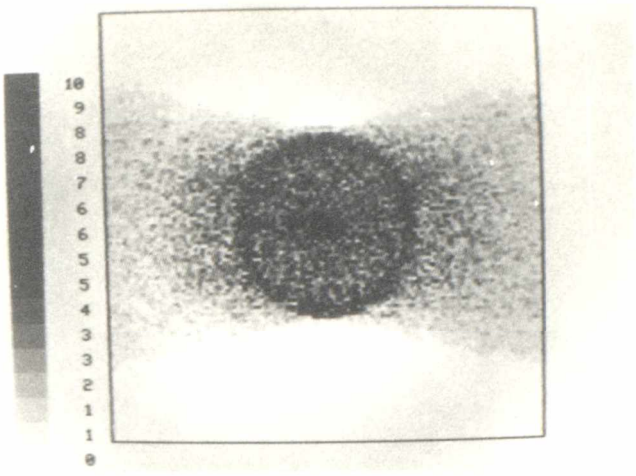

(10) corrected " three faced cube"

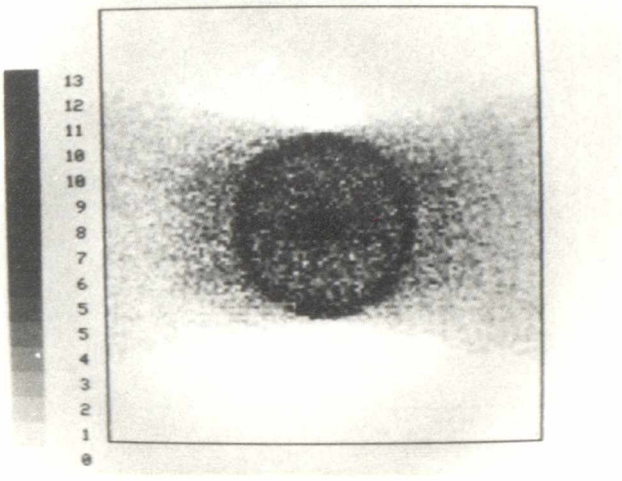

(11) corrected "three faced cube with shifted base"

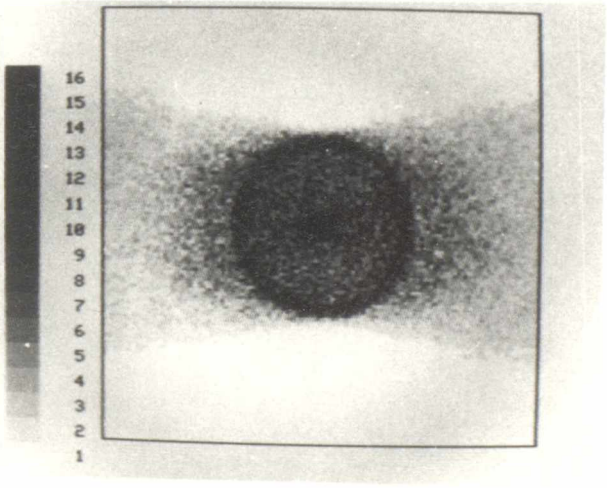

(12) corrected "three faced cube with all faces shifted"

Figure 6.2 continued

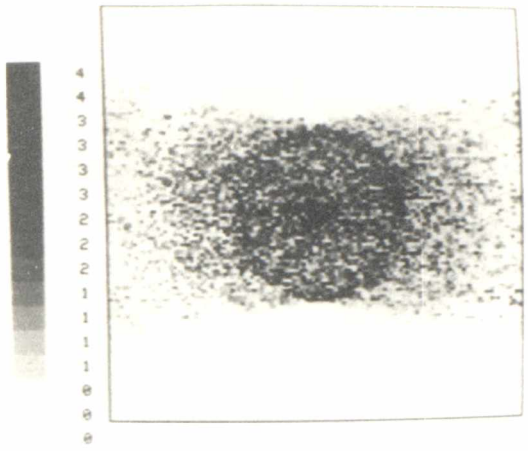

(13) corrected "three faced cube"+ modified minimum

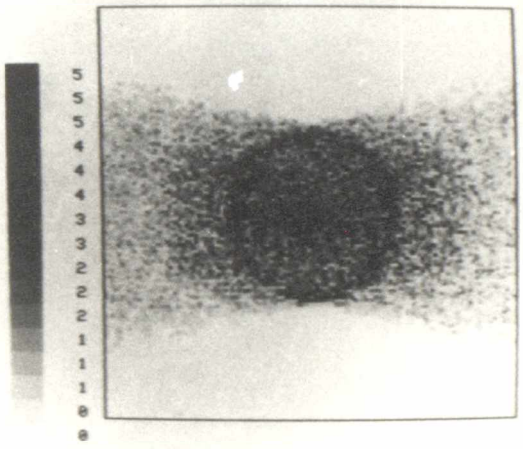

(14) corrected "three faced cube with shifted base" + modified minimum

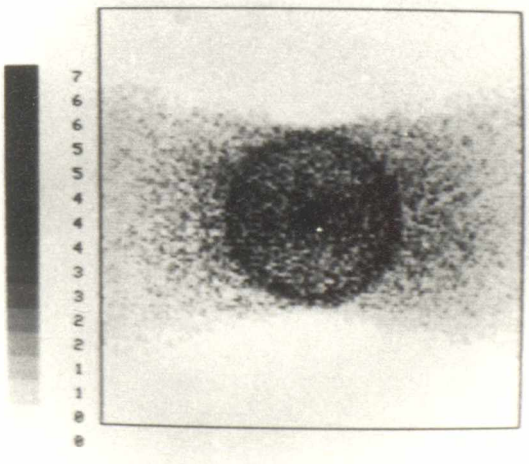

(15) corrected "three faced cube with all faces shifted + modified minimum

Figure 6.2 continued

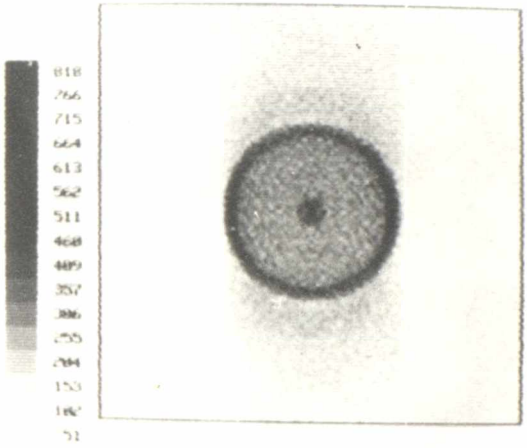

(16) Fourier

Figure 6.2 continued

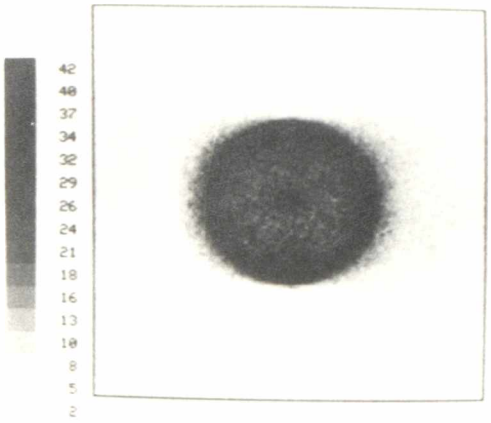

(1) " unprocessed "

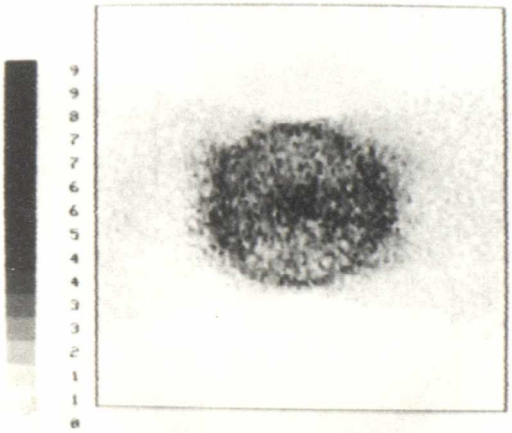

(2) " six faced cube " + modified minimum

Figure 6.3 Pictures in Y direction

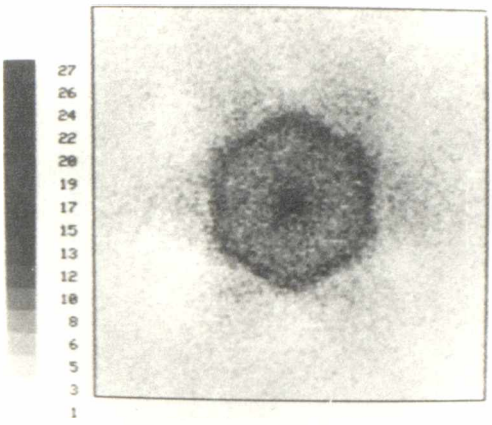

(1) " unprocessed "

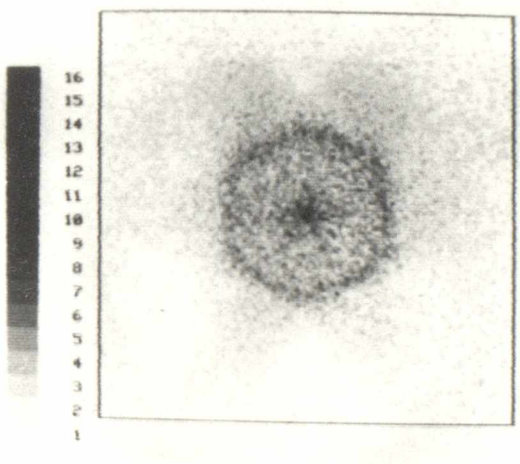

(2) "six faced cube" + modified minimum

Figure 6.4 Pictures in X direction

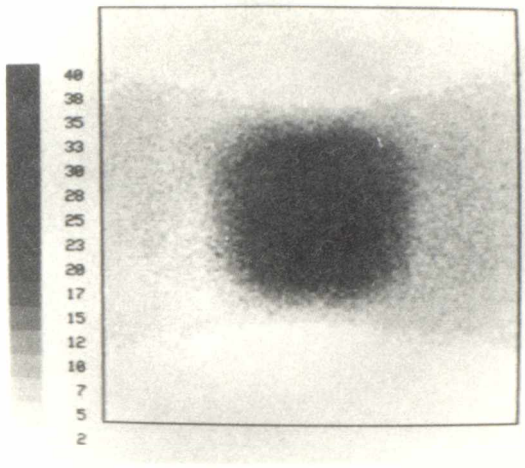

(1) " unprocessed"

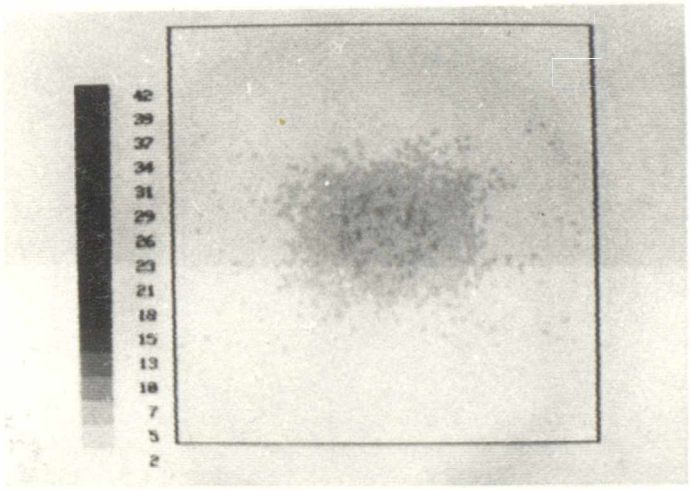

(2) "six faced cube" + modified minimum

Figure 6.5 Pictures of another level through the phantom

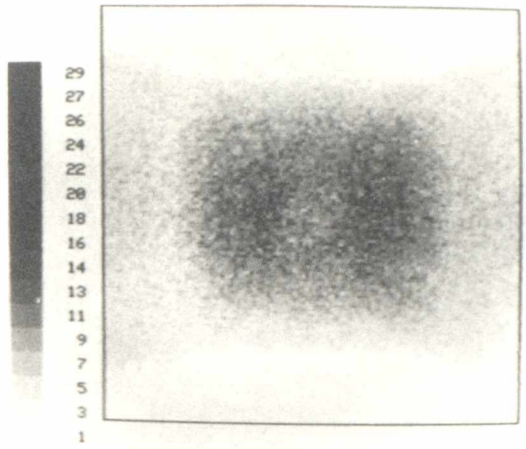

(1) " unprocessed "

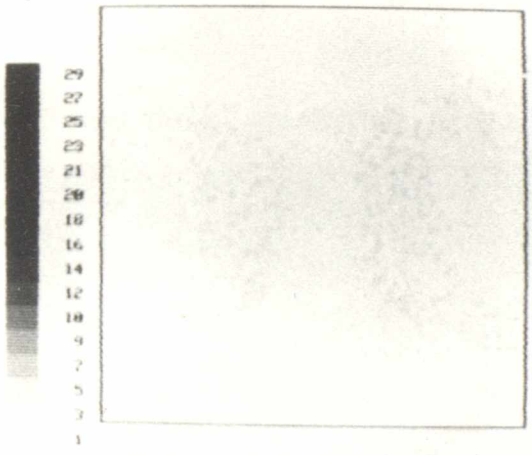

(2) "six faced cube" + modified minimum

Figure 6.6 Pictures of a level outside phantom

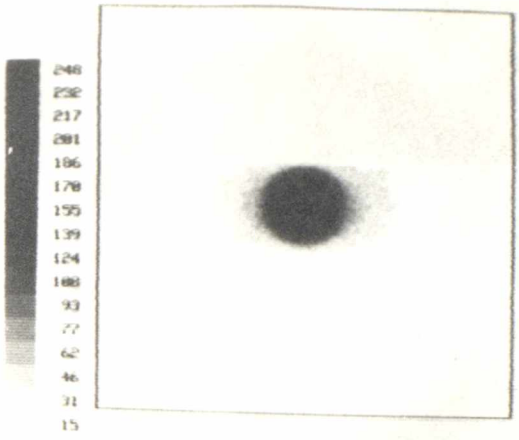

(1) "unprocessed"

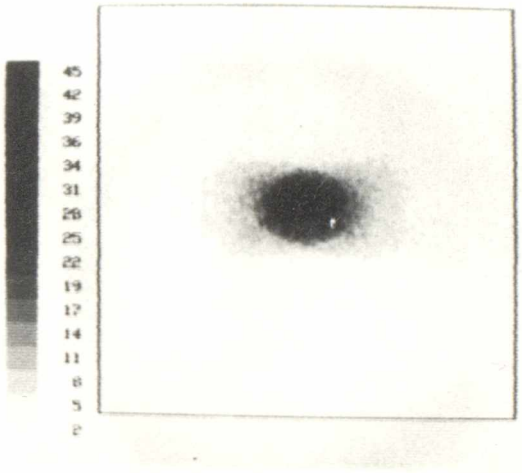

(2) "six faced cube" + modified minimum

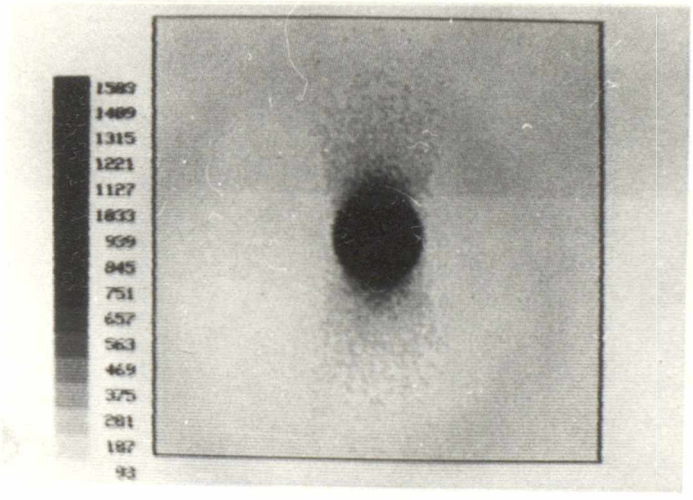

(3) Fourier

Figure 6.7 Phantom - solid sphere

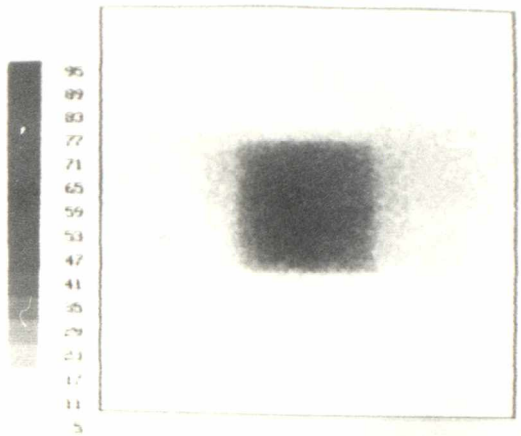

(1) "unprocessed"

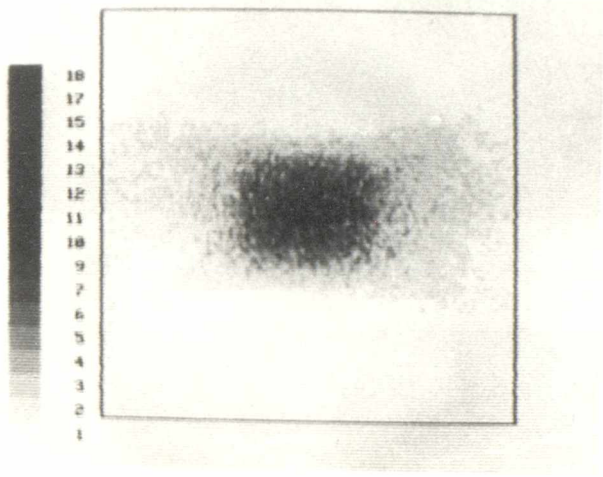

(2) "six faced cube" + modified minimum

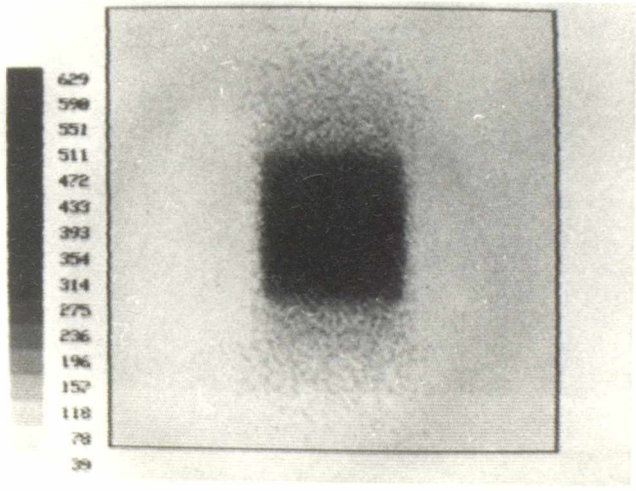

(3) Fourier

Figure 6.8 Phantom - solid cube

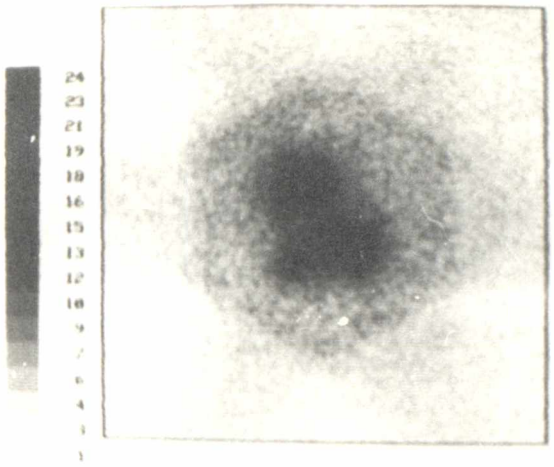

(1) " unprocessed "

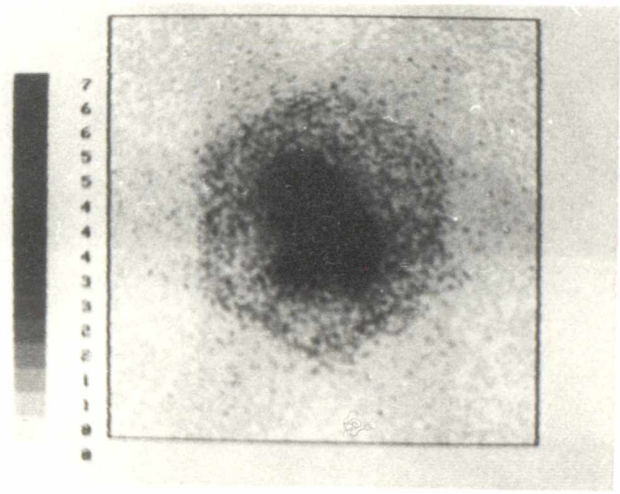

(2) " six faced cube" + modified minimum

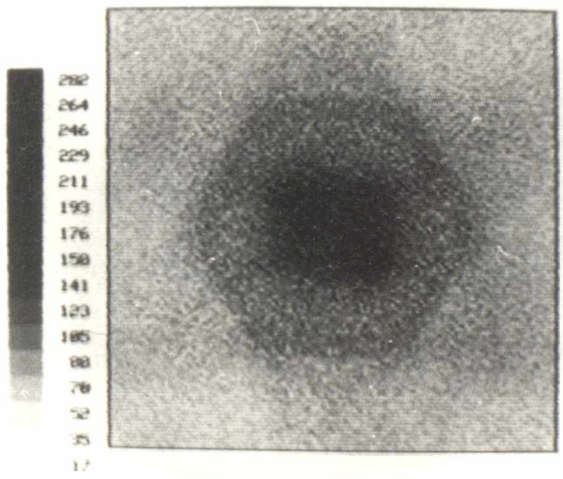

(3) Fourier

Figure 6.9 Phantom - simulated body

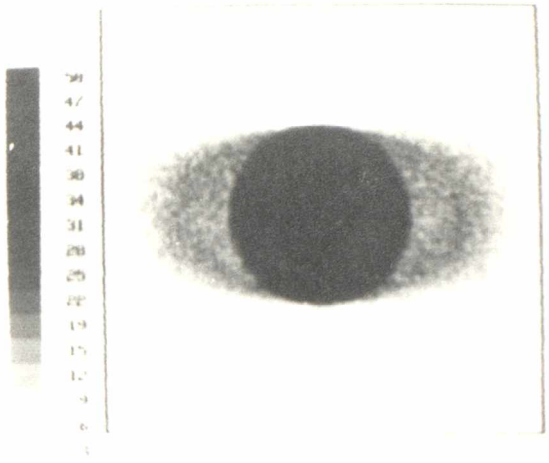

(1) " unprocessed"

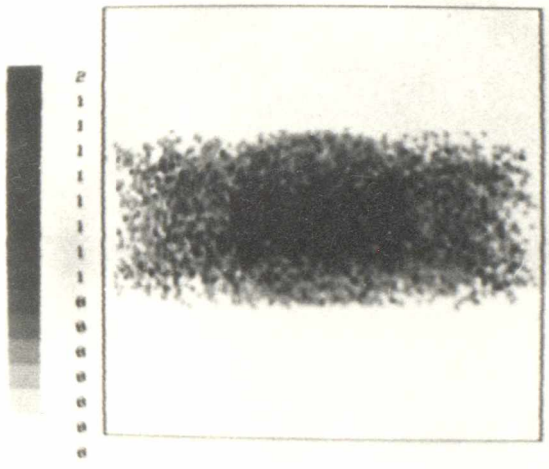

(2) "six faced cube" + modified minimum

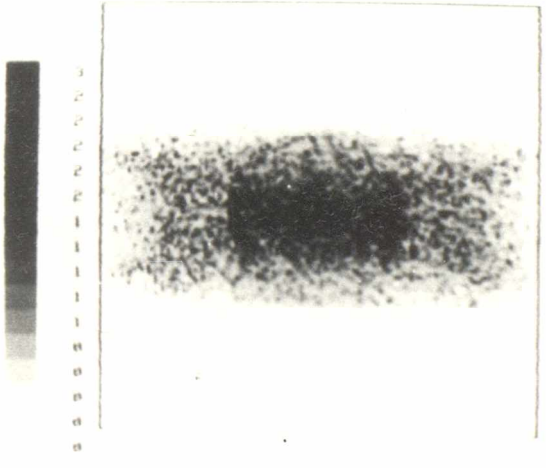

(3) "three faced cube with raised base" + modified minimum

Figure 6.10 Non-detecting boundary set on detector

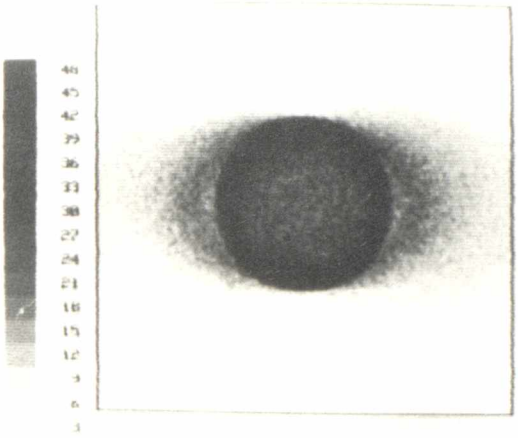

(1) "unprocessed"

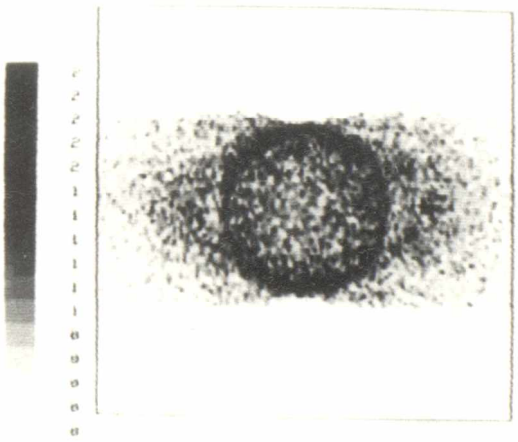

(2) "six faced cube" + modified minimum

Figure 6.11 Limitation on angular acceptance of detector

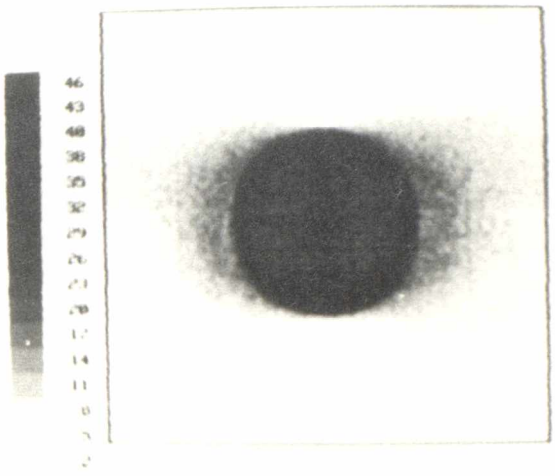

(1) " unprocessed

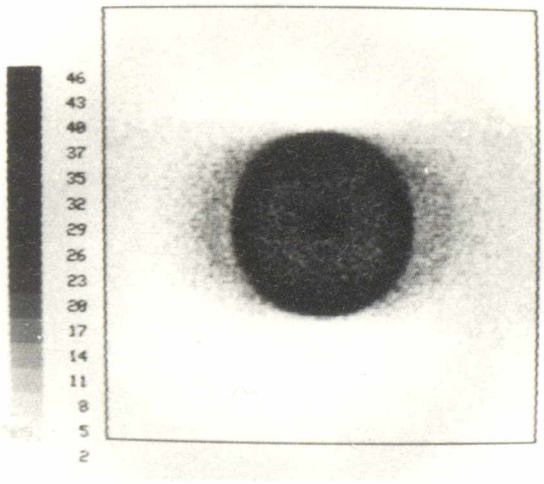

(2) "six faced cube" + modified minimum

Figure 6.12 Limitation on number of detecting elements within each detector

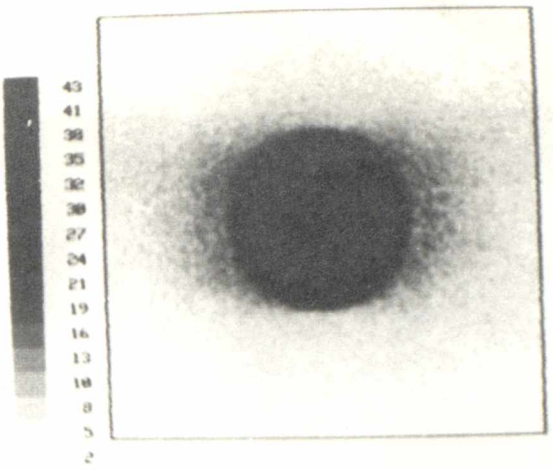

(1) " unprocessed "

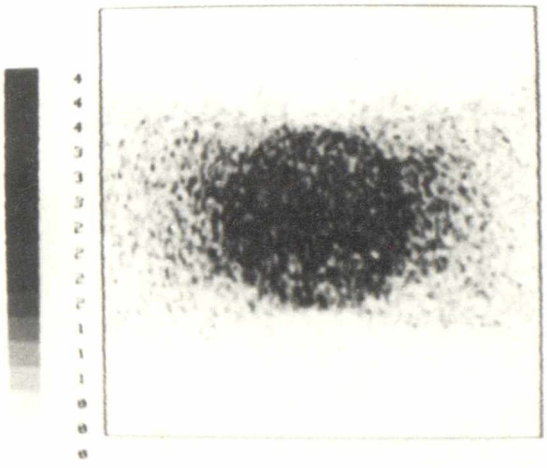

(2) "six faced cube" + modified minimum

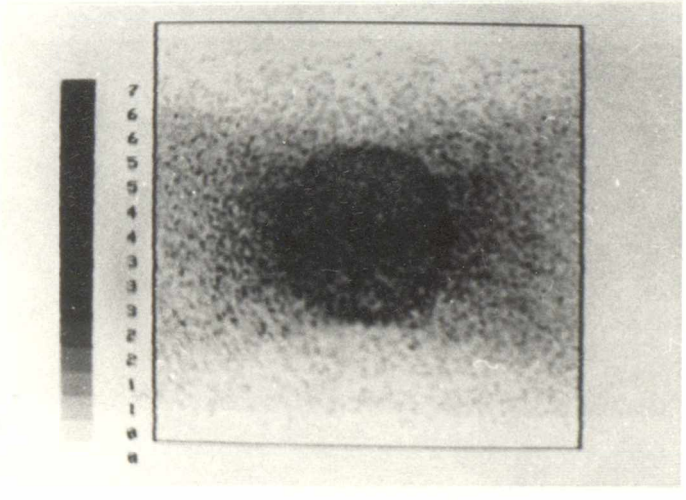

(3) "three faced cube with raised base"
+ modified minimum

Figure 6.13 Simultaneous emission

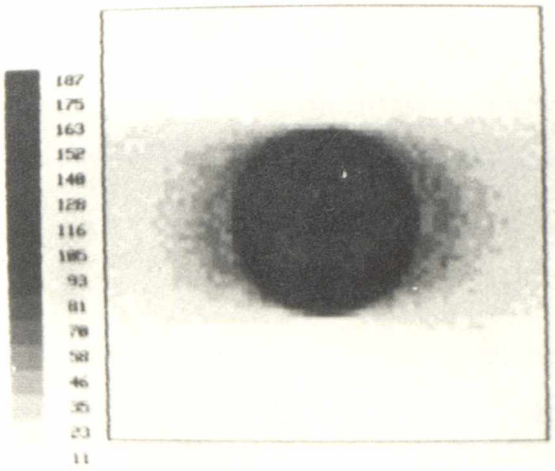

(1) 64 × 64

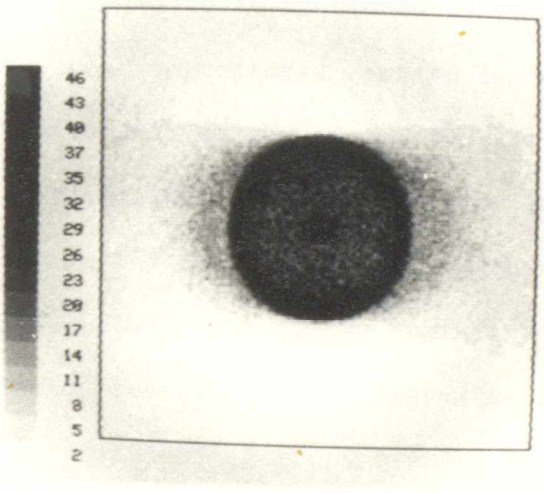

(2) 128 × 128

Figure 6.14 Two different array sizes

CHAPTER SEVEN

COMPARISON WITH PREVIOUS METHODS

Most of the techniques of reconstruction tomography that have been studied up to now by workers in the field, fall into three distinct areas. These are iterative processes, exact solution using matrix techniques and those employing Fourier filtering techniques.

The iterative technique [7.1,7.2,7.3,7.4] involves starting with an even level of intensity throughout the array, and modifying the values contained in it using the 'unprocessed' array. The difference between the two arrays is calculated, and is then used to modify the generated array further. This procedure is continued until the difference between the generated and the unprocessed arrays is below a set limit. The generated array is then used as the output to the picture. The main problem with this technique is the possibility that the difference may never become lower than the set limit. This means that the generated array would oscillate between two states just outside the limit.

The exact solution technique [7.5] involves modification of the unprocessed picture, by removing the effect of the transfer function of the detector system. The transfer function is described as a matrix, whose size is the same as the picture array to be corrected. To remove the effect of the transfer function, involves multiplying the picture array by the inverse of the transfer function matrix. The main problems involved with this technique, include the generation of the inverse matrix as a large number of elements of the first array are zero. Also if noise is present on low or zero values, when the inverse is found

these are amplified and produce erroneous results.

The Fourier filtering methods are of two basic types, those that are applied to the scans before they are projected across the array, and those that are applied to the array after the rays have been projected. This chapter will describe in detail these two Fourier techniques, and will also compare the best process described in Chapter Four, with one of the Fourier techniques.

7.1 Fourier Theory

The basic theory of Fourier analysis is that any waveform consists of only a set of specific frequencies. These frequencies are multiples of the fundamental (lowest) frequency contained in the waveform, and are described by their relative amplitude and phase to that frequency. The breaking up of the waveform into these component frequencies is achieved by using the forward Fourier transform. The original waveform can be reconstructed by the summation of these component waveforms in their correct magnitude and phase. This process is normally carried out using the inverse Fourier transform.

Any waveform that is applied to a system, has the resultant waveform affected by that system's transfer function. This phenomenon can be mathematically described by saying that; "the output of the system results from the convolution of the waveform and the system transfer function." The process of convolution, however when viewed in the frequency domain, is a simple matter of multiplying the transformed waveform and system transfer function together.

The system that the waveform is applied to can be thought of as filtering the original waveform, i.e. enhancing or degrading specific frequencies. Alternately the effects of a system can be removed by applying a filter which has the inverse characteristics to that of the

system. Hence the system effectively becomes transparent to the signal (ie the output equals the input). Due to the introduction of noise within the system, the direct application of this technique introduces erroneous results. However, a filter can be applied which does have the desired effect.

7.2 Description of the Fourier Filtering Technique

The most common method of applying the Fourier filtering technique to reconstruction tomography technique is by filtered back projection [7.6,7.7]. This technique involves Fourier transforming each profile from the scanner (see section 1.2.1), filtering the transformed profile, with a software filter, and reconstructing the filtered profile using the inverse Fourier transform. The values of the filtered profiles are then projected, orthogonal to the scan, across the display array, and all the elements that are passed through are incremented by that value of the profile.

The technique of filtered back projection uses the intensity of detected radiation to produce the final filtered picture. As the Bateman camera does not deal with the intensities of the detected radiation but only its position, it would have been extremely difficult to reconstruct scan profiles to enable using this type of filter. Therefore the second type of Fourier filtering [7.8,7.9,7.10,7.11] was used. This involved constructing the 'unprocessed' picture array (see section 4.1), and two dimensional Fourier transforming it. The transformed array is filtered using a software filter such as that shown in Figure 7.1 and the corrected picture is reconstructed by inverse Fourier transforming the array.

7.2.1 Application of Fourier Technique

In this particular application, the information from the camera, is used to produce a picture of a particular section through the body, using the 'unprocessed' technique described in 4.1. The array of values representing the picture is then Fourier transformed in two dimensions. As the waveform is not continuous but is descrete, the descrete Fourier transform (DFT) has to be used. As the DFT is relatively slow in computation of the Fourier transform, a fast Fourier transform (FFT) [7.12,7.13] routine was used. This produced the same result as the DFT, but in a far shorter time.

The two dimensional Fourier transform is carried out by the following method. Each row of the array in turn is transferred into a separate vector, where the waveform is Fourier transformed. This transformed vector is multiplied by the filter to produce the effect of being convoluted. The resultant vector is replaced in the array. When all the rows have been processed, the same procedure is carried out for the columns. After all the columns have been done, the array is transformed into real space by applying the inverse Fourier transform in the same manner as described above, except with no filter being used.

As the vector being used is a finite size, care has to be taken to minimise effects to discontinuities at the ends of the vector. To reduce these effects the whole vector is reflected about its end. This produces a vector twice as long, with the waveform followed by a mirror image.

7.2.2 Description of Filter

The filter that is used to affect the picture, is dependent on what error is contained in the original information. Some background information on the particular problem is required. The main source of erroneous data contained in the pictures, are from valid sources of radiation which are not in the surface of interest. Consider Figure 4.2, source A should appear in the final picture, but source B should not. The fundamental problem is how to remove the contribution B from the picture.

The concept behind the filter, is to enhance the higher frequencies. If an object is in the plane of interest, this will produce a signal that has a large proportion of high frequency components. If, however, the source is not in the plane of interest, the radiation emanating from the source will be spread out before reaching it. This, in effect, has lowered the frequencies content of the signal on the surface. Thus, if the low frequencies are gradually removed using a filter characteristic like that shown in Figure 7.1, this should enhance the information in the plane of interest.

To use the type of filter described directly introduces 'ringing' into the waveform (Gibbs phenomena [7.14]). To overcome this problem, the basic characteristic of the filter is altered to that shown in Figure 1.5.

7.3 Comparison of Performance of Process

To compare the Fourier filtering technique with the best of the processes described in Chapter Four, requires the same techniques as used in Chapter Six. Using the impulse test gives the result shown in Figure 7.2 along with the '6-faced cube' method with modified minimum. As can be seen the Fourier result is a curve which has a low value at

both low and high frequencies with a maximum in the mid frequency region. This curve is not linear and level.

The Chi Squared test was used on the Fourier filtering technique when it was applied to the four test phantoms. The results obtained were made meaningless due to the constant background level that was introduced. This left only the judgement of a human being looking at the pictures of both processes. On the phantoms the Fourier technique produced the better of the two pictures.

7.4 Conclusion

The Fourier filtering technique relies on the theory that the waveform is of infinite length and is continuous. In a computer study, this is obviously impossible. Therefore, the computer treatment assumes that the waveform is repeative with a fixed period. This induced errors such as 'ghost' sections of the signal appearing. Therefore the manipulation of the waveform has to be done very carefully. The result of a dramatic change on the signal also introduces errors. When a sharp edged filter is applied to a waveform, 'ringing' could appear in the resultant waveform, which can give the impression of hot-spots where none exist.

In Figure 8.1(3) a line source at 45 degrees is shown, with three 'ghost' images appearing as well. These 'ghost' images appear when the source of radiation is not in the centre of the picture. In the previously shown example (Figure 6.2(16)), all the 'ghosting' overlapped to produce a clearer image, as the phantom was symmetrical about the centre of the picture.

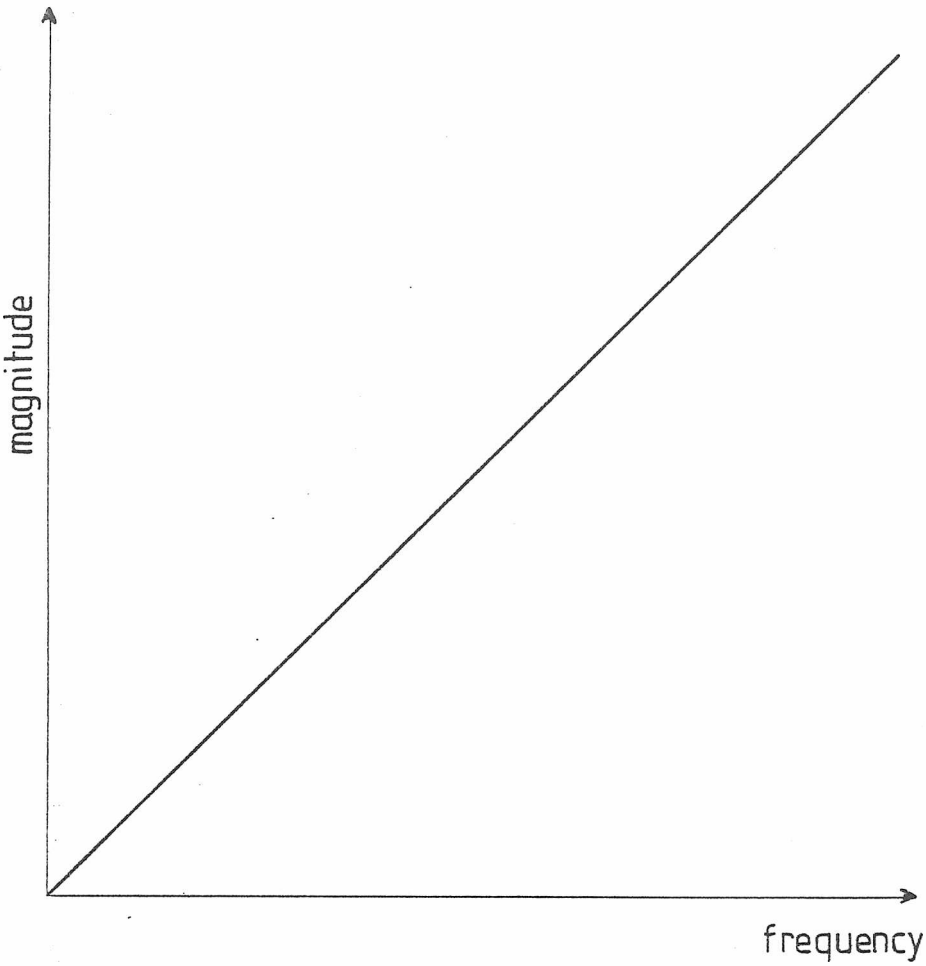

Figure 7.1 Ideal filter

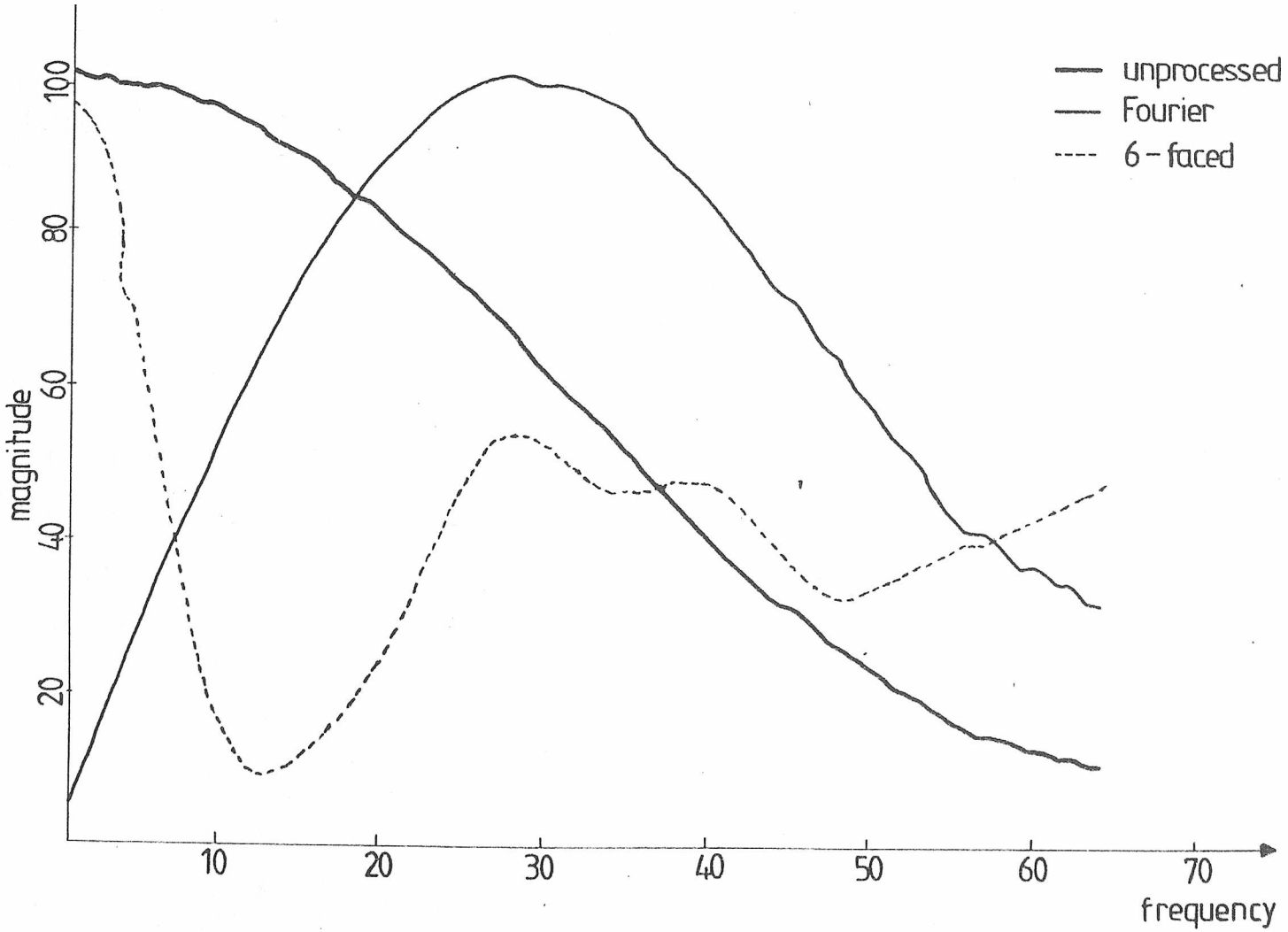

Figure 7.2 Impulse response of Fourier processing

CHAPTER EIGHT

CONCLUSIONS AND FURTHER WORK

8.1 Conclusions

The processes described in Chapter Four were all based round the principle of an array of cubes. Each individual process was a variation upon this theme. Of these, the process that was consistently best was that of the 'six faced cube' using the modified minimum technique (see section 4.4). An explanation why this was the best of the processes considered is as follows.

The processing cube is symmetrical about the surface under consideration, which means that no bias is introduced into the system due to an unbalance such as with the 'three faced cube' and 'three faced cube with shifted base' methods. However, the criteria of being symmetrical also applied to the 'three faced cube with all faces shifted' method. The difference between them was that the 'six faced cube' method enclosed a volume of the emitting material, whereas the 'three faced with all faces shifted' method did not. This appears in the process by the 'six faced cube' method using two 'counting' faces per dimension to only one by the 'three faced cube with all faces shifted'.

8.1.1 Application to Real Data

Two sets of data were available from the real Bateman Camera. These were a line source and a human foot.

The effect on the line source when the best process was applied, as can been seen in Figure 8.1, was the new process removed most of the haze from around the edge of the line source. The Fourier filtering technique produced a sharper line, but it also produced three 'ghost' lines.

The picture produced by the data obtained from the human foot were not very clear. Neither the best process nor the Fourier filtering techniques improved the picture any. This can be seen in Figure 8.2. The main reason for the poor results was the number of samples obtained, which was only 10000.

Without more real data no definite statement can be made on the performance of the new process. But using the results produced by the computer generated phantoms, it looks very promising.

8.2 Further Work

The following sections will describe possible further developments in connection with the processes described in this thesis.

8.2.1 Factors Affecting Program Performance

The times for execution taken by the processes described in Chapter Four, were longer than they should have been, due to the program having to constantly check which process it was to act upon. The final program that would be implemented with the Bateman camera, would have the time for processing reduced, due to only one of these processes being used. One of the factors affecting the time taken, was the reading of the

data. As the amount of space on disc was restricted, the data had to be very efficiently packed, as shown in Appendix B. The time could be reduced by removing the need for packing.

The prototype software was written on a mainframe computer, using a version of Fortran-IV computer language. The selection of a high level language throughout was to increase the portability of the software package. However, this increase in portability meant that the program would take longer to run. To increase speed of execution, critical routines could be written in assembly language. But, these would have to be re-written for each different machine that the software was used.

As the prototype program had to accommodate a number of different processes, a large amount of the memory was used for storing different criteria to do with each process. This in turn meant that the final picture array had to be reduced to accommodate the coding for all these processes. In the final software package, these extra variables would not be needed, and the output array, used with the picture, could be increased to provide a higher spatial resolution. These processes are not dependent on an array that need its dimensions to be a power of two, as is the case for the Fourier technique.

It would be desirable to mount the software on a mini-computer, as these are much cheaper than mainframes and therefore more economically justifiable. However, the software would have to be modified if applied to a mini-computer due to the reduced size of the available memory.

8.2.2 Extension to Other Whole Body Scanners

The prototype software developed during the project, was designed solely for use with the Bateman camera. However, it could be modified to be used with other types of emission body scanners. This software technique could not be applied to the transmission type of device,

due to the introduction of the value of intensity of the radiation.

8.2.3 Expansion of Output Information Type

The software package has the capability of producing an image of any section through the body. These sections can be in any two dimensional plane in three dimensional space. However, to ease the description of the direction, the planes parallel to the X,Y,Z axes were used. To produce three orthogonal areas of the body simultaneously, 3 two dimensional pictures are produced. At present, this involves carrying out three separate runs by the software. As most of the time is involved in reading in the data, the run time for these separate pictures would be reduced if a program was constructed to produce all these three pictures. The system could also, if wished, produce curved sections through the body. An example of where this could be used, is where the section follows just inside the surface of the skin.

8.2.4 Hardware Implementation

An interesting possibility which develops from the processes described in Chapter Four, is that they could be implemented in hardware. This would increase the speed with which the data could be processed to produce a picture. The time reduction could possibly enable a system to give a moving picture of the section through the body, or a picture of a section that was constantly moving. The obvious application of this is in studying the heart.

The hardware would involve an interface to the Bateman camera to receive the data. This would then be processed to find which 'counting' faces of the cube are cut, and the information stored in random access memory. Every so often, this information would be transfered into the display section of the memory, being passed through a comparator circuit

to provide the minimum of the 'counted' values. The levels of the intensity of the display and the position to be viewed in the body, could be controlled by the user.

A possible system to carry this out is shown in Figure 8.3. The information is taken from the camera at the rate, stated in Chapter Two, of 10kHz. This value determines the maximum amount of time available for processing each ray, i.e. 100us. The 100us time is however an average time interval, and will fluctuate as the detections are dependent on a radioactive decaying source. This can be overcome by use of a FIFO register to provide a steady rate to the rest of the system.

The information from the camera is in the form of detector numbers and their associated (X,Y) co-ordinates. This information is converted into the equation of a straight line, with reference to a three dimensional set of axes. The conversion can be carried out either using a ROM look-up table, which may be rather large but fast, or a microprocessor. The position of the surface, to be displayed, can be set by the positioning of these axes. However, the time taken to convert the data from the camera into an equation of a line, must be within the 100us time interval set by the camera.

The equation generated is passed to three parallel channels. Each of these channels finds all the faces of the cubes cut by the gamma ray in that dimension, and increments the locations in memory associated with these faces. Again the complete process must occur within the 100us time interval. Due to the speed of memory access, these process must be carried out in parallel to enable it to be completed within the 100us. This process may be carried out using a high speed microprocessor with clever use of the instruction set. However, it is more likely to be dedicated hardware as this can easily achieve the speed necessary.

This procedure is carried out until there is a picture update. The picture update signal would be generated using a variable frequency oscillator, which can be adjusted by the user. On the update signal, all the arrays containing the X, Y and Z faces are compared by dedicated hardware, and the smallest or modified smallest is placed into the display memory. However this process would take longer than the maximum time of 100us. Therefore, when the picture enable is set, the whole process is frozen until the comparison of the X, Y and Z faces is completed. As this may take quite a long time, a large amount of data would be thrown away. This can be overcome by providing a LARGER FIFO to store the input data, and increase the speed of operation of the rest of the process.

When the values of the memories are being compared, the locations just compared are set to zero. To prevent disturbing the picture, there are two display memories. These operate such that one displays the picture while the other receives the next picture. Once all the information has been transfered into memory, the two memories swap roles. The brightness of the picture is calculated at the same time as the comparison of the 'counts' on the faces of the cubes.

The quality of the picture produced by such a device as described, is dependent on the frequency of the picture updates. If the picture updates occur at a high rate, the number of rays used to produce the final picture will be small. The information content of the final picture will therefore, be such that only large areas of radiation or high intensity areas will be seen. However, the capability of moving pictures is possible. For good quality pictures the time between each picture enable has to be long, of the order of several seconds. In this system there is a compromise between speed of update of picture (ie movement) and quality of the picture produced.

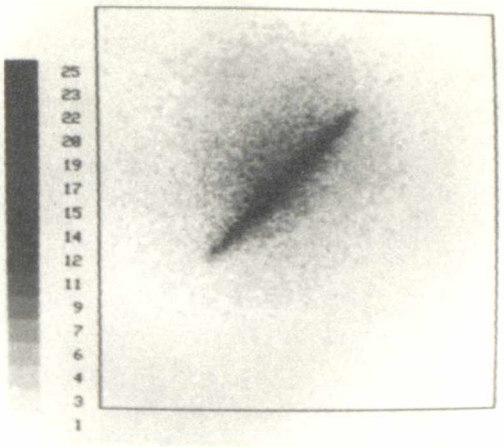

(1) " unprocessed

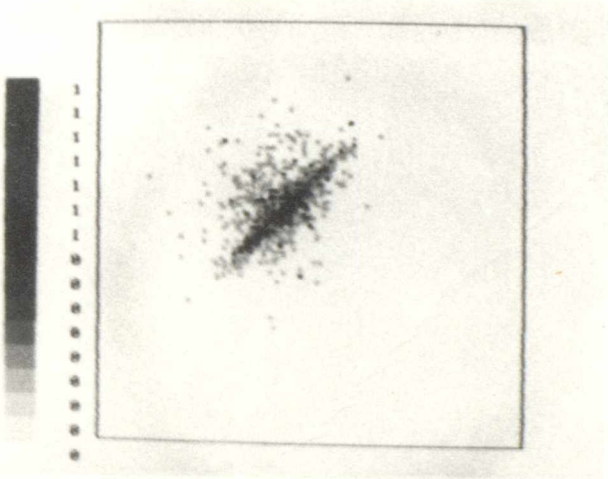

(2) "six faced cube"+ modified minimum

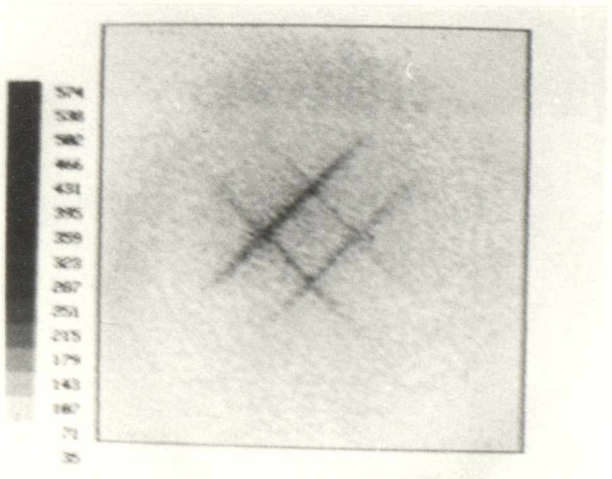

(3) Fourier

Figure 8.1 REAL DATA - Line source

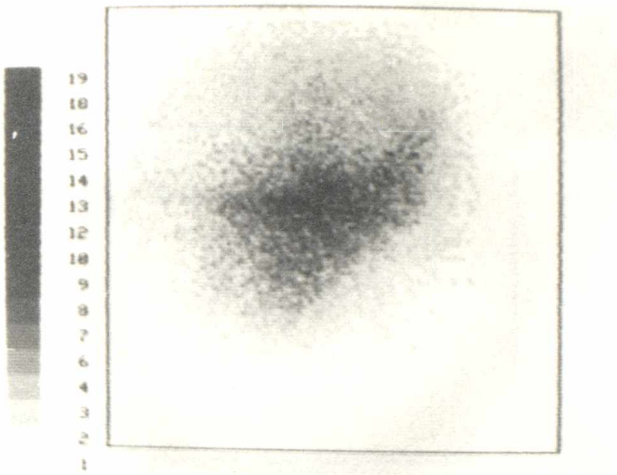

(1) "unprocessed"

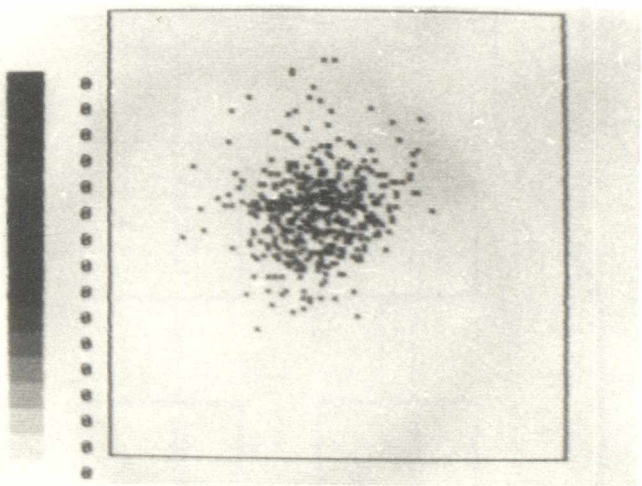

(2) "six faced cube"+ modified minimum

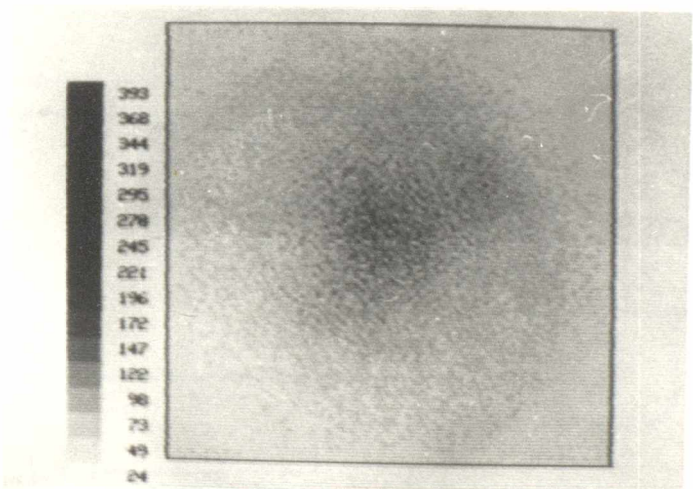

(3) Fourier

Figure 8.2 REAL DATA - Human foot

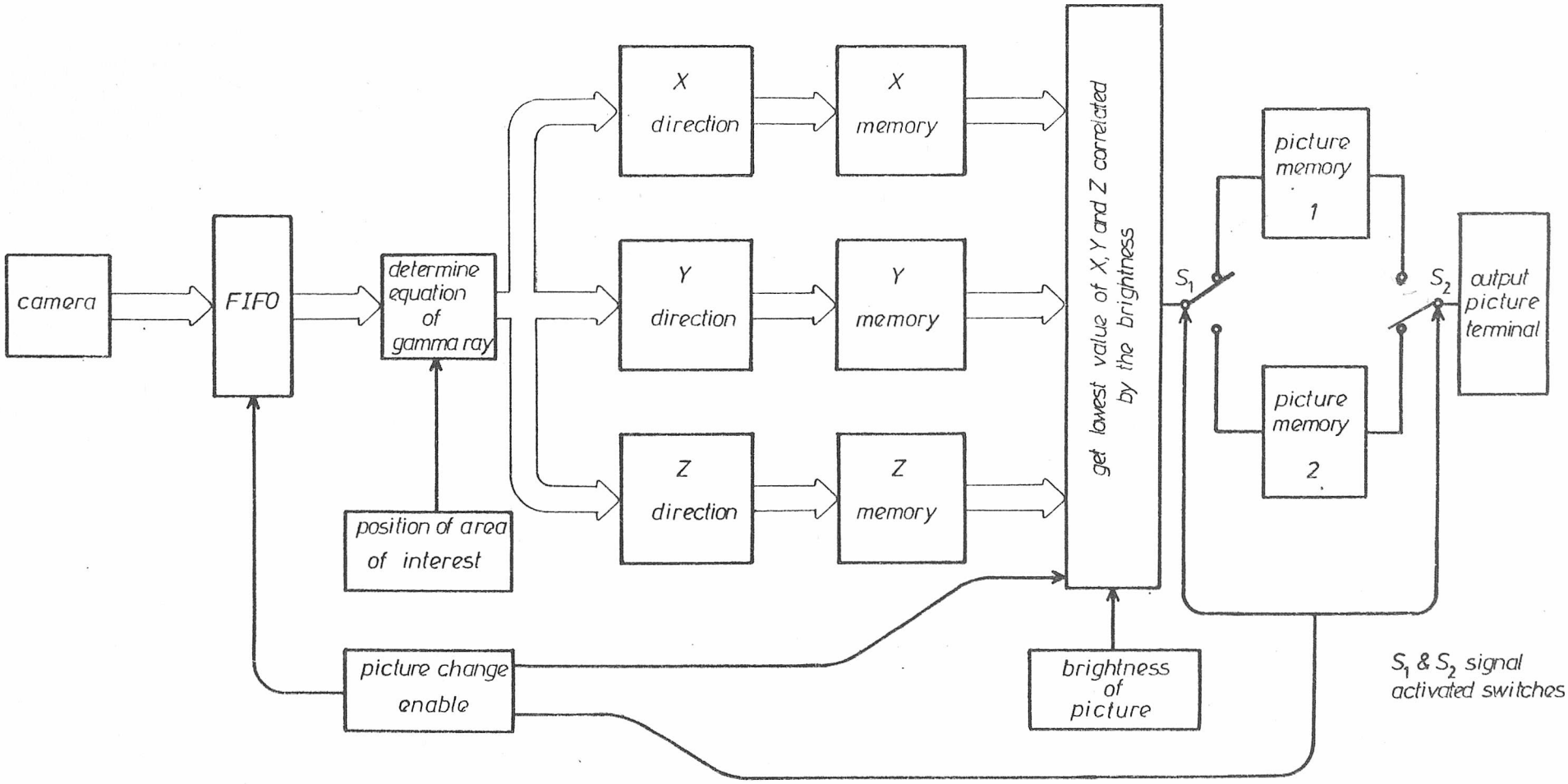

Figure 8.3 Possible hardware configuration

APPENDIX A

CO-ORDINATE CONVERSION

A.1 Conversion of Detector to Real Coordinates

The information received from the camera is received in the form of a detector number and the co-ordinates ('Xd','Yd') of the position on that detector. To use this information easily, the position was converted to a three dimensional co-ordinate system. The system chosen was the normal (X,Y,Z) co-ordinate system with the axes positioned, with respect to the detectors, as shown in Figure 4.3. The following equation gives the conversion from the six detector system to the (X,Y,Z) co-ordinate system. Px is the X dimension of one of the detectors.

The Y co-ordinate remained the same through the transfer (ie Y = Yd).

('*' is used to indicate multiplication)

Detector one:

$$X = Xd + Px * COS(60)$$
$$= Xd + Px / 2.0$$

$$Z = 0$$

APPENDIX A

Detector two:

$$X = Px + Px * COS(60) + Xd * COS(60)$$

$$= 1.5 * Px + Xd / 2$$

$$Z = Xd * SIN(60)$$

Detector three:

$$X = Px + 2.0 * Px * COS(60) - Xd * COS(60)$$

$$= 2.0 * Px - Xd / 2.0$$

$$Z = Px * SIN(60) + Xd * SIN(60)$$

$$= (Px + Xd) * SIN(60)$$

Detector four:

$$X = Px + Px * COS(60) - Xd$$

$$= 1.5 * Px - Xd$$

$$Z = 2.0 * Px * SIN(60)$$

Detector five:

$$X = Px * COS(60) - Xd * COS(60)$$

$$= (Px - Xd) / 2.0$$

$$Z = 2.0 * Px * SIN(60) - Xd * SIN(60)$$

$$= (2.0 * Px - Xd) * SIN(60)$$

APPENDIX A

Detector six:

$$X = Xd * COS(60)$$

$$Z = Px * SIN(60) - Xd * SIN(60)$$

$$= (Px - Xd) * SIN(60)$$

A.2 Conversion of Real to Detector Coordinates

When generating data for a simulated 'phantom', the detector number and its associated co-ordinates ('Xd','Yd') have to be generated from the absolute position (X,Y,Z). The following equations can be used to find the position ('Xd','Yd'). As in A.1, the Y co-ordinate does not change (ie Yd = Y).

(^ is the method used in computing to indicate 'to the power of')

Detector one:

$$Xd = X - Px * COS(60)$$

$$= X - Px / 2.0$$

Detector two:

$$Xd = \sqrt{(X - (Px + Px * COS(60))^2 + Z^2}$$

$$= \sqrt{(X - 1.5 * Px)^2 + Z^2}$$

APPENDIX A

Detector three:

$$Xd = \sqrt{(2.0 * Px - X)^2 + (Z - Px * SIN(60))^2}$$

Detector four:

$$Xd = Px + Px * COS(60) - X$$

$$= 1.5 * Px - X$$

Detector five:

$$Xd = \sqrt{(Px * COS(60) - X)^2 + (2.0 * SIN(60) * Px - Z)^2}$$

Detector six:

$$Xd = \sqrt{X^2 + (Px * SIN(60) - Z)^2}$$

APPENDIX B

METHODS OF STORING THE DATA

The data generated for a particular simulated phantom has to be stored, to used later by the analysis program. The option of using a magnetic tape for storing the data was not feasible, due to the tapes having to be mounted by the computer operators. Therefore, all the data had to be stored on disc within a defined user area. As this area was of a limited size, an efficient method of storing the data had to be devised. The following description shows the route to the final method of storing the data. It will also show the relative speeds of access of the different types.

B.1 Type one - Sequential ASCII

This stores the data as a sequential ASCII file.

Each ray is stored as:

NPL1 NX1 NY1 NPL2 NX2 NY2

where NPL1 - number of first plate struck
NX1 - X co-ordinate on NPL1
NY1 - Y co-ordinate on NPL1

NPL2 - number of second plate struck
NX2 - X co-ordinate on NPL2
NY2 - Y co-ordinate on NPL2

(all values are integer)

This method is wasteful of space as each character is stored as an ASCII number. These include <SPACE>s and <END of line> control characters. The main advantage of this method, is that the detector size can be as large as the value the maximum integer variables allowed on the computer. This dimension controls the total number of detector wires available for use within the detector.

B.2 Type two - Packed Sequential ASCII

This stores the data as a packed sequential file. The data shown above in B.1 is combined into two words, which are constructed by the following arithmetic operation:

IST1 = 16777216 * NPL1 + 4096 * NX1 + NY1

IST2 = 16777216 * NPL2 + 4096 * NX2 + NY1

These multiplications are carried out by logically shifting the word, the appropriate number of bits. For 4096 it is shifted 12 bits and for 16777216 it is shifted 24 bits to the left. Shifting the word, rather than using multiplication, enables the sign bit to also be used for storage. With multiplication it is difficul' to use the sign bit. However, the packing of the information restricts the maximum dimension of the detectors to be 4095.

Each ray is stored as:

IST1 IST2

This reduces the storage space required for the same information. There is also a marked reduction in the time taken to store the data. The time taken to transfer information to disc is large compared to operations carried out by the processor. The reduction in time is due to less data being transfered. However, <SPACE>s and <End of Line>

control characters are still stored.

B.3 Type three - Packed Binary

This takes takes the data described in B.2 and stores it in a BINARY file instead of a SEQUENTIAL file.

Each ray is stored as:

```
START WORD
   IST1
   IST2
STOP  WORD
```

The START and STOP words are used to identify the position of data blocks. This reduces the amount of space required to store the data, as each value is stored as its actual value, not a list of ASCII equivalents. The <SPACE>s and <End of line> characters that were stored when using sequential ASCII files, are not stored in a binary file. As there is no conversion to ASCII, this method is faster than that shown in B.2.

B.4 Type four - Optimally Packed Binary

This takes the data shown in Type two and stores it in a BINARY file, but instead of having a START word and STOP word for each ray, as in B.3, 63 rays are stored for each, as shown below.

```
START WORD
 IST1(1)
 IST2(1)
 IST1(2)
 IST2(2)
    .
    .
    .
 IST1(63)
 IST2(63)
STOP  WORD
```

As the data is sent to disc in blocks of 63 rays, this reduces the time of transfer further, because writing to disc is comparatively slow. 63 pairs of words per block was chosen because each page on the computer holds 128 words, and when the start and stop words are removed there are only 126 words left for data.

B.5 Conclusion

Using the above four methods in turn, for storing a 50000 sample phantom produces the following results.

(1) Page size and number of bytes used:

Type	Pages	Bytes
1	879	449998
2	684	350000
3	391	200003
4	199	101588

(2) The CPU time taken to produce the phantom:

Type	Time (s)
1	111.4
2	108.0
3	75.8
4	67.7

(3) The CPU time taken to produce a picture of a section through the centre of the phantom using the technique described in 4.1:

Type	Time (s)
1	69.1
2	64.6
3	36.4
4	30.2

As can be seen, type four is consistently better than the other three types. In all the comparisons that are carried elsewhere, type four is the method of storing data that was always used.

APPENDIX C

PROOFS

C.1 Bias in Spherical Phantom Generation

In section 3.3.1, a method of producing a randomly placed point within a sphere was described. This technique produced a bias in two out of the three dimensions. The mathematical proof why there should be a bias, is now shown:

Proof

Consider an elementary volume of the sphere defined by:

$$R < r < (R + \delta R)$$

$$A < \text{Theta} < (A + \delta A)$$

$$B < \text{Phi} < (B + \delta B)$$

If the distribution within the sphere is uniform:

$$P[\text{Point in elementary vol}] = \frac{\text{Elementary vol}}{\text{Total vol of sphere}}$$

$$= \frac{\delta X * \delta Y * \delta Z}{(4 * PI * a\hat{}3) / 3}$$

(as $\delta X * \delta Y * \delta Z = R\hat{}2 * \text{Sin}(A) * \delta R * \delta A * \delta B$)

APPENDIX C

$$P[\text{Point in elementary vol}] = \frac{R^2 * \text{Sin}(A) * \delta R * \delta A * \delta B}{(4 * PI * a^3) / 3} \qquad (1)$$

If we assume:

r is uniform over (0,a)

Theta is uniform over (0,PI)

Phi is uniform over (0,2 * PI)

Then

$$P[\text{Point in elementary vol}] = \frac{\delta R}{a} * \frac{\delta A}{PI} * \frac{\delta B}{2 * PI}$$

$$= \frac{\delta R * \delta A * \delta B}{2 * PI^2 * a} \qquad (2)$$

As there is a contradiction between equations (1) and (2), this method will not produce a uniformly distributed random point within the sphere.

APPENDIX C

C.2 Solid Angle of a Point to a Rectangle

Consider a rectangle in three dimension space as shown in Figure C.1 with its area vector orthogonal to the Z plane. The solid angle of the origin to this rectangle is now evaluated.

$$w = \int_S \int \frac{\underline{r} \cdot d\underline{s}}{r^3}$$

$$= \int_S \int \frac{(x\underline{i} + y\underline{j} + e\underline{k}) \cdot \underline{k} \; dx \; dy}{(x^2 + y^2 + e^2)^{3/2}}$$

$$= \int_d^{d+b} \int_c^{c+a} \frac{e \; dx \; dy}{(x^2 + y^2 + e^2)^{3/2}}$$

Solving this gives:

$$w = \tan^{-1}\left[\frac{(c + a)(d + b)}{e\sqrt{(d + b)^2 + e^2 + (c + a)^2}}\right]$$

$$- \tan^{-1}\left[\frac{c\,(d + b)}{e\sqrt{(d + b)^2 + e^2 + c^2}}\right]$$

$$- \tan^{-1}\left[\frac{(c + a)\,d}{e\sqrt{d^2 + e^2 + (c + a)^2}}\right]$$

$$+ \tan^{-1}\left[\frac{c\,d}{e\sqrt{d^2 + e^2 + c^2}}\right]$$

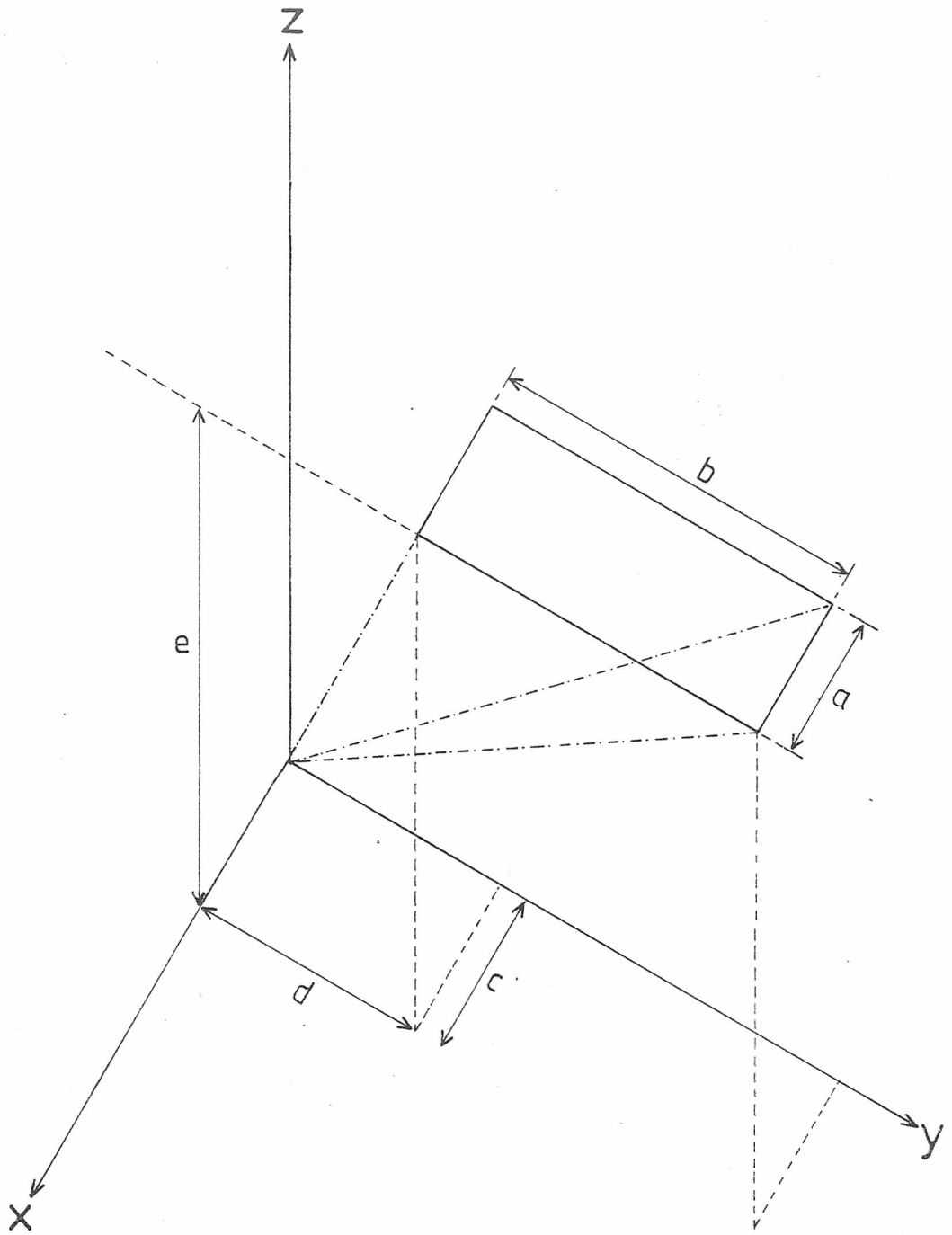

Figure C.1 Solid angle of a rectangle to the origin

APPENDIX D

DECsystem-20 Technical Summary

Computer Type:	DECsystem-2050
C.P.U:	36 bit word 383 element instruction set
Memory size:	256 kilo-words (1152 kilo-bytes)
Operating System:	TOPS-20
Processing method:	Virtual memory system with multi-process job structure
Disc capacity:	80 Mega-words (400 Mega-bytes)

REFERENCES

1.1 Hounsfield G N
Br. J. Radial, 1973, No. 46, Pages 1016-1022

1.2 Keyes W I
'Current Status of Single Photon Emission Compterised Tomography'
I.E.E.E. Trans. Nucl. Sci., 1979, Vol. NS-26, No. 2, Pages 2752-2755

1.3 Rowe R W and Keyes W I
'Comparison of Scanner and Camera Systems for Quantitative Single Photon Emission Tomography'
I.E.E.E. Trans. Nucl. Sci., 1979, Vol. NS-26, No. 2, Pages 2768-2771

1.4 Glasstone S
'Sourcebook on Atomic Energy'
Litton Educational Publishing, Pages 211-224

1.5 Kuhl D E, Edwards R Q and Ricci A R
'The Mark IV System for Radionuclide Computed Tomography of the Brain'
Radiology, 1976, No. 121, Pages 405-413

1.6 Budinger T F, Derenzo S E and Gullberg G T
'Emission Computer Assisted Tomography with Single Photon and Positron Annihilation Photon Emitters'
Journ. Comp. Ass. Tom., 1977, Vol. 1, Pages 131-145

1.7 Keyes W I
'The Fan Beam Gamma Camera'
Phys. Med. Biol., 1975, Vol. 20, No. 3, Pages 489-493

1.8 Anger H O
'Intrumentation in Nuclear Medicine'
New York:Academic Press, 1967, Pages 485-552

REFERENCES

1.9 Burnham C A and Brownell G L
'A Multi-Crystal Positron Camera'
I.E.E.E. Trans. Nucl. Sci, 1972, Vol. NS-19, No. 3, Pages 201-205

1.10 Lim C B, Chu D, Perez-Mendez V, Kaufman L, Hattner R S and Price C
I.E.E.E. Trans. Nucl. Sci. , 1975, Vol. NS-22, No. 1, Pages 388-394

1.11 Hattner R S, Lim C B, Swann S J, Kaufman L, Perez-Mendez V, Chu D, Huberty J P, Price D C and Wilson C B
I.E.E.E. Trans. Nucl. Sci., 1976, Vol. NS-23, No. 1, Pages 523-527

1.12 Jeavons A P
'The CERN Proportional Chamber Positron Camera'
5th Inter. Conf. Positron Annihilation, 1979

1.13 Jeavons A P, Townsend D N, Ford N L, Kull K, Fischer O and Peter M
'A High-Resolution Proportional Chamber Positron Camera and Its Applications'
I.E.E.E. Trans. Nucl. Sci, 1978, Vol. NS-25, No. 1, Pages 164-173

1.14 Townsend D N, Schorr B and Jeavons A P
I.E.E.E. Nucl. Sci. Symp., 1979

1.15 Cho Z H, Cohen M B, Singh M, Eriksson L, Chan J, MacDonald N and Spolter L
'Performance and Evaluation of the Circular Ring Transverse Axial Positron Camera (CRTAPC)'
I.E.E.E. Trans. Nucl. Sci., 1977, Vol. NS-24, No. 1, Pages 532-543

1.16 Bohm C, Eriksson L, Bergstrom M, Litton J, Sundman R and Singh M
'A Computer Assisted Ringdector Positron Camera System for Reconstruction Tomography of the Brain'
I.E.E.E. Trans. Nucl. Sci., 1978, Vol. NS-25, No. 1, Pages 624-631

1.17 Jones T
'Positron Emission Tomography and Measurements of Regional Tissue Functions in Man'
Brit. Med. Bull., 1980, Vol. 36, No. 3, Pages 231-236

2.1 Bateman J E and Connolly J F
'A Multiwire Proportional Gamma Camera for Imaging (99)Tc(m) Radionuclide Distributions'
Phys. Med. Biol., 1978, Vol. 23, No. 3, Pages 455-470

REFERENCES

2.2 Bateman J E and Connolly J F
'A Hybrid MWPC Gamma Ray Detecting System for Applications in Nuclear Medicine'
Nucl. Instr. Meth., 1978, Vol. 156, Pages 27-31

2.3 Glasstone S
'Sourcebook on Atomic Energy'
Litton Educational Publishing, Pages 198-209

2.4 Bateman J E
'Signal to Noise Ratio and Data Rates in Positron Cameras - A Theoretical Analysis'
Rutherford Laboratory Internal Report no. RL-78-006/B, 1978

5.1 Frei W
'Display Processing of Computed Tomography Images'
I.E.E.E. Trans. Nucl. Sci., 1978, Vol. NS-25, No. 2, Pages 939-943

5.2 Eades J D
'The Design of an Interactive Computer System for Microelectronic Mask Making'
Ph. D. Thesis, 1976, Pages 184-216

5.3 'Tektronix 4014 and 4014/1 Computer Display Terminal Users Instruction Manual'
Rev. B, 1974

5.4 Newman W M and Sproull R F
'Principles of Interactive Graphics'
McGraw-Hill Book Company, Pages 211-290

5.5 'User Manual for 5500 Series'
GOC5500(jss A)-jrm, 1978, Issue A

5.6 Keyes W I, Chesser R and Undrill P E
'Transverse-Section Emission Tomography'
7th L H Gray Conference: Medical Images

6.1 Siegel S
'Non-parametric Statistics for the Behavioral Sciences'
McGraw-Hill Book Company, Pages 35-60

6.2 Siegel S
'Non-parametric Statistics for the Behavioral Sciences'
McGraw-Hill Book Company, Pages 42-47

REFERENCES

7.1 Schlindwein M
'Iterative Three-Dimensional Reconstruction from Twin-cone Beam Projections'
I.E.E.E. Trans. Nucl. Sci., 1978, Vol. NS-25, No. 5, Pages 1135-1143

7.2 Colsher J G
'Iterative Three Dimensional Image Reconstruction from Tomographic Projections'
Computer Graphics Image Processing, 1977, Vol. 6, Pages 513-537

7.3 Bernard E and Oppenheim M D
'More Accurate Algorithms for Iterative 3-Dimensional Reconstruction'
I.E.E.E. Trans. Nucl. Sci., 1974, Vol. NS-21, Pages 72-77

7.4 Lim C B, Cheng A, Boyd D P and Hattner R S
'A 3-D Iterative Reconstruction Method for Stationary Planar Positron Cameras'
I.E.E.E. Trans. Nucl. Sci., 1978, Vol. NS-25, No. 1, Pages 196-201

7.5 Townsend D, Piney C and Jeavons A
'Object Reconstruction from Focused Positron Tomograms'
Phys. Med. Biol., 1978, Vol. 23, No. 2, Pages 235-244

7.6 Keyes W I
'A Practical Approach to Transverse-Section Gamma-Ray Imaging'
Brit. Jour. Rad., 1976, Vol. 49, Pages 62-70

7.7 Cormack A M
'Reconstruction of Densities from their Projections, with Applications in Radiological Physics'
Phys. Med. Biol., 1973, Vol. 18, Pages 195-207

7.8 Budinger T F and Gullberg G T
'Three Dimensional Reconstruction in Nuclear Medicine Emission Imaging'
I.E.E.E. Trans. Nucl. Sci., 1974, Vol. NS-21, Pages 2-20

7.9 Colsher J G
'Fully Three-Dimensional Positron Emission Tomography'
Phys. Med. Biol., 1980, Vol. 25, No. 1, Pages 103-115

7.10 Tam K C, Chu G, Perez-Mendez V and Lim C B
'Three-Dimensional Reconstruction in Planar Positron Cameras Using Fourier Deconvolution of Generalized Tomograms'
I.E.E.E. Trans. Nucl. Sci., 1978, Vol. NS-25, No. 1, Pages 152-159

REFERENCES

7.11 Chu G and Tam K C
'Three-Dimensional Imaging in the Positron Camera Using Fourier Techniques'
Phys. Med. Biol., 1977, Vol. 22, No. 2, Pages 245-265

7.12 Cochran W T, Cooley J W, Favin D L, Helms H D, Kaenel R A, Lang W W, Maling G c, Nelson D E, Rader C M and Welch P D
'What is the Fast Fourier Transform?'
I.E.E.E. Trans. Audio Electroacoustics, 1967, Vol. AU-15, No. 2, Pages 45-55

7.13 Uhrich M L
'Fast Fourier Transforms Without Sorting'
I.E.E.E. Trans. Audio Electroacoustics, 1969, Vol. AU-17, Pages 170-172

7.14 Champeney D C
'Fourier Transforms and Their Physical Applications'
Academic Press, London, 1973, Page 6

BIBLIOGRAPHY

1. Ackroyd M H
'Digital Filters'
Butterworth, London 1973

2. Bracewell R N
'The Fourier Transform and its Applications'
McGraw-Hill Book Company Inc

3. Brigham E O
'The Fast Fourier Transform'
Prentice-Hall Inc

4. Brooks R A and Di Chiro G
'Principles of Computer Assisted Tomography (CAT) in Radiographic and Radioisotopic Imaging'
Phys. Med. Biol., 1976, Vol. 21, No. 5,

5. Champeney D C
'Fourier Transforms and their Physical Applications'
Academic Press, London

6. Evans A L
'Evaluation of Medical Images'
Adam Hilger Ltd, Bristol

7. Glasstone S
'Sourcebook on Atomic Energy'
Litton Educational Publishing

8. Giloi K
'Interactive Computer Graphics'
Prentice-Hall Inc

9. Gold B and Rader C M
'Digital Processing of Signals'
McGraw-Hill Book Company Inc

10. I.E.E.E. Trans. Nucl. Sci., Vol. NS-21

11. I.E.E.E. Trans. Nucl. Sci., Vol. NS-25

12. Kowalski G and Wagner W
'Generation of Pictures by X-ray Scanners'
Optica Acta, 1977, Vol. 24, No. 4, Pages 327-348

13. Llacer J
'Nuclear Medical Imaging'
I.E.E.E. Spectrum, 1981, Vol. 18, No. 7, Pages 33-37

14. Newman W M and Sproull R F
'Principles of Interactive Computer Graphics'
McGraw-Hill Book Company Inc

15. Phelps M E
'Emission Computed Tomography'
Seminars Nucl. Med., 1977, Vol. 7, No. 4, Pages 337-365

16. Siegel S
'Non-parametric Statistics for the Behavioral Sciences'
McGraw-Hill Book Company Inc

17. Spiegel M R
'Advanced Mathematics'
Schaum Series, McGraw-Hill Book Company Inc